

MARWALA, T

A MULTIPLE CRITERION UPDATING METHOD FOR
DAMAGE DETECTION ON STRUCTURES

MEng

UP

1997

**A MULTIPLE CRITERION UPDATING METHOD
FOR DAMAGE DETECTION ON STRUCTURES**

by

Tshilidzi Marwala

Submitted in partial fulfilment of the requirements for the degree

of M.Eng (Mechanical) in the Faculty of Engineering

University of Pretoria

Pretoria

13 August 1997

**A MULTIPLE CRITERION UPDATING METHOD FOR DAMAGE
DETECTION ON STRUCTURES**

by

Tshilidzi Marwala

Supervisor: Prof. PS Heyns

Department of Mechanical and Aeronautical Engineering

Degree for which the dissertation is submitted:

Master of Engineering

Summary

Damage in structures may be identified and quantified by using measured frequency response functions (FRFs) or identified modal properties as a basis for updating. The main shortcoming of these methods is that if they are used individually the methods using modal properties do not necessarily predict the measured FRFs and vice versa.

A Multiple Criterion Method (MCM) which uses the measured FRFs and identified modes simultaneously in an optimisation fashion, is developed in this study. The Euclidean norm of the error vector resulting from the integration of the mass and stiffness matrices from the Finite Element Model (FEM) and the measured FRFs in the equation of motion is minimised. The same procedure is performed using identified modal properties. The modulus of elasticity of each element in the FEM of the structure is used as design variables.

The new procedure is tested on a simple beam, a complex beam (with drilled holes that are hard to model) and an irregular H-shaped structure. The effectiveness of MCM was compared to other methods that use FRFs and modal properties individually. The comparison was made by using methods such as Modal Assurance Criterion (MAC), Coordinate Modal Assurance Criterion (COMAC) and the Frequency Response Functions Assurance Criterion (FRFAC), which is a new procedure developed specifically as part of this work.

It was found that the method is capable of obtaining an updated model which assimilates the two sets of data from the FRFs and modal properties. It was also discovered that the method is more successful in determining the presence of damage on the structure; its location; and its the extent of damage.

**'n MULTI-KRITERIUM OPDATERINGSMETODE FOR SKADE-OPSPORING
OP STRUKTURE**

deur

Tshilidzi Marwala

Studieleier: Prof P S Heyns

Departement Meganiese en Lugvaartkundige Ingenieurswese

Graad waarvoor die verhandeling voorgelê word:

Meester in Ingenieurswese

Samevatting

Skade in strukture kan geïdentifiseer en gekwantifiseer word deur die meting van frekwensieresponsiefunksies (FRFs) of deur die identifikasie van modale parameters as 'n basis vir opdatering. Die belangrikste tekortkoming van hierdie metodes is dat as hulle individueel gebruik word, die metodes wat modale parameters gebruik nie noodwendig die gemete FRFs voorspel nie, en omgekeerd.

'n Multi-kriterium metode wat die gemete FRFs en die geïdentifiseerde modusse gelyktydig in 'n optimeringsmodus gebruik, word in hierdie studie ontwikkel. Die Euklidiese norm van die foutvektor wat resulteer uit die integrasie van die massa- en styfheidsmatrikse van die eindige-elementmodel en die gemete FRFs, in die bewegingsvergelyking word geminimeer. Dieselfde prosedure word deurgevoer met gebruik van die geïdentifiseerde modale eienskappe. Die elastisiteitsmodulus van elke element in die eindige-elementmodel word as ontwerpveranderlikes gebruik.

Die nuwe prosedure word getoets op 'n eenvoudige balk, 'n komplekse balk (met geboorde gate wat moeilik is om te modelleer) en 'n onreëlmatige H-vormige struktuur. Die effektiwiteit van die multi-kriterium metode is vergelyk met ander metodes wat FRFs en modale parameters afsonderlik gebruik. Die vergelyking is gedoen deur gebruik te maak van metodes soos die modale korrelasiekriterium, die koördinaat modale korrelasiekriterium en die frekwensieresponsiefunksie korrelasiekriterium, 'n nuwe prosedure wat spesiaal ontwikkel is as deel van hierdie werk.

Daar is gevind dat hierdie metode in staat is om 'n opgedateerde model te vind wat die twee stelle data uit die FRFs en die modale parameters assimileer. Daar is verder gevind dat die metode meer suksesvol is in die bepaling van die teenwoordigeheid van skade in strukture, die posisie en omvang van die skade.

ACKNOWLEDGEMENTS

I wish to thank the following people and organisations:

- Prof. PS Heyns, for being a superb role model, an excellent supervisor, and for implanting in me the unwavering desire to leave no stone unturned.
- Mr. A Engelbrecht and Mr. S. MacWherter.
- Prof. N Stander for the insightful discussions on optimisation.
- AECI Limited
- The Foundation for Research Development
- The University of Pretoria.
- My parents for all they have done for me.

This thesis is dedicated to the memory of my grandmother Vho-Tshianeo Marwala whose warmth, I shall forever feel, as long as I live. My final expression of gratitude goes to the LORD for giving me the wisdom to repent in his Son's name.

TABLE OF CONTENTS

	List of Figures	
	List of Tables	
	List of Symbols	
	Nomenclature	
1.	Introduction	1
2.	Formulation of The Problem	7
	2.1. Introduction	7
	2.2. D'Ambrogio Method (DAM)	9
	2.2.1 Getting the FRFs	10
	2.2.2 Damage Detection	12
	2.3 The Modal Properties Method (MPM)	13
	2.3.1 Damage Detection	15
	2.4 Multiple Criterion Method (MCM)	15
	2.5 Conclusion	16
3.	Computational Techniques	17
	3.1 Introduction	17
	3.2. Comparison of Experiment and Prediction	18
	3.2.1 Direct Comparison	19
	3.2.2 The Frequency Response Functions Assurance Criterion (FRFAC)	21
	3.2.3 The Modal Assurance Criterion (MAC)	22
	3.2.4 The Co-ordinate Modal Assurance Criterion (COMAC)	23
	3.3 Model Expansion and Reduction Procedures	24
	3.3.1 Model Reduction	24
	3.3.2 Model Expansion	27
	3.4 Optimisation	28
	3.5 Comparison of Methods	29
4.	Updating of Finite Element Model	32
	4.1. Introduction	32
	4.2. Example 1. Simple Beam	34
	4.2.1. Updating The Beam Before Damage	35

4.2.2.	The Beam With Damage Case 1	37
4.2.3.	The Beam With Damage Case 2	39
4.2.4.	The Beam With Damage Case 3	41
4.3.	Example 2: Freely Suspended Beam With Holes	43
4.3.1	Updating Before Damage	43
4.3.2.	The Beam With Damage Case 1	45
4.3.3.	The Beam With Damage Case 2	46
4.3.4.	The Beam With Damage Case 3	47
4.4.	Example 3: Freely Suspended H-shaped Structure	49
4.4.1.	The Updating Case Before Damage Occurs	49
4.4.2.	The Damage Case 1	51
4.4.3.	The Damage Case 2	52
4.4.4.	The Damage Case 3	53
4.5.	Conclusion	54
5.	Damage Detection Using Updating Procedure	55
5.1.	Introduction	55
5.2.	Example 1	56
5.2.1.	Damage Case 1	56
5.2.2.	Damage Case 2	58
5.2.3.	Damage Case 3	61
5.3.	Example 2	63
5.3.1.	Damage Case 1	64
5.3.2.	Damage Case 2	67
5.3.3.	Damage Case 3	69
5.4.	Example 3	71
5.4.1.	Damage Case 1	72
5.4.2.	Damage Case 2	73
5.4.3.	Damage Case 3	75
5.5.	Conclusion	77
6.	Conclusion	78
	References	82
	Appendix A: The Expansion and Reduction Programs	90

Appendix B: The Expansion of Measured FRFs	105
Appendix C: Programs Used for the Examples	106
Appendix D: Pictures of the Experiment Conducted	126
Appendix E: The Graphical Illustration of the Results	128
Appendix F: Details of the Structures Used	134

LIST OF FIGURES

Figure 2.1. (a)	Theoretical route to vibration analysis	7
Figure 2.1. (b)	Experimental route to vibration analysis	7
Figure 3.1	Comparison between experimental and analytical natural frequencies	19
Figure 3.2. (a)	Comparison of measured and predicted mode shapes for single mode	20
Figure 3.2. (b)	Comparison of measured and predicted mode shapes for three modes	20
Figure 3.3	Experimental and analytical FRFs	21
Figure 3.4	The schematic diagram of a beam which is fixed at the end	30
Figure 4.1	The structure of the updating procedure	33
Figure 4.2	Illustration of the change in E	34
Figure 4.3	The discretised beam that was tested freely suspended	35
Figure 4.4	Experimental set-up damage was imposed on element 3 as indicated	37
Figure 4.5	Damage on element 3 and 5	39
Figure 4.6	Damage case 3	41
Figure 4.7	A beam with holes	43
Figure 4.8	An irregular H-shaped structure	49
Figure 5.1	Experimental set-up damage was imposed on element 3 as indicated	56
Figure 5.2	Damage detection using DAM	56
Figure 5.3	Damage detection using MPM	57
Figure 5.4	Damage detection using MCM	58
Figure 5.5	Damage at elements 3 and 5	59
Figure 5.7	Damage detection using MPM	59
Figure 5.8	Damage detection using MCM	60
Figure 5.9	Damage at 3, 5 and 6	61
Figure 5.10	Damage detection using DAM approach	62
Figure 5.11	Damage detection using MPM	62
Figure 5.12	Damage detection using MCM	63

Figure 5.13	The schematic representation of the beam with holes	64
Figure 5.14	Damage detection using DAM	65
Figure 5.15	Damage detection using MPM	66
Figure 5.16	Damage detection using MCM	66
Figure 5.17	Damage detection using DAM	67
Figure 5.18	Damage detection using MPM	68
Figure 5.19	Damage detection using MCM	68
Figure 5.20	Damage detection using DAM	69
Figure 5.21	Damage detection using MPM	70
Figure 5.22	Damage detection using the MCM	70
Figure 5.23	The schematic representation of the irregular H-shaped structure	71
Figure 5.24	Damage detection using DAM	72
Figure 5.25	Damage detection using MPM	72
Figure 5.26	Damage detection using MCM	73
Figure 5.27	Damage detection using DAM	74
Figure 5.28	Damage detection using MPM	74
Figure 5.29	Damage detection using MCM	75
Figure 5.30	Damage detection using DAM	76
Figure 5.31	Damage detection using MPM	76
Figure 5.32	Damage detection using MCM	77
Figure D.1	Freely suspended beam	126
Figure D.2	Freely suspended beam with holes	127
Figure D.3	Freely suspended H-shaped structure	127
Figure E.1	The FRFs of the undamaged and the three damage cases	128
Figure E.2	The FRFs of the undamaged and the three damage cases	129
Figure E.3	The FRFs of the undamaged and the three damage cases	130
Figure E.4	The FRFs of damage case 1 of example 1	131
Figure E.5	The phase of damage case 1 of example 1	132

Figure E.6	The modes of damage case 1 of example 1	133
Figure F.1	The detailed diagram of a beam used to select reduction/expansion method	134
Figure F.2	The detailed diagram of a beam used in example 1	134
Figure F.3	The detailed diagram of a beam used in example 2	135
Figure F.4	Details of an irregular H-shaped structure used in example 3	135

LIST OF TABLES

Table 3.1	Results obtained from using expansion and reduction methods	32
Table 4.1	The COMAC, MAC_0 and FRFAC results for example 1 before damage.	36
Table 4.2	Table showing natural frequencies in Hz (example 1 before damage)	37
Table 4.3	The COMAC, MAC_0 and FRFAC for damage case 1	38
Table 4.4	Table showing natural frequencies in Hz for damage case 1	39
Table 4.5	The COMAC, MAC_0 and FRFAC for damage case 2	40
Table 4.6	Table showing natural frequencies in Hz for damage case 2	41
Table 4.7	The COMAC, MAC_0 and FRFAC for damage case 3	42
Table 4.8	Table showing natural frequencies in Hz for damage case 3	42
Table 4.9	The COMAC, MAC_0 and FRFAC for undamaged case (example 2)	44
Table 4.10	Table showing natural frequencies in Hz for undamaged case (example 2)	44
Table 4.11	The COMAC, MAC_0 and FRFAC for damage case 1	45
Table 4.12	Table showing natural frequencies in Hz for damage case 1	45
Table 4.13	The COMAC, MAC_0 and FRFAC for damage case 2	46

Table 4.14	Table showing natural frequencies in Hz for damage case 2	46
Table 4.15	The COMAC, MAC_0 and FRFAC for damage case 3	47
Table 4.16	Table showing natural frequencies in Hz for damage case 3	47
Table 4.17	The COMAC, MAC_0 and FRFAC for undamaged case	50
Table 4.18	Table showing natural frequencies in Hz for undamaged case	50
Table 4.19	The natural frequencies in Hz for damage case 1	51
Table 4.20	The COMAC, MAC_0 and FRFAC for damage case 1	51
Table 4.21	Table showing natural frequencies in HZ for damage case 2	52
Table 4.22	The COMAC, MAC_0 and FRFAC for damage case 2	52
Table 4.23	Table showing natural frequencies in Hz for damage case 3	53
Table 4.24	The COMAC, MAC_0 and FRFAC for damage case 3	53

NOMENCLATURE

Basic terms, dimensions, subscripts, matrices, vectors and scalars

i	$\sqrt{-1}$
b	the simplified scalar representing the COMAC
i, j, n, r	integers
ω	frequency of vibration (rad/s)
N	number of modes measured
M	number of frequency points measured, number of constraints equations
$\{F(t)\}$	System force input vector
$\{x\}$	displacement vector
$\dot{\{x\}}$	velocity vector
$\ddot{\{x\}}$	acceleration vector
$\{\varepsilon\}, \varepsilon$	error vector, error scalar
e	Euclidean norm of error
λ	eigenvalue

Subscripts

A	analytical
X	experimental
s	slave
m	master (measured)
R	reduced
S	static
D	dynamic
d	damaged
u	updated
I	IRS method
U	SEREP method

Frequency response properties

$H(\omega)$	frequency response functions
R_{ff}, R_{fx}	Autocorrelation function, cross spectral density
S_{ff}, S_{fx}	power spectral density, cross spectral density
α_{ij}	receptance FRF
$\{X(\omega)\}$	response vector
$[B(\omega)]$	dynamic stiffness matrix

Matrices, vectors and scalars

$[I]$	identity matrix
$[0]$	null matrix
$\{0\}$	null vector
$[]$	matrix
$\{ \}$	column vector
$ $	absolute value or magnitude of a vector
$[]^{-1}$	inverse of a matrix
$[]^{+}$	generalised / pseudo inverse of a matrix
$[]^T, \{ \}^T$	transpose of a matrix; vector (i.e. row vector)
$[]^{*}$	complex conjugate

Material properties

ρ	density
ν	Poisson ratio
α, β	proportional damping coefficients
I	second moment of area
A	cross-sectional area
E	modulus of elasticity

Spatial properties

$[M],[K],[C]$	mass, stiffness, viscous damping matrices
$[M_A]$	analytical/theoretical/predicted/FE mass matrix

[T]	transformation matrix
[S]	matrix used in IRS and contains zeros and the inverse of the slave part of the stiffness matrix

Modal properties

$\{\phi\}, [\phi]$	eigenvector (matrix)
$\{\phi_{\Lambda}\}$	analytical eigenvector
$\{\phi_x\}$	experimental eigenvector
$[\phi]$	modal matrix
$[\Lambda]$	diagonal matrix of eigenvalues

Acronyms

CSD	cross spectral density
COMAC	co-ordinate modal assurance criterion
DAM	D'Ambrogio approach
DOF(s)	degree(s) of freedom
$E(x,y)$	variance between x and y
EMS	expansion using mass and stiffness matrices
EMD	expansion using modal data
FEM	finite element model
FEA	finite element analysis
FRF(s)	frequency response function(s)
FRFAC	frequency response functions assurance criterion
GSR	Guyan static reduction method
GDR	Guyan dynamic reduction method
IRS	improved reduced system
MAC	modal assurance criterion
MAC_0	zero normalised MAC
MPM	modal properties method
MCM	multiple criterion method
MSF	modal scale factor

SEREP

system equivalent reduction expansion
process

1. Introduction

In this study, a multiple criterion updating method is proposed. This method uses measured frequency response functions (FRFs) and extracted modal properties simultaneously to update the finite element model. The method is proposed to solve the problem of uniqueness of the updated finite element model which the methods currently in use cannot solve (Ibrahim *et al.* 1989). It has been argued (Nobari *et al.* 1989), that to enhance the chances of getting a unique solution a number of restrictive conditions must be satisfied. The proposed multiple criterion method satisfies the measured FRFs and modal parameters. Ibrahim *et al.* (1989) uses two sets of structural responses to enforce a unique solution. The responses used were two identical modes.

The proposed method is compared to the methods that use measured FRFs and modal properties. The comparison uses the Modal Assurance Criterion (MAC) (Allemang and Brown, 1982), Co-ordinate Modal Assurance Criterion (COMAC) (Lieven, 1988) and the FRF Assurance Criterion (FRFAC). The FRFAC is a new method which compares two sets of FRFs, and is also proposed as part of this study. The proposed updating method is applied using selective updating method to detect damage on a simple beam, a beam with holes and an irregular H-shaped structure. In this chapter different updating methods are discussed and some are chosen to detect damage on the structure.

The development of modern computers which are capable of processing large matrices has led to the construction of large and sophisticated numerical models. One of these numerical models is the finite element model. The Cooley-Tukey algorithm, and related techniques, which are used to obtain Fourier transformations, has led to the development of sophisticated techniques in experimental modal analysis. The finite element model often gives results that are not the same as the results given by the experiment. The reasons for the discrepancy between finite element model and measured data include the difficulty in modelling damping, joints, welds and edges, and the linear assumption of the finite element model. Due to this discrepancy between measured and finite element data,

techniques have been developed to update the finite element model so that it can predict measured results.

Techniques developed to update the finite element model can be divided into two categories: direct and iterative methods. Direct methods update the finite the element model without any regard to changes in physical parameters. Because of this reason, direct methods tend to give models that represent the measured parameters without any regard to the structure that is being analysed. This results in mass and stiffness matrices that have little physical meaning and cannot be related to physical changes to the finite elements of the original model. Furthermore, the connectivity of the nodes is not ensured and generally the matrices are fully populated and not sparse. When using iterative methods, physical parameters are changed until the finite element model reproduces measured data. Because of this nature of iterative methods, they give finite element models which ensure connectivity of nodes, and have mass and stiffness matrices that have physical meaning. Because of the objective of using the proposed updating method on damage detection, iterative techniques will be applied in this study.

Before we go on with this study, it is advisable to investigate some of the updating methods that have been proposed and applied in the past so that suitable methods may be chosen. These methods are:

Optimal Matrix Modification (Berman et al., 1971)

This method updates the matrix in order to ensure that the modes and frequencies are reproduced.

Lagrange Multipliers (Baruch, 1978)

This method assumes that the mass matrix is correct and updates the stiffness matrix by minimising the distance between the updated and analytical stiffness matrices.

Sensitivity Based Methods (Collins et al., 1974)

These methods utilise the derivatives of eigenvalues and/or eigenvectors with respect to changes in physical and material parameters. These sensitivities are used to calculate changes in the parameters that would force the analysis frequencies and mode shapes to match those that were measured.

Eigenstructure Assignment Techniques (Zimmerman and Widengren, 1990)

In these methods which are based on control system theory, a structure is forced to respond in a predetermined manner. In damage detection the desired eigenstructure is the one that is measured in the test.

Minimum Rank Perturbation Methods (Chen et al., 1983)

In these methods the mass and stiffness matrix are updated using the measured modes and natural frequencies.

Error Matrix Methods (Sidhu and Ewins, 1984)

The error matrix is the difference between measured stiffness or mass matrices and analytical ones. Updating is performed to ensure that the difference between measured and analytical matrices is minimised.

Matrix Mixing Methods (Link, 1986 and Caesar, 1987)

These methods combine the analytical and experimental mode shapes to obtain a complete eigenvector set.

Methods Based on Force Balance (Berger, et al., 1984)

These methods use the analytical mass and stiffness matrices and utilises the force balance method to locate the error given the measured modal properties and natural frequencies.

Statistics and Sensitivity Methods (Collins, et al., 1974)

The variance associated with structural parameters is minimised to determine those that reproduce measured modal properties. From this work sensitivity based methods were developed where an iterative process was used to produce modal properties.

Updating Using Frequency Response Functions (Sestieri and D'Ambrogio, 1989)

The FRFs are measured directly as opposed to modal properties which are extracted from the measured FRFs. Because of this reason, unnecessary errors introduced when modal properties are extracted from measured FRFs. Sestieri and D'Ambrogio in 1989 used the measured FRFs directly to update the finite element model.

From the methods mentioned above, two approaches are chosen. The first approach uses the measured FRFs directly. Sestieri and D'Ambrogio (1989), minimise the equation of error to update the finite element model. The second approach minimises the error

obtained by pre-multiplying the eigenvalue equation by the transpose of the modal vector. Since these two approaches give error vectors, Euclidean norms of these vectors are minimised. The multiple criterion method minimises the sum of the Euclidean norms from these two approaches. Since these errors have different dimensions, the two equations are non-dimensionalised by dividing each one of them by a certain factor. In this study it is assumed that the accuracy of the FRF and modal data is the same. Because of this assumption, the Euclidean norms of errors from the two methods are given equal weighting functions.

The method proposed is tested using real experimental data. The problem faced when comparing experimental data with numerically generated data is incompleteness. The response is measured at limited degrees of freedom and over a limited frequency range. In order to apply this proposed updating technique, two things may be done. Either the measured degrees of freedom may be expanded to the same number as the finite element model or the finite element model can be reduced to the same number of degrees of freedom as the measured ones. In this study all the available expansion and reduction methods are theoretically studied using computer generated data. The reduction methods are the Guyan reduction (Guyan, 1965), dynamic reduction (Paz, 1984), improved reduced system (IRS) (O'Callahan, 1989), and system equivalent reduction expansion process (SEREP) (O'Callahan *et al.*, 1989). The expansion methods are: the expansion using mass and stiffness matrices, and expansion using modal data. From the results, the most suitable method is chosen for use in this study based on the following criterion:

- the cost of each method in terms of speed
- the accuracy of each method
- the stability of each method

Now that the method is fully proposed the next step is to apply this updating technique on damage detection. The sophistication of modern technology has caused structures to be designed to minimise the weight without compromising on the strength. However, the loads that are applied on the structure are usually unknown and consequently structures must be monitored and this information be used to ensure that structures are functioning

within certain safety parameter constraints. To ensure that the monitoring process is implemented for maximum benefit, the data obtained during monitoring process should be utilised to determine whether critical damage has occurred on the structure or not.

For the proposed method to be utilised effectively, it is necessary to investigate the causes of damage. Typical causes of damage are corrosion, erosion, fatigue, wear, creep, time dependent changes in the boundary conditions, impact damage, substandard material and pitting. Some of the areas which often experience damage include spacecraft, composite materials and offshore structures. Some of the causes of damage in spacecraft include fatigue due to long exposure to extreme temperatures and temperature fluctuations of space environment, gravity gradient, aerodynamic, attitude control, and dynamic structural behaviour due to solar winds and impinging particles. Composite materials which are highly desirable when designing structures, experience failures due to debonding between skin and core, and delamination between laminae. Offshore structures experience damage due to chaotic impingement of water waves upon the structures, blowouts, fires, explosions, weather changes, and other time dependent changes.

Having discussed the causes of damage, it is advisable to highlight some of the techniques developed to detect damage. Such techniques rely on monitoring structures after a period of time. The decreasing price of computers and an increase in their computational capabilities, will enable monitoring to be performed on a continual basis. Techniques employed in the past are visual inspection, liquid penetrant inspection, magnetic methods, radiographic techniques, ultrasonic testing, acoustic methods which include vibration, eddy current testing, potential drop techniques, acoustic emission technique, infrared thermography, laser holography and X-ray diffraction.

Now that different methods have been highlighted, the advantages of the proposed multiple criterion method over the other techniques are discussed briefly.

- Damage detection is not limited to a local area

- Since natural frequencies can be measured from sensor located at a single point, access to the whole structure is not necessary
- Because of recent developments in electronic technology, real time analysis of vibration response in frequency and time domain is facilitated.
- Direct exposure of structural elements are not required which is useful for space structures
- Can be applied to composite structures which are finding more usage.

Even though the proposed method has many advantages, it is necessary to summarise some of the problems that the proposed method has. These are:

- It is time consuming and therefore expensive
- Difficult to apply to inaccessible structural components.
- Difficult to quantify the extent of damage.

Despite all these disadvantages, if the proposed method is implemented with several points in mind most of these problems are overcome.

The next issue to be resolved is how the method will be implemented in a computer program. The optimisation toolbox (Grace, 1990) is implemented and all the parameters that have not been accurately modelled are used as design variables in conjunction with a finite element software structural toolbox (Balmès, 1995).

2. Formulation of The Problem

2.1. Introduction

In this study, a multiple criterion updating method is proposed and is used to detect damage on the structure. In order to fully understand how updating is performed it is appropriate to discuss the theoretical foundations of modal analysis.

Any given vibrating structure may be described in terms of three models: spatial, modal and response models. Spatial, modal and response models entail the expression of a dynamic system in terms of mass, damping and stiffness matrices, natural frequencies and mode shapes as well as frequency or impulse response functions respectively. The schematic representation of the routes to vibration analysis is shown in figure 2.1.

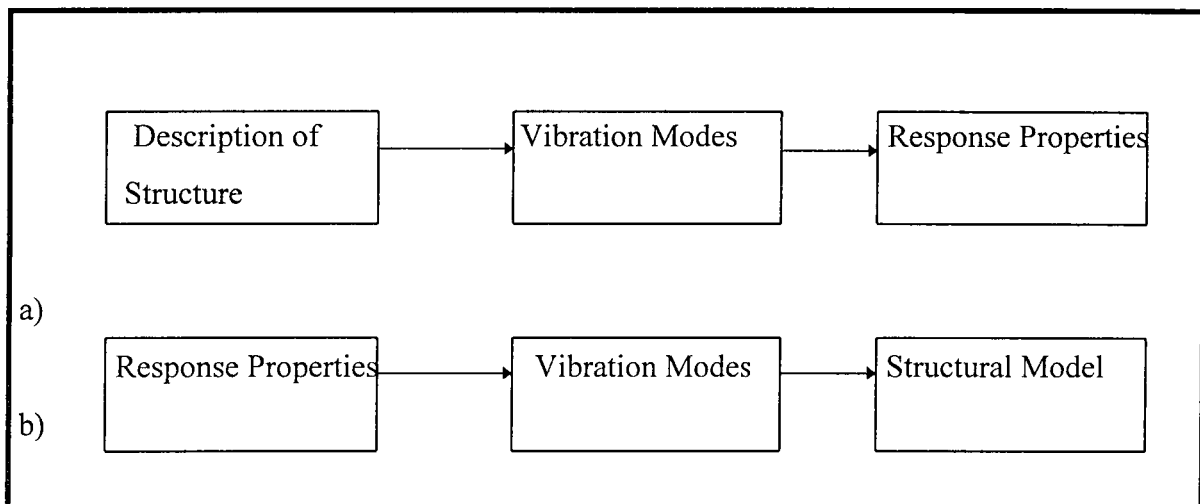


Figure 2.1. (a) and (b) Theoretical and experimental route to vibration (Ewins, 1984)

Figure 2.1 (a) is the theoretical route to vibration analysis. Figure 2.1 (b) is the experimental route to vibration analysis and is called experimental modal analysis. The spatial model is usually obtained from the finite element model (FEM) while the response model is obtained from the experiment. FRFs are measured by artificially exciting the structure and measuring the corresponding responses. The set of FRF measurements may be used to determine the mode shapes at different resonant frequencies. Many methods

have been proposed and successfully used to extract modal properties from measured FRFs.

The measured FRFs and mode shapes have been intensively used in finite element updating, by exploiting their characteristics. FRFs are measured directly, and therefore a considerable amount of labour is saved by using them directly for finite element updating. The problem of updating may also be alternatively approached by using the measured mode shapes and natural frequencies. Even though both methods give the updated finite element model, it often occurs that the solutions that are given by the modal approach are different from the solution which is given by the FRFs approach. This is because the updating techniques do not give a unique solution. If the FRF and modal approaches are used simultaneously, the updated finite element model should reproduce the measured modal properties as well as measured FRFs. In this study, it was assumed that solving the problem of updating from two different perspectives: measured FRFs approach and measured modal properties approach, will increase the chances of obtaining a representative solution.

In this study the measured FRFs will be substituted in the equation of motion obtained from the finite element model and the resulting error will be measured. The Euclidean norm (Burden and Faires, 1995) of the error will be minimised by employing an optimisation procedure and by engaging the physical parameters that are not accurately known as design variables. In the second phase of this work the measured mode shapes and natural frequencies will be substituted into the equation derived from the orthogonality properties where the mass and stiffness matrices from the finite element model will be used. The Euclidean norm error due to the combination of measured mode shapes and natural frequencies with finite element mass and stiffness matrices will be minimised by taking inaccurate physical parameters as design variables. In the third phase of this study the Euclidean norms of errors obtained from the FRF approach and the orthogonality approach will be added using equal weighting functions and the resulting error will be minimised by taking physical parameters as design variables.

The FRF approach will be based on the work done by (D'Ambrogio and Zobel, 1990) while the modal properties approach will be based on the modified version of the orthogonality properties.

2.2. D'Ambrogio Method (DAM)

DAM uses the measured FRFs directly, and therefore eliminates the error that is usually incurred during the extraction of modal properties from measured FRFs. D'Ambrogio and Zobel (1990) use the measured FRFs directly to update the finite element model by updating the stiffness matrices. In this study the stiffness matrices will be updated by varying the physical parameters such as the modulus of elasticity. The process of varying physical parameters will be repeated until the Euclidean norm of the error that is caused by the integration of the experimental results and the FEM computed parameters is minimised. The physical parameter that minimises the Euclidean norm of the error will be used to obtain the new mass and stiffness matrices.

If damage was to occur on the structure, the new FRFs measured will have a Euclidean error norm even though the previously updated physical parameters are used. The physical parameters will then be varied iteratively until the Euclidean norm of the error is minimised. The newly updated physical parameters will be compared with the previously updated physical parameters to localise and quantify damage.

The equation of motion describing the dynamic characteristics of a structure may be obtained using Newton's second law or by employing a suitable energy principle to obtain an N degree-of-freedom viscously damped system:

$$[M]\{\ddot{x}\} + [C]\{\dot{x}\} + [K]\{x\} = \{F(t)\} \quad (2.1)$$

where,

[M] is the inertia matrix

[C] is the damping matrix

[K] is the stiffness matrix

{F(t)} is the forcing function

$\{x\}$, $\{\dot{x}\}$ and $\{\ddot{x}\}$ are the displacement, velocity and acceleration vectors.

The damping matrix will be assumed to be proportional and may be expressed in terms of mass and stiffness matrices as follows:

$$[C] = \alpha[M] + \beta[K] \quad (2.2)$$

Equation 2.1 may be rearranged by taking all terms to the left hand side and may be rewritten as follows:

$$[M]\{\ddot{x}\} + [C]\{\dot{x}\} + [K]\{x\} - \{F(t)\} = \{0\} \quad (2.3)$$

If it is assumed that

$$\{x\} = \{X(\omega)\}e^{i\omega t} \quad (2.4)$$

it follows, by taking the appropriate derivatives, that

$$\{\dot{x}\} = i\omega\{X(\omega)\}e^{i\omega t} \quad (2.5)$$

$$\{\ddot{x}\} = -\omega^2\{X(\omega)\}e^{i\omega t} \quad (2.6)$$

Substituting equations 2.5 and 2.6 into equation 2.3 the equation may be written in the frequency domain as follows:

$$(-\omega^2[M] + i\omega[C] + [K])\{X(\omega)\} - \{F(\omega)\} = \{0\} \quad (2.7)$$

or

$$[B(\omega)]\{X(\omega)\} - \{F(\omega)\} = \{0\} \quad (2.8)$$

where $[B(\omega)]$ is the dynamic stiffness matrix of the structure.

2.2.1 Getting the FRFs

If periodic excitation of a system $\{F(t)\}$ is at co-ordinate i , and the measurement $\{x(t)\}$ is taken at co-ordinate j , then the FRF vector ($\{\alpha_{ij}(\omega)\}$) of such a system may be obtained by performing the Fast Fourier Transform to obtain $\{F(\omega)\}$ and $\{X(\omega)\}$ respectively and then dividing to obtain:

$$\{\alpha_{ij}(\omega)\} = \frac{\{X(\omega)\}}{\{F(\omega)\}} \quad (2.9)$$

For a random excitation the FRFs are obtained by first calculating the auto spectrum of the response and excitation signals and the cross spectrum between these two signals. The autocorrelation (R_{ff}) is defined as the average of the product ($F(t).F(t+\tau)$) computed along the time axis and may be expressed as follows (Ewins, 1986)

$$R_{ff}(\tau) = E[F(t).F(t + \tau)] \quad (2.10)$$

This equation does satisfy the Dirichlet condition for the Fourier transform, unlike $f(t)$ and therefore its Fourier transform equation may be obtained. The Power Spectral Density (PSD) may be calculated by using the following formula:

$$R_{ff}(\omega) = \frac{1}{2\pi} \int_{-\infty}^{\infty} R_{ff}(\tau) e^{-i\omega\tau} d\tau \quad (2.11)$$

A similar approach may be applied for cross correlation and cross spectral density. The cross correlation (R_{fx}) is defined as the average of the product ($F(t).F(t+\tau)$) computed along the time axis and may be expressed as follows

$$R_{fx}(\tau) = E[F(t).F(t + \tau)] \quad (2.12)$$

The Cross Spectral Density (CSD) may be calculated by using the following formula:

$$S_{xf}(\omega) = \frac{1}{2\pi} \int_{-\infty}^{\infty} R_{xf}(\tau) e^{-i\omega\tau} d\tau \quad (2.13)$$

The FRFs may be obtained from equations 2.11 and 2.13 by the following formulae:

$$H(\omega) = \frac{S_{fx}(\omega)}{S_{ff}(\omega)} \text{ or } H(\omega) = \frac{S_{xx}(\omega)}{S_{xf}(\omega)} \quad (2.14)$$

Comparing the two estimates in equations 2.14 provides a means for ensuring that the quality of the FRF data.

In equation 2.7 the $\{X(\omega)\}$ and $\{F(\omega)\}$ are measured quantities. The difficulty with equation 2.7 is that FRFs are measured instead of displacement and force individually. To solve this problem the excitation is assumed white, and hence the vector $\{F(\omega)\}$ has a unit force magnitude at all frequencies, and the displacement is replaced by the FRFs.

If the measured FRFs are substituted into equation 2.3, using the $[M]$, $[C]$ and $[K]$ from the FE model, then there will be an error which will depend on the accuracy of the FE

model. This system error vector may be introduced on the right hand side of equation 2.8 and the resulting equation is

$$[B(\omega)]\{X(\omega)\} - \{F(\omega)\} = \{\varepsilon(\omega)\} \quad (2.15)$$

Due to the cumbersome nature of investigating the elements of the error vector, the Euclidean norm (e) (Burden and Faires, 1995) which is the square root of the sum of the squares of the error vector elements will be used. If the error vector has zero elements, then e will be equal to zero. The equation of e is

$$e = \left(\sum_{j=1}^M |\varepsilon(\omega_j)|^2 \right)^{1/2} \quad (2.16)$$

The stiffness and damping matrices amongst other things depend on the area (A), density (ρ), Poisson ratio (ν) and the modulus of elasticity (E) of each element. By varying one of these physical parameters, e can be minimised. The A , ρ , ν , and E obtained by updating the FEM are called updated parameters.

2.2.2 Damage Detection

When damage is introduced into the system the stiffness and the damping matrices are changed and the new equation may be written as follows:

$$(-\omega^2[M] + i\omega[C_d] + [K_d])\{X(\omega)\} - \{F(\omega)\} = \{\varepsilon\} \quad (2.17)$$

or

$$[B_d(\omega)]\{X(\omega)\} - \{F(\omega)\} = \{\varepsilon\} \quad (2.18)$$

where subscript d refers to damage.

If the FRFs of the damaged system are measured, and are substituted into the updated $[M]$, $[C]$, and $[K]$ matrices of the undamaged structure, then the system will have a non-zero e . The physical parameters which were updated previously may be updated again by changing physical parameters until e is minimised. The updated physical parameters will change. These changes that had to be introduced to the undamaged system to reproduce measured FRFs from the damaged system will be assumed to have resulted from damage.

2.3. Modal Properties Method (MPM)

The measured FRFs may be used for the extraction of measured modal parameters. Some of the methods that are commonly utilised to achieve the conversion, are the peak-picking method and the circle fitting method. The peak-picking method uses the peak of the graph of the FRF magnitude versus frequency to identify the modes. The circle-fitting method uses the geometrical properties of the Nyquist plot to identify the natural frequencies, mode shapes and damping information. Mode shapes have several special properties such as orthogonality. The MPM uses orthogonality approach to update the finite element model. The modified version of the eigenvalue equation will be developed in the next few paragraphs.

If the equation of motion for a dynamic system (equation 2.1) is modified by setting $\{F(t)\}=\{0\}$, then the resulting free vibration equation may be written as follows:

$$[M]\{\ddot{x}\} + [C]\{\dot{x}\} + [K]\{x\} = \{0\} \quad (2.19)$$

Using the differential equation theory, the solution may be assumed to be of the form:

$$\{x\} = \{X(\omega)\}e^{i\omega t} \quad (2.20)$$

By differentiating appropriately equations 2.5 and 2.6 may be obtained. If these equations are substituted into equation 2.19 then the resulting equation

$$(-\omega^2[M] + i\omega[C] + [K])\{x\} = \{0\} \quad (2.21)$$

By substituting $\{X\}=\{\psi\}$

$$(-\omega_j^2[M] + [K])\{\psi_j\} = \{0\} \quad (2.22)$$

Equation 2.22 is a set of simultaneous equations with unknowns ω_j and $\{\psi_j\}$ for $j=1,N$ where N is the number of degrees of freedom. From the theory of differential equations, to obtain the non-trivial equation, the determinant of the coefficient matrix must be equal to zero.

$$|-\omega^2[M] + i\omega[C] + [K]| = 0 \quad (2.23)$$

If equation 2.23 is expanded a polynomial which is in terms of ω is obtained and is called the characteristic equation.

$$a_N\lambda^N + a_{N-1}\lambda^{N-1} + a_{N-2}\lambda^{N-2} + \dots + a_1\lambda + a_0 = 0 \quad (2.24)$$

where $\lambda = \omega^2$

The roots of the polynomial may be solved for ω_j and are called eigenvalues and correspond to the natural frequencies. Using ω_j the non-unique $\{\psi_j\}$ may be obtained. The solutions $\{\psi_j\}$ are called eigenvectors and correspond to mode shapes. Due to their non-uniqueness, eigenvectors $\{\psi_j\}$ have to be scaled. If one of the elements of the vector $\{\psi_j\}$ is given a specific value, then the vector has a unique value. The process of scaling modal vector to obtain a unique vector is called normalisation. When the mass matrix is pre-multiplied by a transpose of the normalised vector and post-multiplied by a normalised vector, then the modal mass is obtained. When the stiffness matrix is pre-multiplied by a transpose of the normalised vector and post-multiplied by a normalised vector, then the modal stiffness is obtained.

$$\{\psi_j\}^T[M]\{\psi_j\} = m_j \text{ and } \{\psi_j\}^T[K]\{\psi_j\} = k_j \quad (2.25)$$

If equations 2.25 are scaled such that $m_j=1$, then the vector $\{\psi_j\}$ becomes orthonormalised and may be replaced by $\{\phi_j\}$, and the new equation is:

$$\{\phi_j\}^T[M]\{\phi_j\} = 1 \text{ and } \{\phi_j\}^T[K]\{\phi_j\} = \omega_j^2 \quad (2.26)$$

By setting $\{\psi_j\}=\{\phi_j\}$ in equation 2.22 then,

$$(-\omega_j^2[M]+[K])\{\phi_j\} = 0 \quad (2.27)$$

If equation 2.26 is pre-multiplied by $\{\phi_j\}^T$ then the resulting expression is

$$\{\phi_j\}^T(-\omega_j^2[M]+[K])\{\phi_j\} = 0 \quad (2.28)$$

This equation may be rewritten as follows:

$$\omega_j^2\{\phi_j\}^T[M]\{\phi_j\} = \{\phi_j\}^T[K]\{\phi_j\} \quad (2.29)$$

When an experiment is conducted and modal properties of the system are extracted from the measured FRFs, it is often the case that the measured properties differ with the finite element predictions (Friswell and Mottershead, 1995). The measured modal properties, the mass and the stiffness matrices from the finite element model may be substituted in equation 2.29. In this case the left hand side of equation 2.29 is often different from the right hand side. Because of this reason, equation 2.29 may be written in terms of an error scalar ε as follows:

$$\varepsilon_j = \omega_j^2 \{\phi_j\}^T [M] \{\phi_j\} - \{\phi_j\}^T [K] \{\phi_j\} \quad (2.30)$$

Equation 2.30 gives an error for a given measured mode j . If more than one modes are measured then the e (see equation 2.16) of all the measured modes may be computed.

Since the mass and stiffness matrices depend on the modulus of elasticity and other parameters, these parameters may be varied iteratively thereby updating the mass and stiffness matrices until the e is minimised. The physical parameters that will give rise to the minimum e will give the updated finite element model.

2.3.1 Damage Detection

The idea of using changes in modal properties to detect damage has been used by many researchers (Cawley and Adams, 1979; Rizos *et al.*, 1990; Ju and Mimovitch, 1988; Wolff and Richardson, 1989). If damage is introduced on the system, the modal properties will change. If the modal properties are substituted together with updated matrices, then e will be non-zero. The stiffness matrices may be updated again by varying the physical parameters until the e is minimised. The discrepancy between the previously updated parameters and the newly updated parameters will be assumed to have resulted from the presence of damage.

2.4. Multiple Criterion Method (MCM)

The method based on the DAM and MPM work well except for the fact that they do not give a unique solution. In order to increase the probability of obtaining a unique solution a new method which will be the combination of the two methods will be used. The error obtained in equations 2.18 and 2.30 may be combined together using equal weighting functions to obtain the equation.

$$\varepsilon = \sum_{j=1}^M \left| [B(\omega_j)] \{X(\omega_j)\} - \{F(\omega_j)\} \right| + \sum_{j=1}^N [\omega_j^2 \{\phi_j\}^T [M] \{\phi_j\} - \{\phi_j\}^T [K] \{\phi_j\}] \quad (2.31)$$

where M is the number of frequency points measured and N is the number of modes measured.

It was discovered that the method works better if a normalisation factor is introduced to equation 2.30.

$$\varepsilon = \frac{\sum_{j=1}^M \left| [\mathbf{B}(\omega_j)] \{X(\omega_j)\} - \{F(\omega_j)\} \right|}{f_1} + \frac{\sum_{j=1}^N [\omega_j^2 \{\phi_j\}^T [\mathbf{M}] \{\phi_j\}] - [\{\phi_j\}^T [\mathbf{K}] \{\phi_j\}]_j}{f_2} \quad (2.32)$$

where

$$f_1 = \sum_{j=1}^M \left| [\mathbf{B}_0(\omega)] \{X_0(\omega)\}_j - \{F(\omega)\}_j \right| \quad (2.33)$$

and

$$f_2 = \sum_{j=1}^M [\omega_{0j}^2 \{\phi_{0j}\}^T [\mathbf{M}] \{\phi_{0j}\}] - [\{\phi_{0j}\}^T [\mathbf{K}_0] \{\phi_{0j}\}] \quad (2.34)$$

In equations 2.33 and 2.34 the subscript 0 indicates the parameters of the initial design variables of the optimisation technique.

Equation 2.32 is minimised subject to the following constraint

$$[\mathbf{K}]^T - [\mathbf{K}] = [0] \quad (2.35)$$

which ensures that the stiffness matrix remain symmetrical.

The design variable which was used in this optimisation problem is the modulus of elasticity of each element.

2.5 Conclusion

Several techniques will be required to solve the MCM. These techniques will be fully discussed in the next chapter.

This study will satisfy the following objectives:

- The method proposed will be implemented in a computer program that will utilise the Structural Dynamics Toolbox (Balmès, 1994), and Optimisation Toolbox (Grace, 1990) which run in a MATLAB environment.
- The updating problem will be solved using D'Ambrogio; Modal Properties and Multiple Criterion approaches, and the results will be compared.
- The new method will be applied on the simple beam, a beam with holes and an irregular H-shaped structure.

3. Computational Techniques

3.1 Introduction

In order to successfully complete this study, several computational techniques need to be fully analysed. The first logical issue to be resolved in updating, is making the comparison between experimental and computational results. To make this comparison, several techniques have been developed and successfully used. Most of these methods use the modal properties to make the comparison. Since mode shapes are extracted from measured FRFs, methods using FRFs for comparison purposes save time and money. As part of this study, a new technique was proposed in the previous chapter and uses the measured FRFs and modal properties to update the finite element model to the measured data. Several methods have been developed to compare experimental and computational results. These methods will be discussed in detail in the following sections. All comparison methods that have been developed so far, use the modal properties and not measured FRFs directly. In this work a new method that uses the FRFs directly was fully developed and is called the Frequency Response Functions Assurance Criterion (FRFAC). This method will be fully explained in the next few sections.

The new updating technique introduced in the previous chapter will not be complete unless it is evaluated by using experimental results. The experimental and computational results are incompatible in the sense that the measured modes and co-ordinates are less than the computed modes and co-ordinates. Consequently, techniques that may be used to either reduce the computational results to the same number of degrees of freedom or expand the measured degree of freedom, to the computed results have been developed and will be explained in this chapter. These methods are programmed to determine the most effective ones when the new updating technique introduced in the previous chapter is used.

The problem that was developed in the previous chapter is an optimisation problem. The MATLAB Optimisation Toolbox (Grace, 1990) is implemented to solve the problem.

This toolbox uses a Sequential Quadratic Programming procedure and the procedure will be discussed in this chapter.

3.2. Comparison of Experiment and Prediction

The most important aspect of modal testing is the comparison between the computed dynamic properties and those actually observed in practice. This process is often referred to as 'validating' a theoretical model and it involves several steps. The first step is to compare the specific dynamic properties, measured vs. predicted. The second step is to quantify the extent of the differences (or similarities) between the two sets of data. The third phase is to bring the theoretical model closer to the measured data. When this is achieved, the theoretical model is said to have been updated. In this section we will take a closer look at the computational techniques used in the first, second and third stages.

In most cases a great deal of effort goes into deriving the theoretically based model on one hand, and the experimentally derived model on the other hand. Because of this reason, it is sensible to make as many different levels of comparison as possible. In the previous chapter it was discussed that the dynamic model of a structure may be classified into *Spatial*, *Modal*, and *Response* models. It now becomes convenient to return to this classification and try to make the comparison between the experiment and the theoretical model at each of these. Therefore we shall make comparisons of response properties as well as modal properties. Comparisons between spatial properties are difficult and shall therefore not be considered.

In using whichever medium of comparison, the model will have to be developed extensively from the original form. In conclusion it is recommended that as many different methods of comparison should be used as possible.

3.2.1 Direct Comparison

A) Comparisons of Natural Frequencies

The easiest mode of comparison between the experimental and theoretical model is by comparing the natural frequencies. This may be done by tabulating the experimental and theoretical natural frequencies. The most convenient way of comparison is to plot the graph of the experimental natural frequencies against the analytical ones for all available modes. If the slope of the best straight line passing through the points is close to zero, then the correlation between the experiment and computed model is good. If the points lie scattered widely about a straight line, then there is a serious failure of the model in representing the theoretical model's ability to predict the measured natural frequencies and consequently the theoretical model should be re-evaluated. If the points deviate slightly from the straight line but in a systematic fashion, then this situation suggests that there is a specific characteristic responsible for the deviation. The comparison between natural frequencies is illustrated by figure 3.1. (Ewins, 1984)

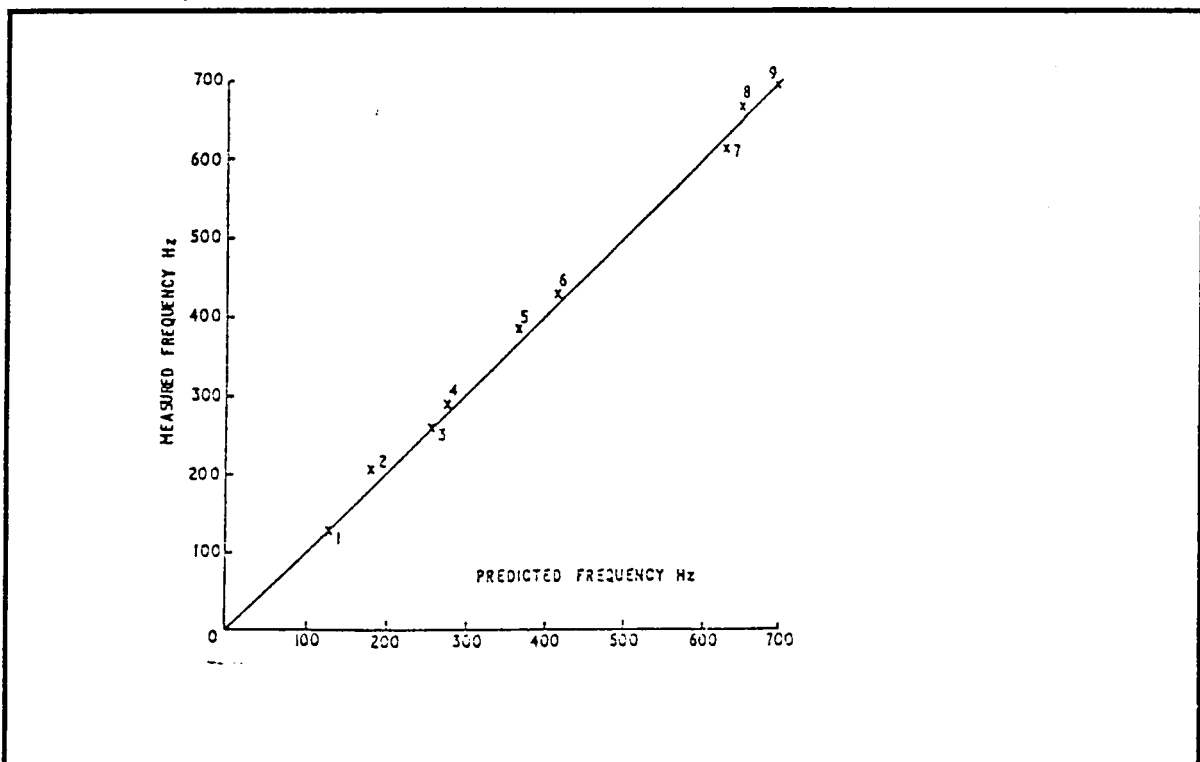


Figure 3.1 Comparison between experimental and analytical natural frequencies

B) Comparisons of Mode Shapes

The mode shapes may also be compared by plotting the analytical modes against the experimental ones. For a simple structure with well separated modes, this method of comparison may be used very easily. However, for a complicated structure with modes that are close to one another this method often becomes difficult to implement. Therefore it is appropriate to make comparisons of mode shapes at the same time as those of the natural frequencies.

In the case where we have more data to handle for each mode, the comparison may be done by plotting the deformed shape for each model, experimental and theoretical, overlaying one plot on another. The disadvantage of this method is that even though the differences show up, they are difficult to interpret and plots are often confused because there is so much information. A convenient method of comparison which is along the lines of the natural frequency plot, is to plot each element in the mode shape vector, experimental and theoretical, on an x-y plot as shown in Graphs 3.2. a and b from (Ewins, 1984).

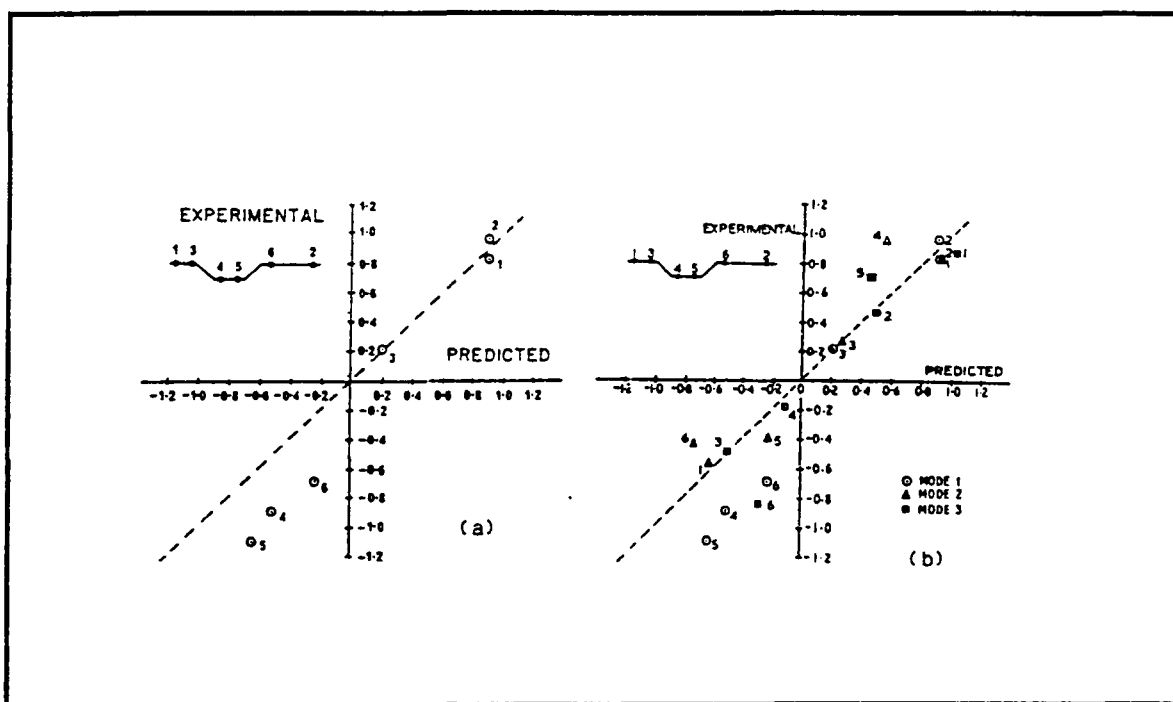


Figure 3.2. (a) Comparison of measured and predicted mode shapes for single mode (b) Three Modes

The individual points on this graph relate to modal co-ordinates, and it is expected that they should lie close to a straight line. If the mode shape vectors are mass-normalised, this straight line should have a slope of ca. 1. If the points lie close to a straight line with a slope that is not ca. 1 then either one of the mode shapes is not mass-normalised or there is scaling error in the data. If the points are widely scattered about the line, then there is inaccuracy in one or the other set. If the scatter is excessive, then it may be that the eigenvectors that are being compared do not relate to the same mode.

The slope of the best straight line, passing through the points plotted in figure 3.2. is called the Modal Scale Factor and is defined as (Ewins, 1991):

$$\text{MSF}(\phi_a, \phi_m) = \frac{\{\phi_a\}^T \{\phi_m\}}{\{\phi_a\}^T \{\phi_a\}} \quad (3.1)$$

where $\{\phi_a\}$ and $\{\phi_m\}$ are the analytical and experimental mode shape vectors respectively.

This parameter gives no indication of the quality of the measured points with respect to the straight line fit.

3.2.2 The Use of Frequency Response Functions (FRFAC)

The advantage of using FRFs directly is that they are measured directly. The easiest way in which measured FRFs may be compared to the computed FRFs is by plotting the measured and theoretical FRFs in one graph as shown in figure 3.3 (Ewins, 1984)

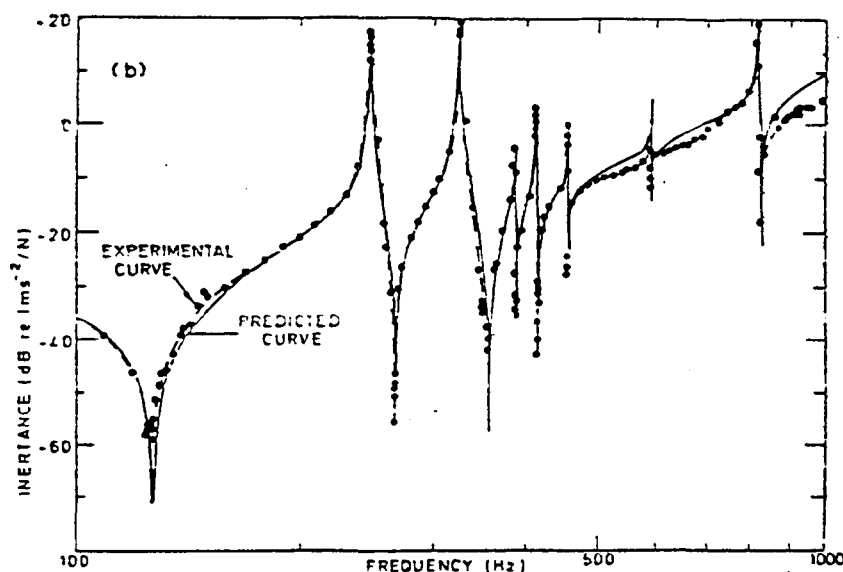


Figure 3.3 Experimental and analytical FRFs

Since for particular FRF measurements there are many measurements to be compared, it becomes necessary to introduce a scalar factor (FRFAC) that gives the correlation between measured and theoretical FRFs. This new scalar factor was developed specifically for this work and uses the measured FRFs directly:

$$\text{FRFAC} = \frac{\left(\sum_{j=1}^M \sum_{n=1}^N |H_a(n, j)| \right)}{\left(\sum_{j=1}^M \sum_{n=1}^N |H_m(n, j)| \right)} \quad (3.2)$$

where N is the number of degrees of freedom; j is the number of the measured frequency; H_m is the measured FRF; and H_a is the analytical FRF.

A FRFAC of 1 indicates that the measured FRFs perfectly reflects the analytical FRFs; the FRFAC which is greater than 1 indicates that the magnitude of the analytical FRF is on average greater than the experimental ones and the FRFAC which is less than 1 indicates that the magnitude of the experimental FRF are on average greater than the analytical ones.

The ability of the FRFAC to give the correlation between experimental and theoretical FRFs is investigated carefully in this chapter.

3.2.3. The Modal Assurance Criterion (MAC)

The MAC compares the measured and the computed mode shapes and can be summarised by the following equation (Allemang and Brown, 1982):

$$\text{MAC}_{jk} = \frac{|\phi_{mj}^T \phi_{ak}|^2}{(\phi_{ak}^T \phi_{ak})(\phi_{mj}^T \phi_{mj})} \quad (3.3)$$

The MAC is a measure of the least squares deviation of the points from the straight line correlation. A value close to 1 suggests that the two mode shapes are well correlated, while a value close to 0 indicates that the mode shapes are not correlated. If equation 3.3 is substituted by a mode shape vector, then the MAC becomes an identity matrix. Due to

the graphical nature of investigating the MAC matrix an expression which is a simplification of the MAC may be defined as follows:

$$[MAC_0] = [I] - [MAC] \quad (3.4)$$

where $[I]$ is the identity matrix.

If the modal vectors that are being analysed are a perfect correlation then the matrix $[MAC_0]$ will have zero entries. A factor which is the sum of the squares of the elements of $[MAC_0]$ may be defined as follows:

$$MAC_0 = \sum_j \sum_i^1 MAC_{0ij}^2 \quad (3.5)$$

If the scalar MAC_0 is equal to zero, then the two mode shape vectors are well correlated. The shortcoming with this method is that it does not discriminate between random scatter being responsible for the deviations or systematic deviations. The main causes of less than perfect MAC results are: non-linearity in the test structure, noise on the measured data and poor modal analysis of the measured data.

3.2.4 The Co-ordinate Modal Assurance Criterion (COMAC)

The COMAC method is based on the same principle as the MAC, and is essentially an indication of the correlation between the measured and the computed mode shapes for a given common co-ordinate. The COMAC for co-ordinate j is given by (Lieven and Ewins, 1988).

$$COMAC(j) = \frac{\left(\sum_{r=1}^L |(j\phi_{ar})(j\phi_{mr}^*)| \right)^2}{\sum_{r=1}^L (j\phi_{ar})^2 \sum_{r=1}^L (j\phi_{mr}^*)^2} \quad (3.6)$$

Unlike the MAC, the COMAC does not have any difficulty comparing modes that are close in frequency or that are measured at insufficient transducer locations. L is the total number of well-correlated modes as indicated by the MAC. A value close to 1 suggests good correlation. If the mode shape vectors are used then the COMAC becomes a vector.

For a perfect co-ordinate correlation, the entries of the COMAC vector are all equal to 1. The product of the elements of the entries of the vector may be defined as follows:

$$b = \prod_{i=1}^N \text{COMAC}(i) \quad (3.7)$$

where N is the number of measured co-ordinates, and the \prod represent the following multiplication:

$$b = \text{COMAC}(1) \times \text{COMAC}(2) \times \dots \times \text{COMAC}(N) \quad (3.8)$$

3.3 Model Expansion and Reduction Procedures

Two approaches may be pursued to ensure that the measured co-ordinates and modes are equal to the computed ones and these are:

- The experimental data may be expanded to the same number of degrees of freedom as the computed ones.
- The computed results may be reduced to the same number of co-ordinates as the measured ones.

Several techniques may be employed and as part of this study, the methods are programmed and their effectiveness are evaluated with respect to each method. The reduction methods applied are: Guyan Static Reduction Method, Guyan Dynamic Reduction Method, Improved Reduced System (IRS) and System Equivalent Reduction Expansion Process (SEREP). The expansion methods applied are: expansion using mass and stiffness matrices and expansion using modal data

3.3.1 Model Reduction

A) Guyan Static Reduction Method (GSR)

In this method the state and force vectors, $\{x\}$ and $\{f\}$, and the mass and stiffness matrices $[M]$ and $[K]$ are partitioned into the measured (master) and unmeasured (slave) co-ordinates.

$$\begin{bmatrix} [M_{mm}] & [M_{ms}] \\ [M_{sm}] & [M_{ss}] \end{bmatrix} \begin{Bmatrix} \ddot{x}_m \\ \ddot{x}_s \end{Bmatrix} + \begin{bmatrix} [K_{mm}] & [K_{ms}] \\ [K_{sm}] & [K_{ss}] \end{bmatrix} \begin{Bmatrix} x_m \\ x_s \end{Bmatrix} = \begin{Bmatrix} f_m \\ 0 \end{Bmatrix} \quad (3.9)$$

where the subscripts m and s correspond to master and slave co-ordinates respectively.

The inertia terms are neglected to obtain the equation

$$[K_{sm}]\{x_m\} + [K_{ss}]\{x_s\} = \{0\} \quad (3.10)$$

This equation may be used to eliminate the slave co-ordinate to remain with the following equation (Guyan, 1965):

$$\begin{Bmatrix} x_m \\ x_s \end{Bmatrix} = \begin{bmatrix} [I] \\ -[K]_{ss}^{-1}[K_{sm}] \end{bmatrix} \{x_m\} = [T_s]\{x_m\} \quad (3.11)$$

The T_s denotes the static transformation between full state vector and master co-ordinates.

The reduced mass $[M_R]$ and stiffness $[K_R]$ matrices are as follows:

$$[M_R] = [T_s]^T [M] [T_s] \quad (3.12)$$

and

$$[K_R] = [T_s]^T [K] [T_s] \quad (3.13)$$

The frequency response function generated by the reduced mass matrices are exact at zero frequency because the inertia matrices were neglected.

B) Guyan Dynamic Reduction Method (GDR)

The *Guyan Static Reduction* method neglected the effects of inertia. The Guyan dynamic reduction method takes the inertia effect into account, assuming a particular frequency. The choice of frequency affects the accuracy of the reduced model. In the dynamic reduction method the mass and stiffness matrices are partitioned into slaves and master co-ordinates. The modified transformation matrices are as follows (Paz, 1984):

$$\begin{Bmatrix} x_m \\ x_s \end{Bmatrix} = \begin{bmatrix} [I] \\ -([K_{ss}] - \omega^2 [M_{ss}])^{-1} ([K_{sm}] - \omega^2 [M_{sm}]) \end{bmatrix} \{x_m\} = [T_D]\{x_m\} \quad (3.14)$$

The transformation may then be used in the same way as the static transformation, $[T_s]$, to obtain the reduced mass and stiffness matrices similar to equations 3.12 and 3.13.

C) Improved Reduced System (IRS)

The IRS is an improvement of the Guyan static reduction method. This method uses the transformation, the reduced mass and stiffness matrices from the Guyan reduction method together with the [S] matrix which is made out of the zeros and the inverse of the slave partition of the stiffness matrix, to obtain a new transformation matrix (O'Callahan, 1989):

$$[T_I] = [T_S] + [S][M][T_S][M_R]^{-1}[K_R] \quad (3.15)$$

are

$$[S] = \begin{bmatrix} [0][0] \\ [0][K_{SS}]^{-1} \end{bmatrix} \quad (3.16)$$

Friswell *et al.*, (1994) extended this method by introducing the iterated IRS method that converges to the same transformation as the SEREP.

D) System Equivalent Reduction Expansion Process (SEREP)

The System Equivalent Reduction Expansion Process (SEREP) (O'Callahan *et al.*, 1989) partitions the analytical mode shapes into measured and unmeasured co-ordinates, and obtains the transformation by multiplying that with the generalised pseudo inverse (see equations 3.17 and 3.18).

$$\{\phi\} = \begin{bmatrix} \phi_m \\ \phi_s \end{bmatrix} \quad (3.17)$$

$$[T_U] = \{\phi\}\phi_m^+ \quad (3.18)$$

where

$$\phi_m^+ = (\phi_m^T \phi_m)^{-1} \phi_m^T \quad (3.19)$$

The transformation may then be used in the same way as the static transformation, [T_S], to obtain the reduced mass and stiffness matrices similar to equations 3.12 and 3.13.

3.3.2 Model Expansion

A) Expansion using Mass and Stiffness Matrices (EMS)

This method is in essence the inverse of the Guyan reduction method. Suppose ω_{mj} and ϕ_{mj} are the measured natural frequencies and mode shapes of co-ordinates i . Then the mass and the stiffness matrices from the finite element analysis may be partitioned into measured and unmeasured co-ordinates. The equation of motion may then be written as follows:

$$\begin{pmatrix} -\omega_{mj}^2 \begin{bmatrix} [M_{mm}] & [M_{ms}] \\ [M_{ms}] & [M_{ss}] \end{bmatrix} + \begin{bmatrix} [K_{mm}] & [K_{ms}] \\ [K_{ms}] & [K_{ss}] \end{bmatrix} \end{pmatrix} \begin{Bmatrix} \phi_{mj} \\ \phi_{sj} \end{Bmatrix} = \begin{Bmatrix} 0 \\ 0 \end{Bmatrix} \quad (3.20)$$

where ϕ_{sj} represents the mode shape at the slave or the unmeasured co-ordinates. By rearranging the lower part of the matrix equation produces a solution for the unknown part of the measured mode shape vector. Thus

$$\{\phi_{sj}\} = -(-\omega_{mj}^2 [M_{ss}] + [K_{ss}])^{-1} (-\omega_{mj}^2 [M_{sm}] + [K_{sm}]) \{\phi_{mj}\} \quad (3.21)$$

Other estimates of the unmeasured degrees of freedom may be obtained by using the upper part of equation 3.16. This calculation will involve the pseudo inverse; using the upper part is satisfactory if the number of measured degrees of freedom exceeds the number of unmeasured degrees of freedom. Similarly, the unmeasured FRF may be calculated using the following equation:

$$\{H_{sj}\} = -(-\omega_{mj}^2 [M_{ss}] + [K_{ss}])^{-1} (-\omega_{mj}^2 [M_{sm}] + [K_{sm}]) \{H_{mj}\} \quad (3.22)$$

The details on how equation 3.22 is obtained may be viewed in the appendix B.

B) Expansion using Modal Data (EMD)

This method uses the modal data obtained from the finite element model to estimate the modes at the unmeasured degrees of freedom. The measured modes are assumed to be a linear combination of the analytical modes at measured degrees of freedom and a transformation T as indicated by the following equation:

$$\{\phi_m\} = [\phi_a]_m [T] \quad (3.23)$$

where $[\phi_a]_m$ represents the analytical mode shapes at measured degrees of freedom.

Applying the pseudo inverse to equation 3.23 gives the transformation as:

$$[T] = [\phi_a]_m^+ \{\phi_m\} \quad (3.24)$$

where + indicates the pseudo inverse. This transformation may be used to estimate the modes at unmeasured degrees of freedom from the finite element analysis. It may also be used to smooth out the measured modes. Thus

$$\{\phi_m\}_{\text{smoothed}} = [\phi_a]_m [T] \quad (3.25)$$

$$\{\phi_s\} = [\phi_a]_s [T] \quad (3.26)$$

where $[\phi_a]_s$ represents the analytical mode shapes at the unmeasured degrees of freedom. The transformation may be obtained by using only the analytical modal data or the combination of measured and analytical data. This method is like the inverse of the SEREP method. Similarly the measured FRFs may be expanded and the details for such an expansion may be viewed in the appendix B.

3.4 Optimisation

In an optimisation problem, some function is minimised subject to certain bounds and constraints. To illustrate this a mathematical expression may be written as follows:

$$\text{minimise } f(\{x\}) \quad (3.27)$$

$$\text{subject to } g_i(\{x\}) < 0 \quad (3.28)$$

$$\text{where } \{a\} < \{x\} < \{b\} \quad (3.29)$$

The function to be minimised is $f(\{x\})$; the design variables are the vector $\{x\}$; the constraint equations are $g_i(\{x\}) < 0$ (where $i=1:M$ and M is the number of constraint equations) and the bounds are defined as vector $\{x\}$ being between vectors $\{a\}$ and $\{b\}$.

The initial design parameters have to be chosen carefully because they influence the accuracy of the answer. This improves the efficiency of the execution and helps locate a global minimum instead of a local minimum. Optimisation problems may take many iterations to converge and are sensitive to numerical problems such as truncation and round-off errors in the calculation of finite difference gradients.

The quadratic sequential programming which is implemented in the Optimisation Toolbox (Grace, 1990) which runs on MATLAB uses a quadratic cost function and linear constraints.

3.5 Comparison of Methods

Having discussed the computational tools, the next step is to apply the computational procedures using a simple structure. The structure chosen for this study is a simple beam (see figure 3.4). The details of the beam are shown in figure F.1 (appendix F).

The finite element model of the beam was obtained using the *Structural Toolbox* (Balmès, 1995) which runs in a MATLAB environment. The 'measured' data was computationally simulated through the Structural Toolbox. The 'measured' data had fewer degrees of freedom, than the finite element data. Consequently, the finite element data was reduced to the same number of degrees of freedom as the 'measured' data. All the reduction procedures discussed above were implemented. The other approach was to expand the 'measured' data to the same number of degrees of freedom as the finite element data. All the expansion methods discussed above were implemented in order to select one good expansion or reduction method. To achieve this computationally simulated experimental data was used to update the finite element method using different expansion or reduction techniques and their effectiveness was evaluated using the popular comparisons MAC; COMAC and the newly proposed FRFAC.

The 'experimental' FRFs were obtained by modelling the beam in figure 3.4 with a modulus of elasticity of 7.0×10^{10} MPa for each element. The beam was divided into 10 elements and the modulus of elasticity of each element was used as a design variable. The initial design variable for each element in the finite element model was 3.0×10^{10} MPa. The initial design variables were used to obtain the initial finite element model.

All the reduction and expansion methods were implemented in the program. The simulated FRFs were used to extract the ‘measured’ modal properties. The ‘measured’ FRFs and modal properties were incorporated into the MCM, the DAM and the MPM. The results obtained from each method were used to generate the updated FRFs and modal properties. The ‘measured’ FRFs and modal properties were compared to the FRFs and modal properties of the initial finite element model and that of the updated finite element model by applying the FRFAC, the COMAC and the MAC_0 . The results of the comparisons are shown in table 3.1. Also shown in table 3.1 are the number of iterations and the magnitude of the objective function at the optimum point.

From this study it was found that the reduction methods are more reliable than the expansion methods. This is because the expansion methods are more computationally intensive than the reduction methods. It was found that the SEREP method tends to be unstable by giving the inertia and stiffness matrices that are close to singular especially if the design variables are not scaled properly. The rest of the study utilises the IRS procedures to reduce the finite element results. The FRFAC before updating was on average 0.7046 and after updating it was close to 1. It was also found that the results given by the three methods DAM, MPM and MCM were good and therefore the three approaches were successfully able to update the simulated data.

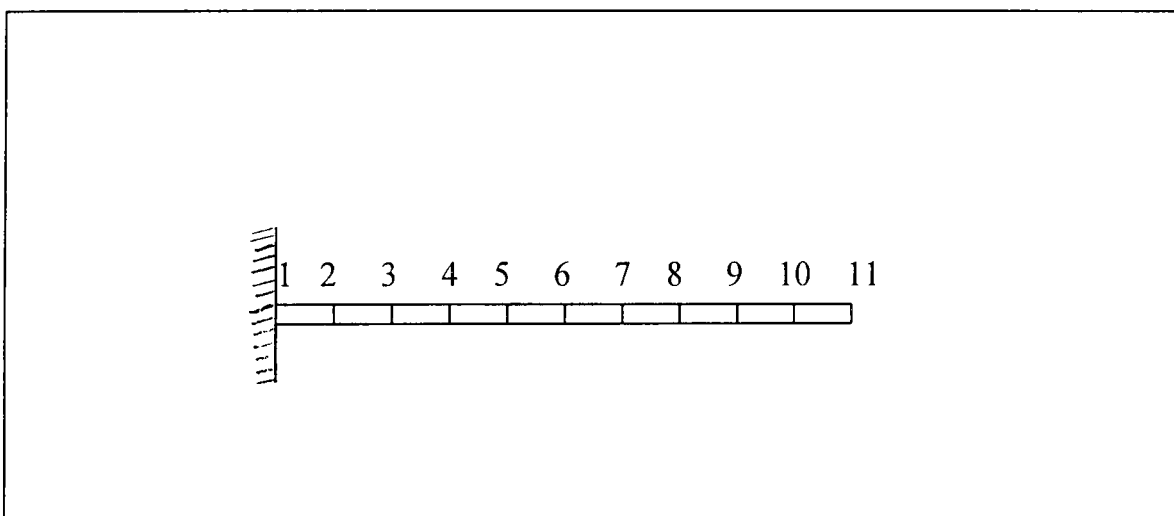


Figure 3.4 The schematic diagram of a beam which is fixed at the end

Table 3.1 Results obtained from using expansion and reduction methods

Method	No. of iterations	Objective functions	FRFAC	MAC ₀	COMAC
GSR and DAM	298	2.1930	1.0050	0.0980	1.0000
GSR and MPM	1148	3.7730	0.9931	0.0980	0.9996
GSR and MCM	612	9.1390	1.0212	0.0990	1.0000
GDR and DAM	552	3.8760	1.0014	0.0980	1.0000
GDR and MPM	1235	1.0645	1.0060	0.0980	1.0000
GDR and MCM	481	6.7220	1.0203	0.0990	1.0000
IRS and DAM	457	2.7220	1.0110	0.0980	1.0000
IRS and MPM	898	0.2720	1.0330	0.0990	0.9996
IRS and MCM	324	5.00	1.0201	0.0990	1.0201
SEREP and MPM	171	6.0E-11	0.9761	0.1007	0.9761
SEREP and DAM	324	4.397	1.0200	0.0992	1.0200
SEREP and MCM	670	288.773	0.9464	0.0995	0.9464
EMS and DAM	598	22.9130	1.0149	0.0980	1.0000
EMS and MPM	1248	13.7370	0.9824	0.0970	0.9996
EMS and MCM	812	19.9310	1.0234	0.0998	1.0000
EMD and DAM	493	50.378	1.0100	0.0998	1.0230
EMD and MPM	781	6.092	0.9861	0.1027	0.9869
EMD and MCM	524	14.937	1.0300	0.0998	1.0224

4. Updating of Finite Element Model

4.1. Introduction

In this study, a new multiple criterion optimisation method (MCM) was formulated. This method incorporates the measured FRFs and identified modal properties. In this chapter this method is tested using three different examples; a beam, a beam with holes and an irregular H-shaped structure. The proposed method is compared with the D'Ambrogio method (DAM) and Modal Property Method (MPM) using the Modal Assurance Criterion (MAC), Co-ordinate Modal Assurance Criterion (COMAC), and the Frequency Response Function Assurance Criterion (FRFAC).

The MAC is the measure of the least square deviation of the points from the expected straight line obtained when experimentally measured mode shape is compared to the theoretically predicted one. The MAC_0 however is a theoretical simplification of the MAC (see equation 3.5) and is obtained by setting the MAC to zero. A MAC_0 value of zero indicates that the least squares deviation of the points from the straight line is zero (perfect correlation).

The COMAC method is based on the same principle as the MAC. It is essentially an indication of the correlation between the measured and the computed mode shapes for a given common co-ordinate. The COMAC scalar of 1 represents a perfect correlation between measured modal co-ordinates and the theoretically predicted ones.

The FRFAC is a proposed method used for comparing the FRFs. This criterion gives the ratio between the magnitudes of the analytical FRFs to the magnitudes of the measured FRFs. The FRFAC of 1 indicates that the measured FRFs are the same as the analytical FRFs.

In this chapter the experimental data are used to update the FEM by using the DAM approach. Thereafter, modal analysis is used to identify modal properties from measured FRFs. The MPM is then used to update the FEM. The proposed MCM

that uses the measured FRFs and modal approach simultaneously is used to update the FEM. Examples used are a simple beam; a complex beam with holes and therefore difficult to model; and an irregular H-shaped structure. The summary of this chapter may be viewed in the diagram in figure 4.1.

In this chapter results are presented in tabular form and the corresponding graphs are demonstrated in Appendix E. A tabular comparison is made using COMAC, MAC_0 and FRFAC between the theoretically predicted data and measured data before and after updating. Furthermore, the natural frequencies before and after updating are compared for each damage case. All these comparisons are made to evaluate the effectiveness of the DAM, MPM and MCM.

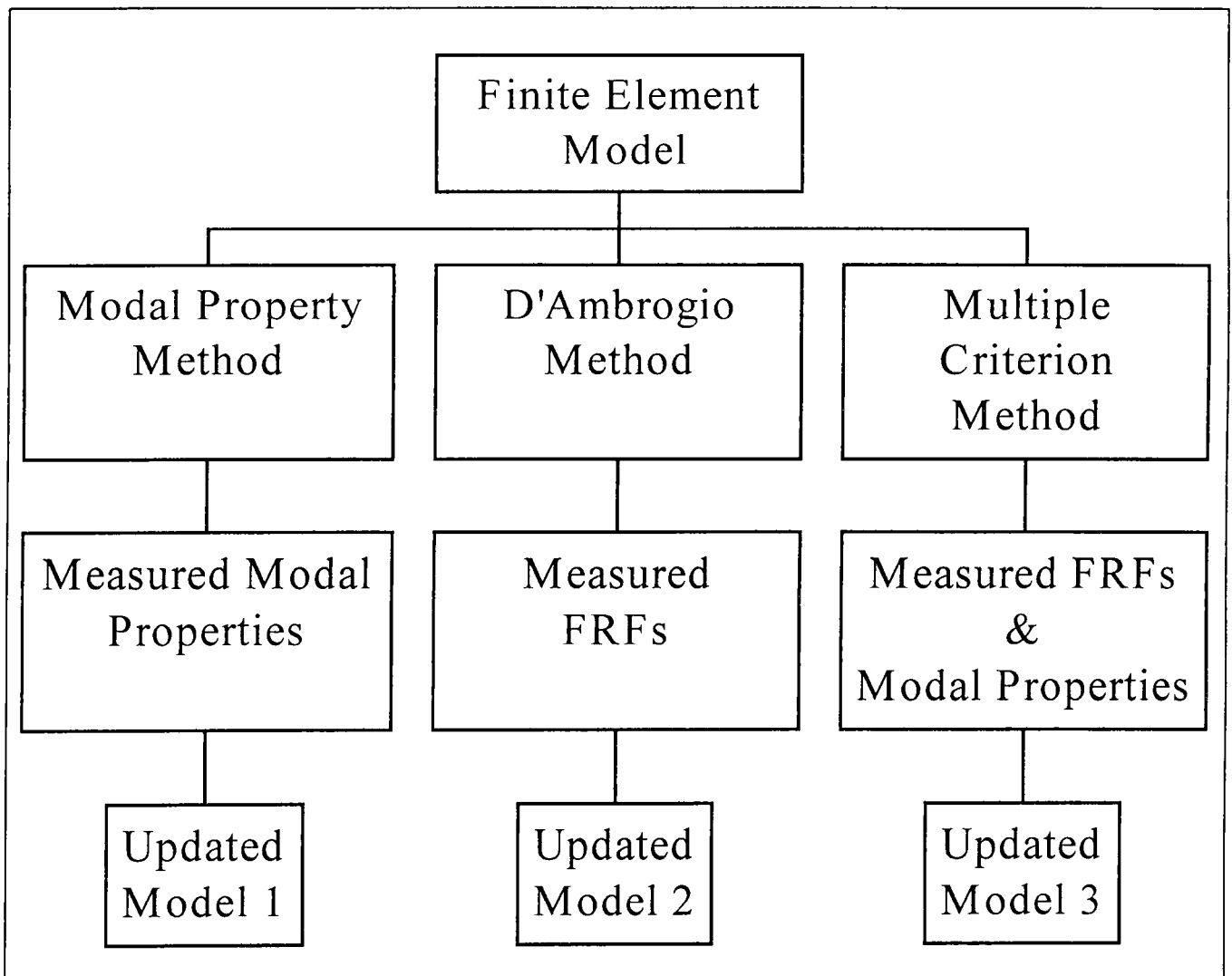


Figure 4.1 The structure of the updating procedure

A vital preliminary step in modal analysis is the preparation of the structure. The decision was taken to test a structure in an approximated free condition. This means that the structure is not attached to the ground at any of its co-ordinates but freely suspended in space. In this study the simple beam, beam with holes and an irregular H-shaped structure were tested free by suspending the structures using elastic bands. In the free suspension, the structures exhibit rigid body modes which are determined by their mass and inertia properties and in which there are no bending or flexing.

4.2. Example 1: Freely suspended beam

In this example an aluminium beam of length 1.0 m, width of 25.4 mm and thickness of 13.4 mm was used. The beam is depicted in figure 4.2 (detailed drawing in figure F.2 in appendix F) and was modelled discretely by 12 elements. The implemented program (see Appendix C) was written in a MATLAB environment and uses the Euler-Bernoulli FEA. Damping was assumed to be proportional because the damping levels were assumed to be low. The modulus of elasticity of each element (E), the Poisson ratio (ν), the cross-sectional area of each element (A) and the density of the beam (ρ) and the damping coefficients, α and β , were used as design variables. After the first updating only E was used as a design variable.

When beam elements are used adjusting E effectively ensures that the factor EI is changed. I represents the second moment of area. Figure 4.2 illustrates this.

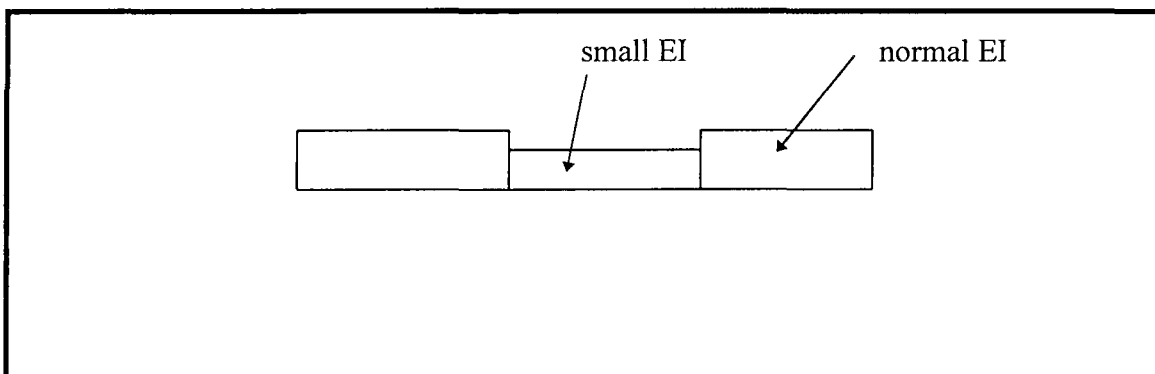


Figure 4.2 Illustration of the change in E

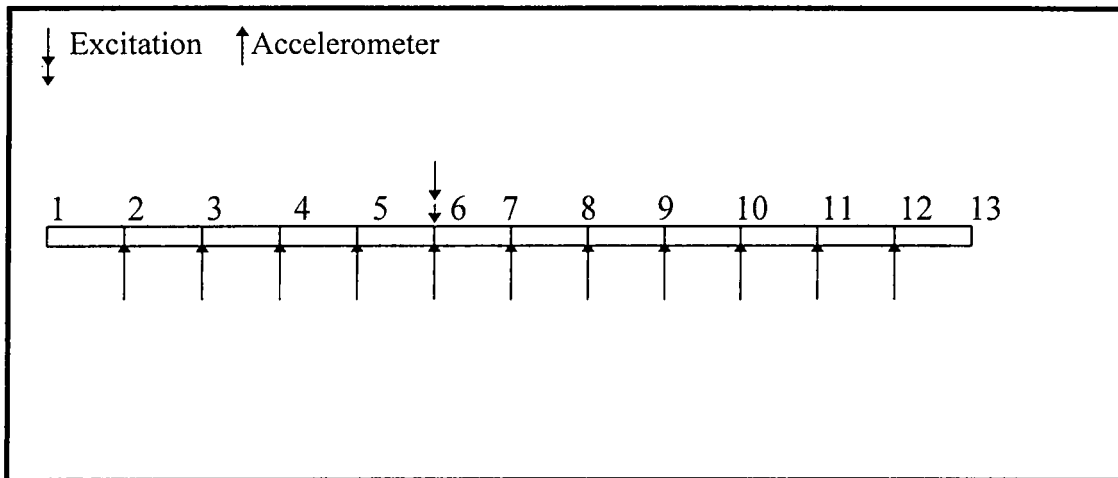


Figure 4.3 The discretised beam tested freely suspended

The beam was excited at node 6 as shown in figure 4.3 and the responses were measured for 11 cases using an accelerometer placed in succession at node 2 to 12. From the measurements a set of 11 FRFs was obtained. These measurements were used to identify modal parameters. Section 2.3 highlights simple techniques developed to identify these parameters. The Structural Toolbox uses an algorithm based on the pole or complex residue parametrization to extract the modal properties from the FRFs. The DAM, MPM and MCM were used to update the FEM. Figures E.4 and E.5 (in appendix E) show the FRFs and the phase diagrams of example 1 before and after updating respectively. The graphical illustration of the FRFs of the undamaged structure and the three damage cases may be viewed in figure E.1 (appendix E).

4.2.1 Updating The Beam Before Damage

The initial FEM was updated using experimental data obtained as explained in section 4.2. The DAM, MPM and the MCM were used (see Appendix C) and the results obtained are given in table 4.1. The DAM gives ν of 0.34 and ρ of 2702 kg.m^{-3} ; the MPM gives ν of 0.34 and ρ of 2650 kg.m^{-3} and the MCM gives ν of 0.34 and ρ of 2650 kg.m^{-3} . The values for α and β were both found to be approximately 0.0005. These parameters are taken as constant when updating of damaged structure is performed. The COMAC, the MAC_0 and the FRFAC were used to compare the results and may be viewed in table 4.1. The 'COMAC before' updating compares the normalised modes

obtained from the experiment to the normalised modes obtained from the initial FEM. The 'COMAC after' compares the normalised modes obtained from the experiment to the normalised modes obtained from the FEM after updating. The ' MAC_0 before' compares the normalised modes obtained from the experiment to the normalised modes obtained from the initial FEM and the ' MAC_0 after' compares the modes obtained from the experiment to the modes obtained from the FEM after updating. The 'FRFAC before' compares the FRFs of the initial FEM to the FRFs obtained from the experiment. The 'FRFAC after' compares the measured FRFs to the FRFs obtained from the FEM after updating.

Table 4.1 The COMAC, MAC_0 and FRFAC results for example 1 before damage

Method	COMAC (before)	COMAC (after)	MAC_0 (before)	MAC_0 (after)	FRFAC (before)	FRFAC (after)
DAM	0.9940	0.9998	0.0313	0.0311	0.7479	0.7778
MPM	0.9940	1.0000	0.0313	0.0313	0.7479	0.7756
MCM	0.9940	0.9999	0.0313	0.0311	0.7479	0.7762

Table 4.1 shows that the DAM, MPM and MCM were able to update the COMAC, MAC_0 and FRFAC factors. The COMAC factor was best updated when the MPM was used followed by the MCM and then the DAM. The MAC_0 was virtually not updated by any of the three approaches. The FRFAC was best updated when the DAM was used followed by the MCM and then the MPM. The results demonstrate that the FRFs based approach (DAM) updated the FRFAC better than the modal property based approaches (MPM). Furthermore, the results show that the MCM updated both the FRFAC and COMAC simultaneously better than the two methods.

The natural frequencies of the three measured modes from the experiment were compared to the natural frequencies from the initial FEM, the DAM updated FEM, the MPM updated FEM and the MCM updated FEM. The results of these comparisons are shown in table 4.2.

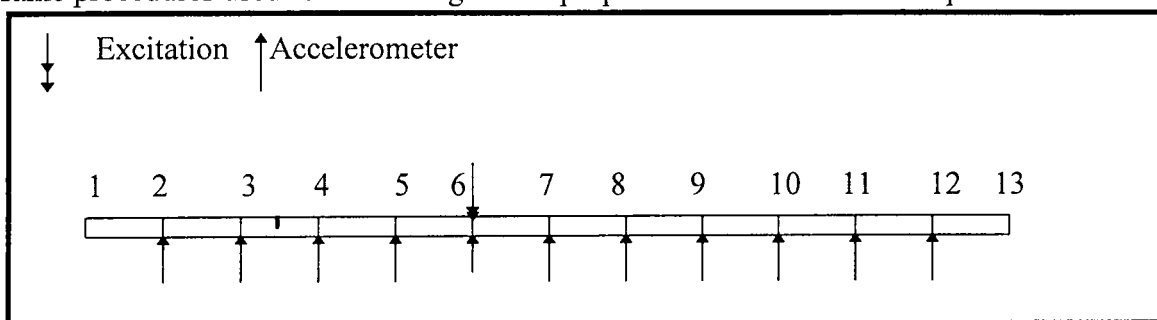
Table 4.2 Table showing natural frequencies in Hz (example 1 before damage)

Mode Number	Experimental Natural Frequencies (Hz)	Initial Natural Frequencies (Hz)	Updated Natural Frequencies (Hz) (DAM)	Updated Natural Frequency (Hz) (MPM)	Updated Natural Frequency (Hz) (MCM)
Mode 1	70.1	64.9	69.0	70.1	70.0
Mode 2	193.6	179.0	192.9	193.2	193.1
Mode 3	380.5	351.0	378.8	379.1	379.2

All the three methods displayed improvements in the updating of natural frequencies for the better. The MPM followed by the MCM displayed the best approximation of the first natural frequency than the DAM. The MPM displayed the best approximation for the second natural frequency, followed by the MCM and then the DAM. The third natural frequency was best approximated when the MCM was used followed by the MPM and then the DAM. These results demonstrate that the method using modal properties (MPM) tends to give better approximation of the measured modes and natural frequencies. It can also be concluded that the ability of the MCM to demonstrate better approximation than the MPM is because the MCM takes into account the modal properties as well as measured FRFs.

4.2.2. The Beam With Damage Case 1

The beam which may be viewed in figure 4.4 was damaged at element 3. The damage introduced was a thin saw cut that went half way through the cross-section of beam. The same experimental procedures that were performed in section 4.2.1 were repeated and the same procedures used for extracting modal properties from FRFs were implemented.

**Figure 4.4** Graph of a structure with damage at element 3

By using the measured FRFs and modal properties the DAM, MPM and MCM were implemented. The modal properties of the updated FEM were compared to the modal properties of the FEM. The FRFs of the updated FEM were compared to the FRFs before updating. The results of these comparisons are displayed in table 4.3.

Table 4.3 The COMAC, MAC_0 and FRFAC for damage case 1 (example 1)

Method	COMAC (before)	COMAC (after)	MAC_0 (before)	MAC_0 (after)	FRFAC (before)	FRFAC (after)
DAM	0.9855	0.9878	0.0335	0.0334	0.9704	1.0255
MPM	0.9855	0.9944	0.0335	0.0327	0.9704	1.0374
MCM	0.9855	0.9971	0.0335	0.0330	0.9704	1.0322

The results in table 4.3 indicate that the COMAC factor shows the MCM giving the best updating followed by the MPM and then the DAM. The MAC_0 factor, shows the MPM giving the best results followed by the MCM and then the DAM. The FRFAC factor shows that the DAM gives the best results followed by the MCM. These results demonstrate that the methods which use FRFs directly (DAM and MCM) tend to update the FRFAC more than the methods that do not use the FRFs directly (MPM). Furthermore, the results show that the methods that use the modal properties approach directly (MPM) tend to update the COMAC and the MAC_0 more effectively than the methods that use measured FRFs only (DAM). The results show that the method that uses both the measured FRFs and modal properties simultaneously (MCM) gives results that take into account the measured modal properties and the measured FRFs. The level in which the method takes into account the FRFs and modal properties depends entirely on the weighting functions chosen.

The natural frequencies for the three measured modes were compared to the natural frequencies of the same modes obtained from the initial FEM, the DAM updated FEM, MPM updated FEM and the MCM updated FEM. The results of these comparisons are shown in table 4.4.

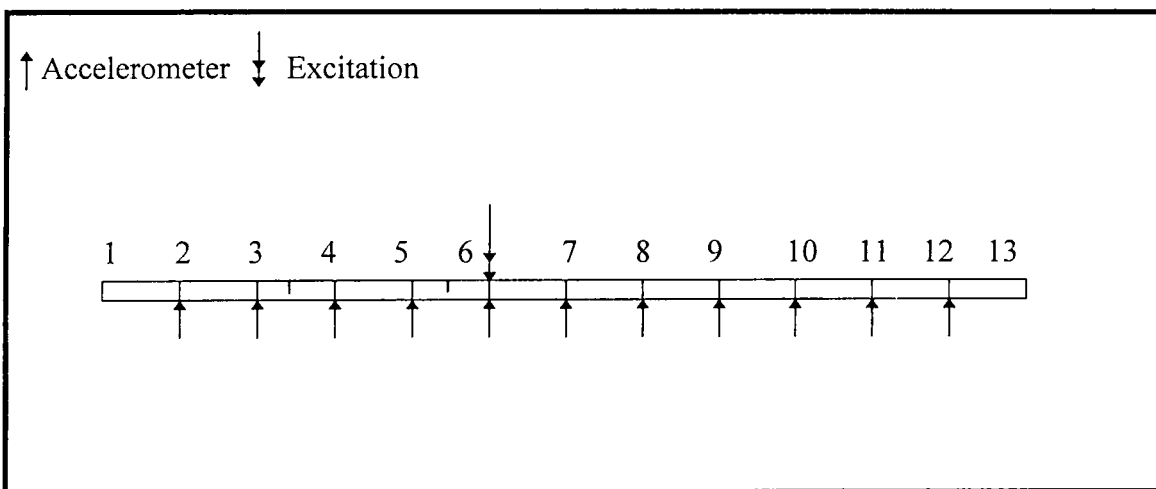
Table 4.4 Table showing natural frequencies in Hz for damage case 1 (example 1)

Mode Number	Experimental Natural Frequencies (Hz)	Initial Natural Frequencies (Hz)	Updated Natural Frequency (Hz) (DAM)	Updated Natural Frequency (Hz) (MPM)	Updated Natural Frequency (Hz) (MCM)
Mode 1	63.8	69.3	64.1	63.7	63.7
Mode 2	183.8	191.1	186.1	183.7	183.6
Mode 3	349.2	373.9	348.1	349.1	349.3

Table 4.4 shows that the MPM and MCM were better able to update the first natural frequency to the measured one than the DAM. It further demonstrates that the MPM was best able to reproduce the second and the third natural frequencies followed by the MCM and then the DAM. For the third mode, the MCM and the MPM were better able to reproduce the measured natural frequency than the DAM.

4.2.3 The Beam With Damage Case 2

The second damage case considered in example 1, was obtained by introducing a saw cut at elements 3 and 5. This case is in essence a multiple damage detection problem. Care must be taken in performing this experiment to avoid exogenous disturbances. The schematic diagram of this example may be viewed in Figure 4.5.

**Figure 4.5** Freely suspended beam with damage at elements 3 and 5

The beam was excited at node 6 as shown in figure 4.5. The response was measured using an accelerometer placed consecutively at nodes 2 to 12. From the measurements, a set of 11 FRFs was obtained. This set of FRFs was used to update the FEM (see Appendix C). The measured modal properties were identified and were also used to update the FEM. Thereafter, the measured FRFs and modal properties were used simultaneously to update the model. The COMAC, MAC_0 and the FRFAC before and after updating were computed and may be viewed in table 4.5.

Table 4.5 The COMAC, MAC_0 and FRFAC for damage case 2

Method	COMAC (before)	COMAC (after)	MAC_0 (before)	MAC_0 (after)	FRFAC (before)	FRFAC (after)
DAM	0.9779	0.9849	0.0344	0.0321	0.9514	0.9934
MPM	0.9779	0.9884	0.0344	0.0302	0.9514	0.9914
MCM	0.9779	0.9872	0.0344	0.0302	0.9514	0.9924

The COMAC factor shows that the MPM gives best results followed by the MCM and then the DAM. The MAC_0 factor shows that the MCM and the MPM give better results than the DAM. The FRFAC approach shows that the DAM approach gives the best results followed by the MCM and then the MPM.

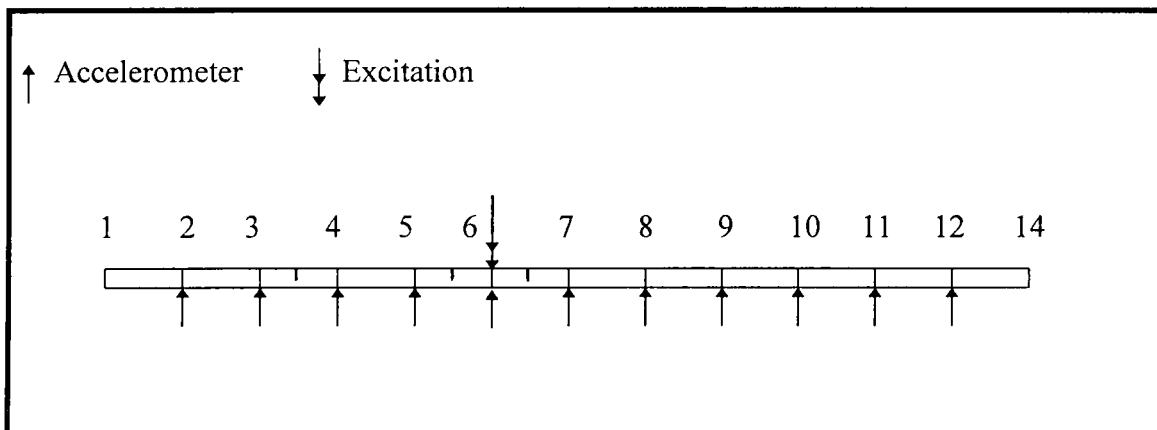
Table 4.6. shows that the MPM gives the best approximation for the first natural frequency followed by the MCM and then the DAM. For the second and the third natural frequencies, the MPM and the MCM give better results than the DAM.

Table 4.6 Table showing natural frequencies in Hz for damage case 2 (example 1)

Mode Number	Experimental Natural Frequencies (Hz)	Initial Natural Frequencies (Hz)	Updated Natural Frequency (Hz) (DAM)	Updated Natural Frequency (Hz) (MPM)	Updated Natural Frequency (Hz) (MCM)
Mode 1	64.7	69.2	64.1	64.4	65.3
Mode 2	175.1	190.5	176.1	176.0	176.0
Mode 3	340.2	372.8	339.0	339.1	339.1

4.2.4 The Beam With Damage Case 3

In the third case damage was introduced at element 6 in addition to the previously introduced damage at elements 3 and 5. The schematic representation for this case is illustrated in figure 4.6.

**Figure 4.6** Freely suspended beam with damage at elements 3 and 5

From the measurements a set of 11 FRFs was obtained. This set of FRFs was used to update the FEM. The measured modal properties were extracted from a set of FRFs and were also used to update the FEM. Thereafter, the MCM was used to update the model. The results showing the COMAC, the MAC_0 , and the FRFAC before and after updating when three updating techniques are implemented may be viewed in table 4.7.

Table 4.7 The COMAC, MAC_0 and FRFAC for damage case 3 (example 1)

Method	COMAC (before)	COMAC (after)	MAC_0 (before)	MAC_0 (after)	FRFAC (before)	FRFAC (after)
DAM	0.9654	0.9987	0.0296	0.0288	1.0212	0.9929
MPM	0.9654	0.9999	0.0296	0.0203	1.0212	0.9913
MCM	0.9654	0.9998	0.0296	0.0288	1.0212	0.9920

The COMAC factor shows that the MPM gives the best results followed by the MCM and then the DAM. The MAC_0 factor shows that the MPM gives better results than the DAM and MCM methods. The FRFAC factor shows that the DAM gives the best results followed by the MCM then the MPM. These results show that the MPM gives the updated FEM which reproduces the modal properties the best followed by the MCM and then the DAM. The DAM gives the updated FEM which predicts the measured FRFs the best, followed by the MCM and then the MPM.

The comparisons of natural frequencies before and after updating using three different updating methods are shown in table 4.8. The three updating techniques were able to update the first natural frequency. The DAM gave the best results, followed by the MPM and then the MCM. The ability to reproduce the third mode, however, was in the following order: the MCM and the MPM and then the DAM.

Table 4.8 Table showing natural frequencies in Hz for damage case 3 (example 1)

Mode Number	Experimental Natural Frequencies (Hz)	Initial Natural Frequencies (Hz)	Updated Natural Frequency (Hz) (DAM)	Updated Natural Frequency (Hz) (MPM)	Updated Natural Frequency (Hz) (MCM)
Mode 1	64.9	65.4	67.3	65.0	65.0
Mode 2	184.2	176.0	184.5	184.2	184.0
Mode 3	356.0	339.1	355.2	355.8	355.8

4.3. Example 2: Freely Suspended Beam With Holes

This example is closely related to the previous one, except that the beam had holes and therefore was more difficult to model. The aluminium beam has the following dimensions: length: 1.1 m, width: 29.2 mm and thickness: 9.6 mm. The beam has holes of diameter 5.8 mm located at nodes 2 to 9 which are separated by 10 cm equal spacing (see details in figure F.3 in appendix F). The same procedure is followed as in section 4.2 and the programs implemented are written in a MATLAB environment and may be viewed in Appendix C (section 2). The beam was modelled by 11 elements and the structure was excited at node 4 (see figure 4.7). The picture of this beam may be viewed in figure D.2 (in appendix D). The responses were measured by placing the accelerometers consecutively at nodes 2 to 12. The DAM; MPM and MCM were implemented and the results were compared by using the COMAC, MAC_0 and FRFAC.

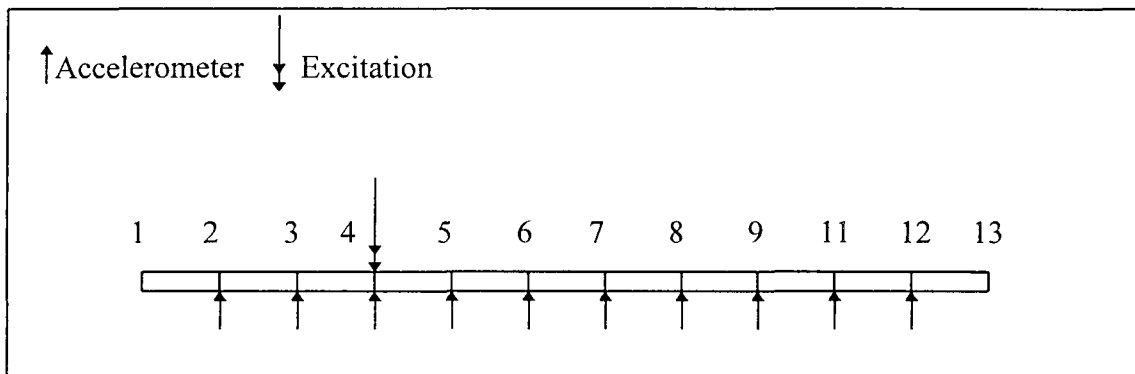


Figure 4.7 A beam with holes

4.3.1. Updating Before Damage

The optimisation procedure was performed with E , ν , ρ , α , and β used as design variables. It was found that the ν was 0.34, ρ was 2650 kg m^{-3} and α was 0.00043, and β was 0.000082. The values of ν , ρ , α and β were stored for later use.

The COMAC, MAC_0 , and FRFAC before and after updating were compared and the results are displayed in table 4.9.

Table 4.9 The COMAC, MAC_0 and FRFAC for undamaged case (example 2)

Method	COMAC (before)	COMAC (after)	MAC_0 (before)	MAC_0 (after)	FRFAC (before)	FRFAC (after)
DAM	0.8326	0.8919	0.0420	0.0419	1.7281	1.6089
MPM	0.8326	0.9859	0.0420	0.0419	1.7281	1.6862
MCM	0.8326	0.9087	0.0420	0.0420	1.7281	1.6183

The COMAC factor shows that the MPM gives the best results followed by the MCM and then the DAM. The MAC_0 factor shows virtually no updating. The FRFAC factor shows that the DAM gives the best results followed by the MCM then by the MPM. These results show that the MPM gives the updated FEM which reproduces the modal properties the best followed by the MCM and then the DAM. The DAM gives the updated FEM which predicts the measured FRFs the best, followed by the MCM and then the MPM.

The natural frequencies before and after updating are displayed in table 4.10.

Table 4.10 Table showing natural frequencies in Hz for undamaged case (example 2)

Mode Number	Experimental Natural Frequencies (Hz)	Initial Natural Frequency (Hz)	Updated Natural Frequency (Hz) (DAM)	Updated Natural Frequency (Hz) (MPM)	Updated Natural Frequency (Hz) (MCM)
Mode 1	40.9	38.5	41.9	41.3	41.4
Mode 2	115.4	106.1	113.0	115.8	113.0
Mode 3	224.6	208.8	221.3	227.0	221.3
Mode 4	376.1	347.1	377.2	376.0	377.2

The MPM gives the FEM which best predicts the measured natural frequencies, followed by the MCM and then the DAM. None of the three methods could give an FEM that gives the third natural frequency closer to the measured one.

4.3.2. The Beam With Damage Case 1

In this case, damage was introduced at element 2. The same procedures as in section 4.3.1 were applied and the results are shown in tables 4.11 and 4.12.

Table 4.11 The COMAC, MAC_0 and FRFAC for damage case 1 (example 2)

Method	COMAC (before)	COMAC (after)	MAC_0 (before)	MAC_0 (after)	FRFAC (before)	FRFAC (after)
DAM	0.8326	0.9019	0.0419	0.0421	1.7870	1.1433
MPM	0.8325	0.9259	0.0419	0.0421	1.7870	1.6979
MCM	0.8326	0.9187	0.0419	0.0421	1.7870	1.5423

The COMAC factor shows that the MPM gives the best updating, followed by the MCM and then the DAM. The MAC_0 scalars demonstrate no updating for any of the three approaches. The FRFAC indicated that the best updating was performed by the DAM, followed by the MCM and then the MPM.

Table 4.12 Table showing natural frequencies in Hz for damage case 1 (example 2)

Mode Number	Experimental Natural Frequencies (Hz)	Initial Natural Frequency (Hz)	Updated Natural Frequency (Hz) (DAM)	Updated Natural Frequency (Hz) (MPM)	Updated Natural Frequency (Hz) (MCM)
Mode 1	41.5	37.9	40.8	40.7	40.2
Mode 2	114.5	107.7	112.5	112.5	113.5
Mode 3	224.5	206.7	220.6	220.6	221.3
Mode 4	371.6	351.4	363.4	366.4	365.6

Table 4.12 demonstrates that the three approaches work well. For all the measured natural frequencies, the MPM gives the best results, followed by the MCM and then the DAM. For the second natural frequency the three methods give same results.

4.3.3. The Beam With Damage Case 2

In this case, damage is introduced at elements 2 and 3. The structure which was used is the same as in figure 4.5. The same procedures as in section 4.3.1 were implemented. The results obtained may be viewed in tables 4.13 and 4.14.

Table 4.13 The COMAC, MAC_0 and FRFAC for damage case 2 (example 2)

Method	COMAC (before)	COMAC (after)	MAC_0 (before)	MAC_0 (after)	FRFAC (before)	FRFAC (after)
DAM	0.6324	0.7326	0.0486	0.0498	1.8340	1.6979
MPM	0.6324	0.8453	0.0486	0.0495	1.8340	1.7734
MCM	0.6324	0.8126	0.0496	0.0496	1.8340	1.7432

Table 4.13 shows that the COMAC and the MAC_0 scalars were most updated when the MPM was used followed by the MCM and then the DAM. The FRFAC approach demonstrated that the best updating is obtained when using DAM, then MCM and then the MPM.

The corresponding changes in natural frequencies may be viewed in table 4.14.

Table 4.14 Table showing natural frequencies in Hz for damage case 2 (example 2)

Mode Number	Experimental Natural Frequencies (Hz)	Initial Natural Frequency (Hz)	Updated Natural Frequency (Hz) (DAM)	Updated Natural Frequency (Hz) (MPM)	Updated Natural Frequency (Hz) (MCM)
Mode 1	41.5	40.2	41.3	41.7	41.3
Mode 2	114.5	113.5	113.0	114.2	113.0
Mode 3	224.5	221.3	221.7	225.6	221.9
Mode 4	371.6	365.6	363.0	373.3	368.1

Table 4.14 shows that all the three approaches update the first, second and third natural frequencies well. However, the MPM on average gives best approximation, followed by the MCM and then DAM.

4.3.4. The Beam With Damage Case 3

In the third case, damage is introduced in elements 2, 3 and 4. The same procedure as in section 4.3.1 was followed and the results are in Tables 4.15 and 4.16.

Table 4.15 The COMAC, MAC_0 and FRFAC for damage case 3 (example 2)

Method	COMAC (before)	COMAC (after)	MAC_0 (before)	MAC_0 (after)	FRFAC (before)	FRFAC (after)
DAM	0.6072	0.7036	0.0419	0.0419	1.8638	1.6528
MPM	0.6072	0.7474	0.0419	0.0419	1.8638	1.7483
MCM	0.6372	0.7128	0.0419	0.0419	1.8638	1.7074

This case demonstrates that the MAC_0 did not offer any improvement. The COMAC demonstrates that the MPM gives better results, followed by the MCM and then the DAM. The FRFAC shows that the best improvements due to updating are obtained when the DAM is used, followed by the MCM, and then MPM.

Table 4.16 Table showing natural frequencies in Hz for damage case 3 (example 2)

Mode Number	Experimental Natural Frequencies (Hz)	Initial Natural Frequency (Hz)	Updated Natural Frequency (Hz) (DAM)	Updated Natural Frequency (Hz) (MPM)	Updated Natural Frequency (Hz) (MCM)
Mode 1	35.4	41.3	38.4	35.9	36.4
Mode 2	110.3	113.0	113.3	109.8	112.3
Mode 3	209.3	221.9	219.3	210.9	219.3
Mode 4	352.7	368.1	359.7	351.8	353.7

Table 4.16 demonstrates that the three approaches work well. On average, it was discovered that the MPM gives better approximation of the natural frequency, followed by the MCM and then the DAM.

The results that show the effect of damage on the measured FRFs for example 2 may be viewed in appendix E (figure E.2).

4.4. Example 3: Freely suspended H-shaped structure

The third example is an irregular H-shaped structure which may be viewed in Figure 4.8.

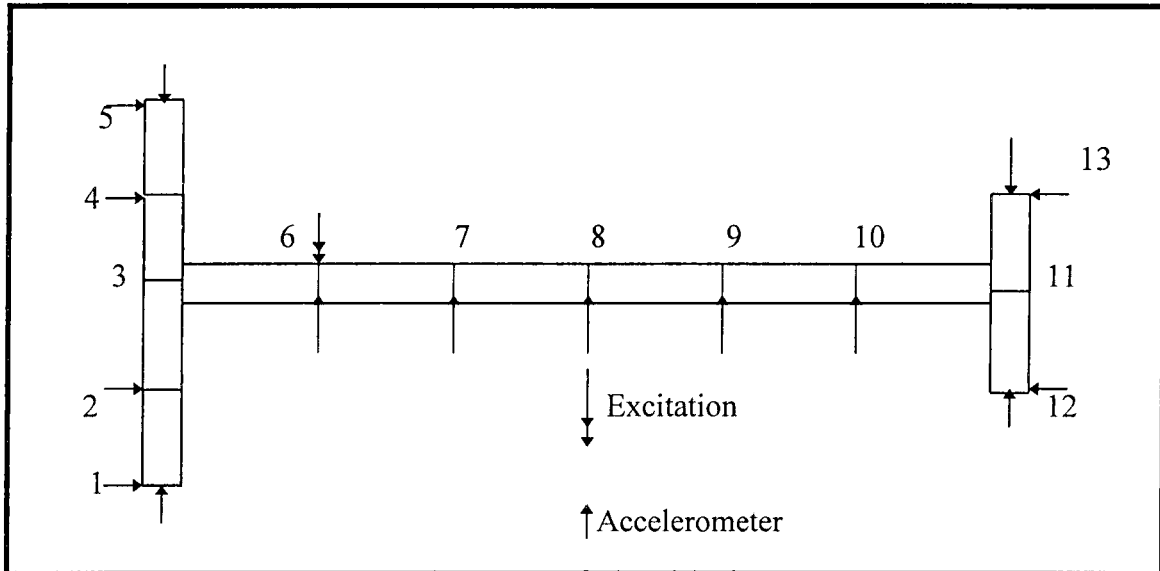


Figure 4.8 An irregular H-shaped structure

The structure displayed in figure 4.8 is made out of aluminium. The dimensions of the structure are shown in figure F.4 (appendix F). The structure was divided into 12 elements. The structure was excited at node 6 and the accelerometer was placed at 15 locations as shown figure 4.8. The picture of the set-up may be viewed in figure D.3 (appendix D). The structure was tested free and a set of 15 FRFs was obtained and used for updating.

4.4.1. The Updating Case Before Damage Occurs

The FRFs obtained as explained in section 4.4. were utilised to update the FEM. The initial updated FEM was updated using experimental data obtained by following the same procedure as in section 4.2. The DAM, MPM and the MCM were used (see Appendix C) and the results obtained are as given in table 4.1. The DAM gives ν of 0.33 and ρ of 2700 kg.m^{-3} ; the MPM gives ν of 0.34 and ρ of 2690 kg.m^{-3} and the MCM gives ν of 0.33 and ρ of 2700 kg.m^{-3} . The values for α and β were found to be approximately equal to 0.0004.

The results in table 4.17 show the comparison of COMAC, MAC_0 and FRFAC before and after updating.

Table 4.17 The COMAC, MAC_0 and FRFAC for undamaged case (example 3)

Method	COMAC (before)	COMAC (after)	MAC_0 (before)	MAC_0 (after)	FRFAC (before)	FRFAC (after)
DAM	1.4281	1.1230	0.2643	0.0658	0.9446	0.9947
MPM	1.4281	1.2630	0.2643	0.0653	0.9446	0.9942
MCM	1.4281	1.1800	0.2643	0.0657	0.9446	0.9947

The results shown in table 4.17 demonstrate that the COMAC was improved the most after updating when DAM was used, then MPM and then MCM. The MAC_0 factor was improved the most by the MPM, then the MCM and then DAM. The FRFAC was improved the most by the DAM and the MCM followed by the MPM.

Table 4.18 shows the comparison between natural frequencies.

Table 4.18 Table showing natural frequencies in Hz for undamaged case (example 3)

Mode Number	Experimental Natural Frequencies (Hz)	Initial Natural Frequency (Hz)	Updated Natural Frequency (Hz) (DAM)	Updated Natural Frequency (Hz) (MPM)	Updated Natural Frequency (Hz) (MCM)
Mode 1	55.37	51.26	55.26	55.40	55.28
Mode 2	125.30	116.01	125.00	124.97	125.30
Mode 3	225.18	208.48	226.68	224.70	225.39
Mode 4	259.71	240.44	258.67	258.70	259.30
Mode 5	446.04	412.96	444.41	444.63	445.55

Table 4.18 demonstrates that all three approaches were capable of reproducing the measured natural frequencies. The results show that the MPM approximated the measured parameters the best, followed by the MCM and then the DAM.

4.4.2. The Damage Case 1

In this case damage was introduced in element 3 of figure 4.8. The same procedure followed in section 4.4.1 is followed in this case. When updating was performed the results in table 4.19 were obtained.

Table 4.19 The natural frequencies in Hz for damage case 1 (example 3)

Mode Number	Experimental Natural Frequencies (Hz)	Initial Natural Frequency (Hz)	Updated Natural Frequency (Hz) (DAM)	Updated Natural Frequency (Hz) (MPM)	Updated Natural Frequency (Hz) (MCM)
Mode 1	55.16	55.38	56.00	55.18	54.26
Mode 2	123.69	125.30	125.74	123.72	120.11
Mode 3	206.76	225.39	208.67	207.85	209.39
Mode 4	258.55	259.30	258.54	259.98	257.77
Mode 5	443.22	445.55	448.35	442.93	442.92

Table 4.19 demonstrates that the MPM was best able to approximate the natural frequencies, then the MPM then the DAM.

Table 4.20 The COMAC, MAC_0 and FRFAC for damage case 1 (example 3)

Method	COMAC (before)	COMAC (after)	MAC_0 (before)	MAC_0 (after)	FRFAC (before)	FRFAC (after)
DAM	1.4281	1.2407	0.2526	0.0724	1.0920	1.0820
MPM	1.4281	1.1020	0.2526	0.0721	1.0920	1.0907
MCM	1.4281	1.1710	0.2526	0.0723	1.0920	1.0902

Table 4.20 demonstrates that the MPM gives the best updated approximation of the COMAC and the MAC_0 scalar, then the MCM and then the DAM. The FRFAC was best updated by the DAM, then the MCM and then the MPM.

4.4.3. The Damage Case 2

In this case, damage was introduced at elements 2 and 3 of the structure shown in figure 4.8. The same procedure in section 4.4.1 was used in this section. The results obtained are shown in table 4.21.

Table 4.21 Table showing natural frequencies in Hz for damage case 2 (example 3)

Mode Number	Experimental Natural Frequencies (Hz)	Initial Natural Frequency (Hz)	Updated Natural Frequency (Hz) (DAM)	Updated Natural Frequency (Hz) (MPM)	Updated Natural Frequency (Hz) (MCM)
Mode 1	55.15	54.26	55.17	55.48	54.27
Mode 2	123.61	120.11	125.74	123.73	120.11
Mode 3	205.82	209.39	206.28	207.85	206.93
Mode 4	258.52	257.77	259.99	258.46	257.77
Mode 5	445.98	442.92	445.55	443.94	442.92

Table 4.21 demonstrates that the DAM gives best results, then the MCM and then the MPM.

When the comparison methods were implemented the following results were shown in table 4.22 were obtained.

Table 4.22 The COMAC, MAC_0 and FRFAC for damage case 2 (example 3)

Method	COMAC (before)	COMAC (after)	MAC_0 (before)	MAC_0 (after)	FRFAC (before)	FRFAC (after)
DAM	0.7436	0.9022	0.2738	0.0166	1.2641	1.0263
MPM	0.7436	0.9232	0.2738	0.0119	1.2641	1.1297
MCM	0.7436	0.9191	0.2738	0.0161	1.2641	1.1262

The results demonstrate that the MPM gives the best COMAC and MAC_0 scalars approximation, then the MCM and then the FRF approach. The FRFAC gives the best results when the DAM is used, followed by the MCM, then the MPM.

4.4.4. The Damage Case 3

In this case damage was introduced in elements 3, 4 and 5 of the structure in figure 4.8. The same procedure as in the previous section was implemented and the results are shown in table 4.23.

Table 4.23 Table showing natural frequencies in Hz for damage case 3 (example 3)

Mode Number	Experimental Natural Frequencies (Hz)	Initial Natural Frequency (Hz)	Updated Natural Frequency (Hz) (DAM)	Updated Natural Frequency (Hz) (MPM)	Updated Natural Frequency (Hz) (MCM)
Mode 1	53.88	54.27	53.89	53.23	53.27
Mode 2	117.32	120.11	117.27	118.66	118.11
Mode 3	208.40	206.93	208.26	208.71	208.93
Mode 4	253.99	257.77	253.85	250.26	254.77
Mode 5	445.17	442.92	445.02	437.89	445.92

Table 4.23 shown that all the three methods give good results. However, it may be observed that the MPM experienced difficulty in updating higher natural frequencies. The MCM gives the best updated approximation of the measured natural frequencies, followed by the DAM and then MPM.

When the comparison methods were implemented, the results in table 4.24 were obtained.

Table 4.24 The COMAC, MAC_0 and FRFAC for damage case 3 (example 3)

Method	COMAC (before)	COMAC (after)	MAC_0 (before)	MAC_0 (after)	FRFAC (before)	FRFAC (after)
DAM	0.7918	0.9114	0.2787	0.0309	1.2723	1.0246
MPM	0.7918	0.9890	0.2787	0.0304	1.2723	1.2360
MCM	0.7918	0.9373	0.2787	0.0299	1.2723	1.0254

Table 4.24 demonstrates that the MPM gives best updating of the COMAC value, followed by the DAM and then the MCM. The MAC_0 value was best updated when MCM was implemented, then MPM and then DAM. The FRFAC approach was best updated when DAM was used, then MCM and then MPM.

The results showing the effects of damage on the FRFs for this example are shown in figure E.3 (appendix E). The results showing the qualities of modes measured are shown in figure E.6. The results demonstrating the effect of updating on the FRFs are in figure E.4 and E.5.

4.5. Conclusion

The MPM and the DAM give a good approximation to the measured FRFs and modal parameters. The MCM approximates both the measured FRFs and modal properties well. It tended to find the middle ground between the measured FRFs and modal properties.

In this chapter it was discovered that the FRFAC factor is a good criterion for comparing measured FRFs. When the FRFAC was used, the frequency range was chosen on the region with minimal noise. It is suggested that for future use of the FRFAC, the FRFs must be smoothed out to minimise the effect of noise.

The MAC_0 scalar was not a very good factor to compare modes. In the future it is suggested that the MAC be normalised by multiplying the elements in its diagonal. This will ensure that perfect correlation gives 1.

The assumption of proportional damping worked well for this study. If the structure being analysed is heavily damped, then proportional damping will not be a good assumption. This may compromise on the effectiveness of the method. For future research, it is suggested that the effect of heavy damping on the effectiveness of the MCM be investigated.

5. Damage Detection Using Updating Procedure

5.1. Introduction

In chapter 4, a new iterative updating method was developed and applied to three examples. In this chapter this new updating method is applied in conjunction with the philosophy of selective updating to detect damage on three different structures. The method is compared to the DAM and MPM. The idea of selective updating was introduced by Ben-Haim in 1992. Ben-Haim reduced the number of updating parameters by applying excitations which produce strong sensitivities. In this study instead of using the E vector of the structure as a design variable, the structure is divided into two halves. Each half is assumed to have the same E. Then the MCM, the DAM and the MPM methods are applied. The half that experiences the least updating of E is restricted by applying a relatively stringent bounds and the other half is further divided into halves. The procedure is repeated until damage is completely located.

In chapter 4, the FEM was updated iteratively by varying the modulus of elasticity of each element of the FEM. Several damage cases were introduced and their respective FEMs were identified. As an extension to the previous work, the results of the updated models for each damage case are compared to the results of the updated model before damage had been introduced. Damage is detected by analysing the difference between the updated damaged model and the updated undamaged model. In this study the extent of damage is represented by the changes in modulus of elasticity. It is argued that a relationship exists between the changes in modulus of elasticity and the amount of damage in the structure. However, to quantify this relationship, a separate study will have to be conducted. In this study it is postulated that the relationship between the changes in modulus of elasticity and the amount of damage that has occurred is a function of the material property of the structure.

Photographs of the structures that were used may be viewed in appendix D. The structure was damaged by introducing saw cuts on several selected elements. The cuts went

further than the centre of the cross-section of the structure. The programs implemented for detection of damage are the same as those used for updating and may be viewed in appendix C.

5.2. Example 1

5.2.1. Damage Case 1

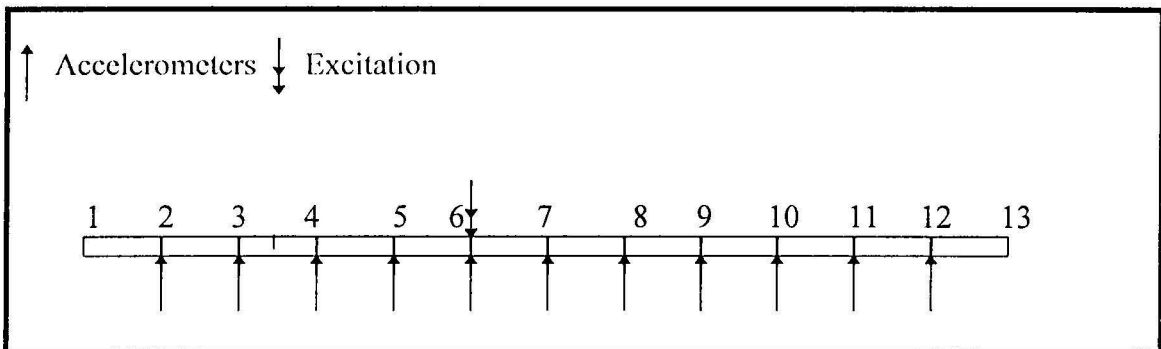


Figure 5.1 Experimental set-up damage was imposed on element 3 as indicated

The beam depicted in figure 5.1 was excited at node 6 and the response measured by an accelerometer placed consecutively at node 2 to 12. From the measurements one set of 11 Frequency Response Functions (FRF's) was obtained. This set of FRFs was used to identify each element's modulus of elasticity of the FEM. The modulus of elasticity of the newly updated model was subtracted from the modulus of elasticity of the previously updated model. The results may be viewed in figure 5.2.

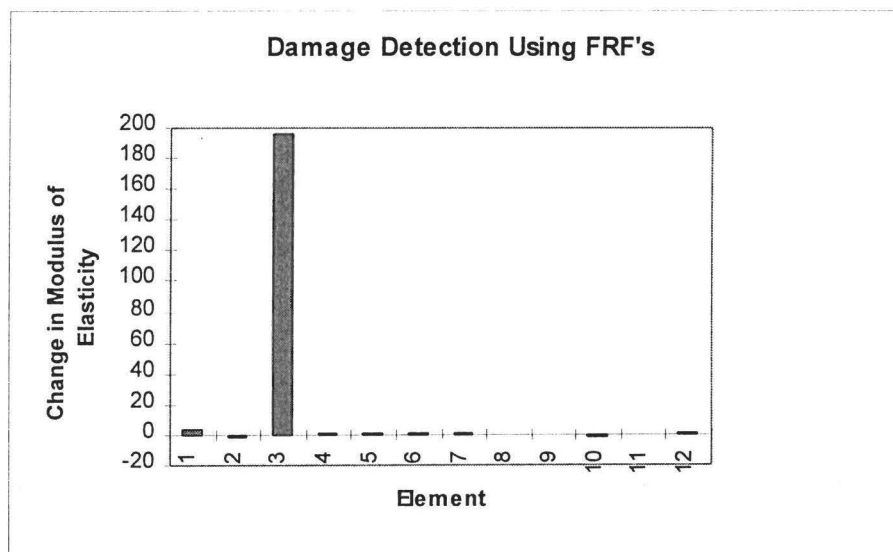


Figure 5.2 Damage detection using DAM (example1, case 1)

Figure 5.2 shows that when the DAM was used the modulus of elasticity of element 3 was updated by approximately 190.0×10^8 MPa. These results indicate the presence of damage at element 3.

From the FRFs measurements the modal properties were extracted and were used in the MPM to update the FEM. The modulus of elasticity vector of the newly updated model was subtracted from the modulus of elasticity vector of the previously updated model. The results may be viewed in Figure 5.3.

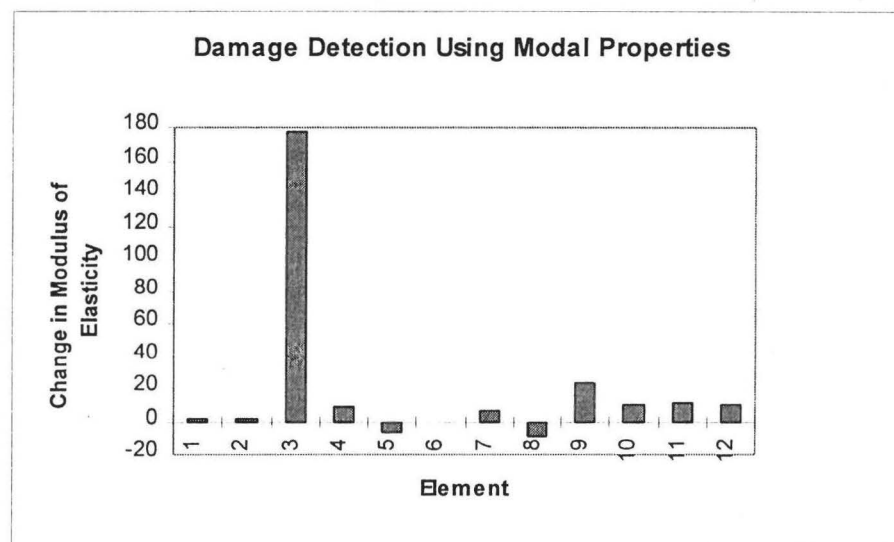


Figure 5.3 Damage detection using MPM (example 1, case 1)

The results show that the MPM updated the FEM by changing the modulus of elasticity of element 3 by about 180.0×10^8 MPa. The results indicate the presence of damage (significant updating was performed), its location at element 3 and its extent (180.0×10^8 MPa).

The MCM was implemented to detect damage. The modulus of elasticity vector obtained after updating was compared to the modulus of elasticity vector before updating. The results are shown in figure 5.4.

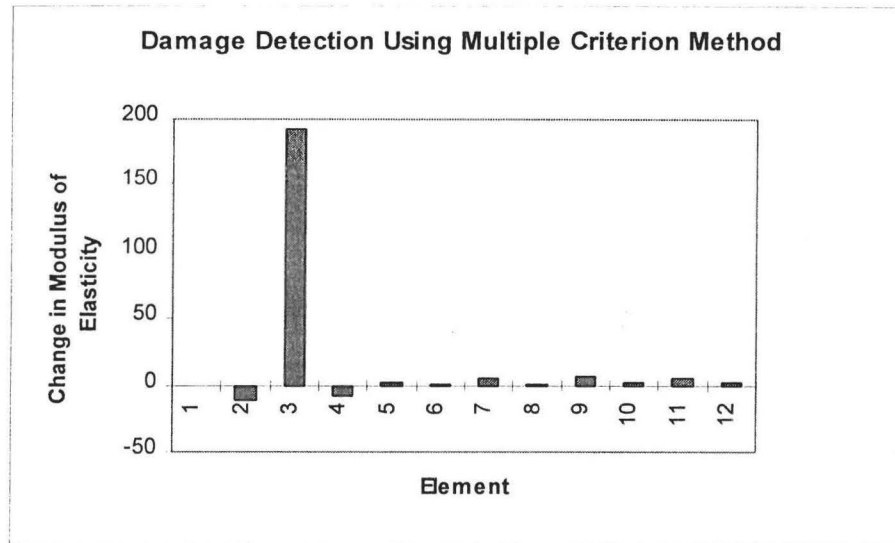


Figure 5.4 Damage detection using MCM (example1, case 1)

The results show that the MCM updated the FEM by changing the modulus of elasticity of element 3 by 180.0×10^8 MPa. The other elements were not updated significantly. The fact that significant updating was performed indicates that the structure was damaged. This MCM predicts the presence of damage (significant updating was performed), its location at element 3 and its extent (180.0×10^8 MPa).

The results obtained by the three methods are consistent with each other. These three approaches were able to indicate the presence of damage (significant updating was performed), its location (at element 3) and its extent (180.0×10^8 MPa). It must be noted that the three approaches give slightly different changes in modulus of elasticity. This is due to the presence of error in the measured parameters.

5.2.2. Damage Case 2

In this case damage was introduced at elements 3 and 5. This case is a multiple damage detection problem. It was discovered that this case is difficult to analyse since it requires experimental data of a higher degree of accuracy. Care must therefore, be taken to minimise exogenous disturbances when performing this experiment. The schematic diagram of this example may be viewed in figure 5.5.

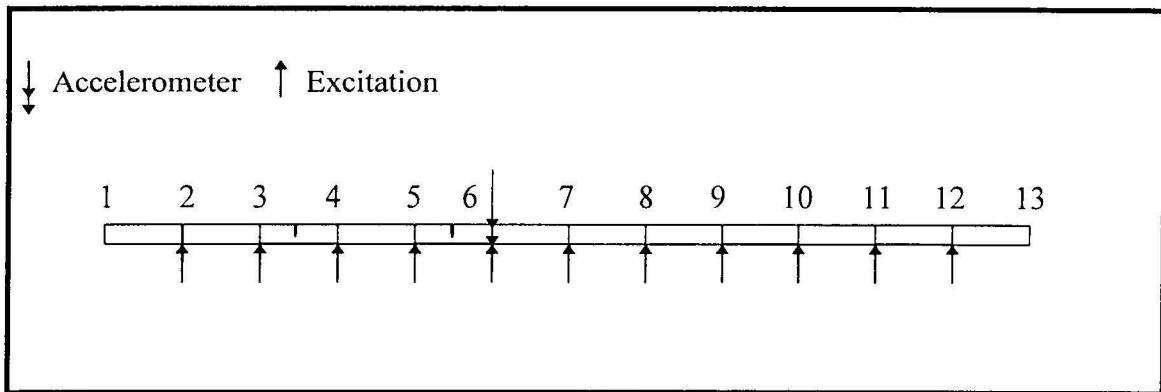


Figure 5.5 Damage at elements 3 and 5

When the DAM was implemented and the updated FEM was obtained and compared to the updated FEM in section 5.2.1. The results obtained may be viewed in figure 5.6.

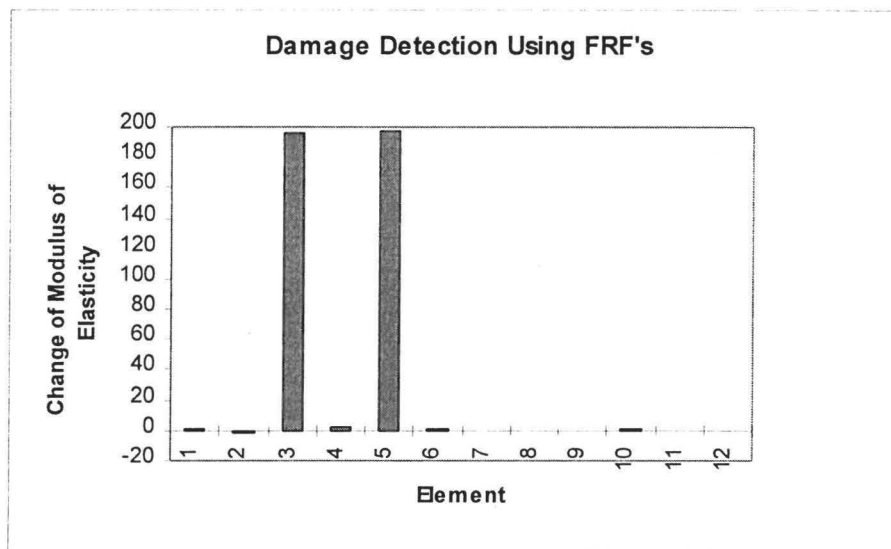


Figure 5.6 Damage detection using DAM (example 1, case 2)

Figure 5.6 shows that elements 3 and 5 were updated by about 180.0×10^8 MPa. The fact that significant updating was performed on the previously updated FEM indicates existence of further damage. The location of damage at elements 5 and 6 and the extent for each is 180.0×10^8 MPa.

By applying modal analysis techniques, modal properties of the system were extracted and subsequently used to detect the location and the extent of damage on the structure.

The results of the MPM are shown by figure 5.7.

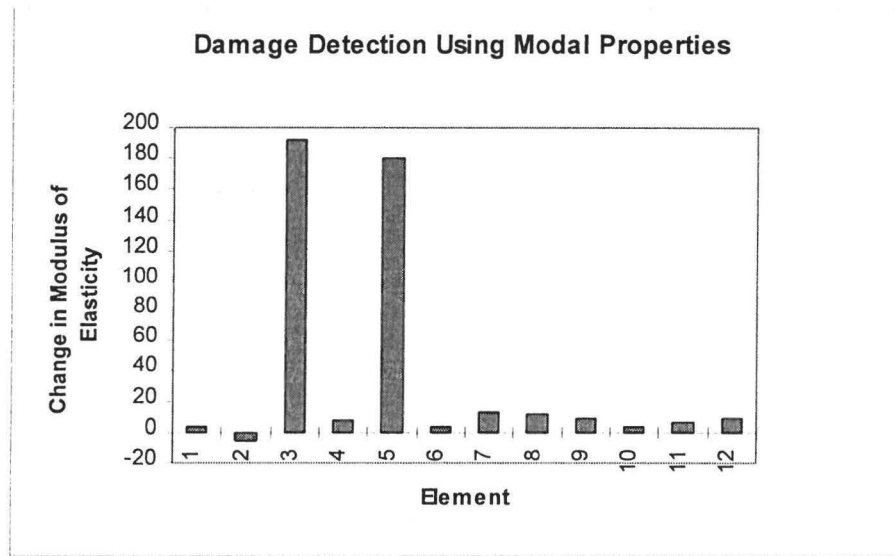


Figure 5.7 Damage detection using MPM (example1, case 2)

As it can be viewed in figure 5.7 updating was performed in elements 3 and 5 and this demonstrates the existence of damage. These results further show the location of damage to be at elements 3 and 5 and the extent of damage to be 190.0×10^8 MPa and 180.0×10^8 MPa respectively.

The MCM was implemented and the results of the process may be viewed in figure 5.8.

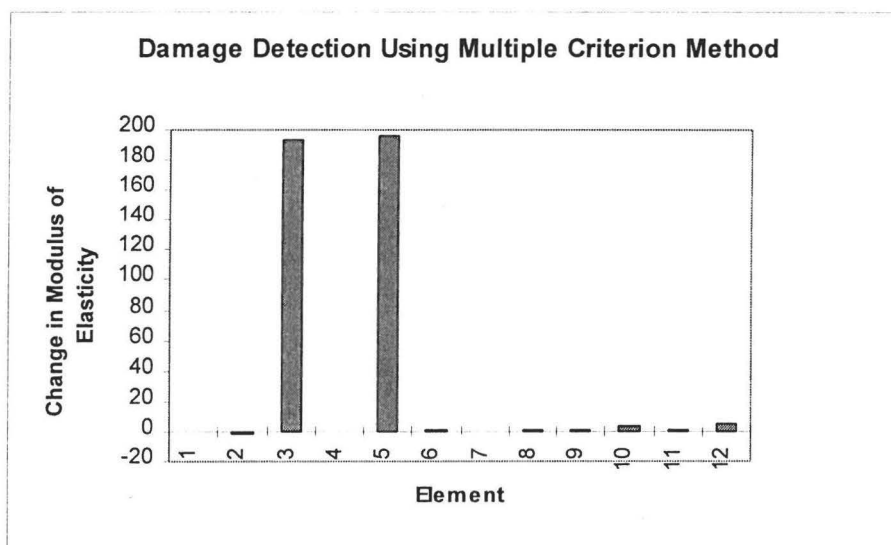


Figure 5.8 Damage detection using MCM (example1, case 2)

The results indicate that updating was performed at elements 3 and 5. This figure indicates that damage has occurred in elements 3 and 5 and the extent for both is 180.0×10^8 MPa.

In this case it was found that the three methods give results that are consistent with one another. The three methods were able to detect the presence of damage, its location and a factor (change in modulus of elasticity) that can be used to determine its extent.

5.2.3. Damage Case 3

In the third damage case an additional damage was introduced at element 6. The schematic representation for such a case may be viewed in figure 5.9.

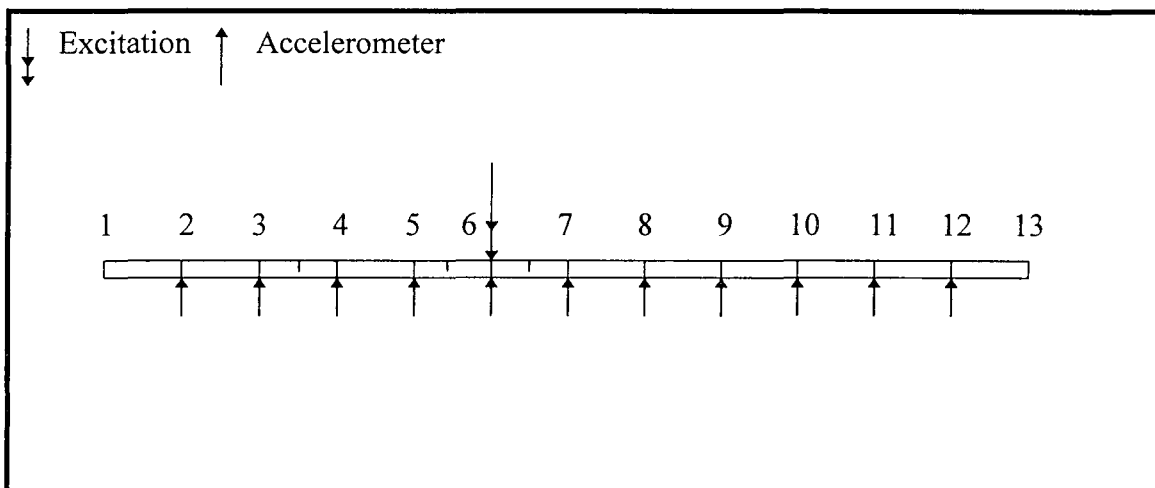


Figure 5.9 Damage at 3, 5 and 6

The DAM approach was implemented to detect damage on the structure. The results obtained may be viewed in figure 5.10. This figure shows that the FEM was updated in elements 3, 5 and 6. From these results it may be deduced that the location of damage occurred at elements 3, 5 and 6 and the extent is 190.0×10^8 MPa for all three.

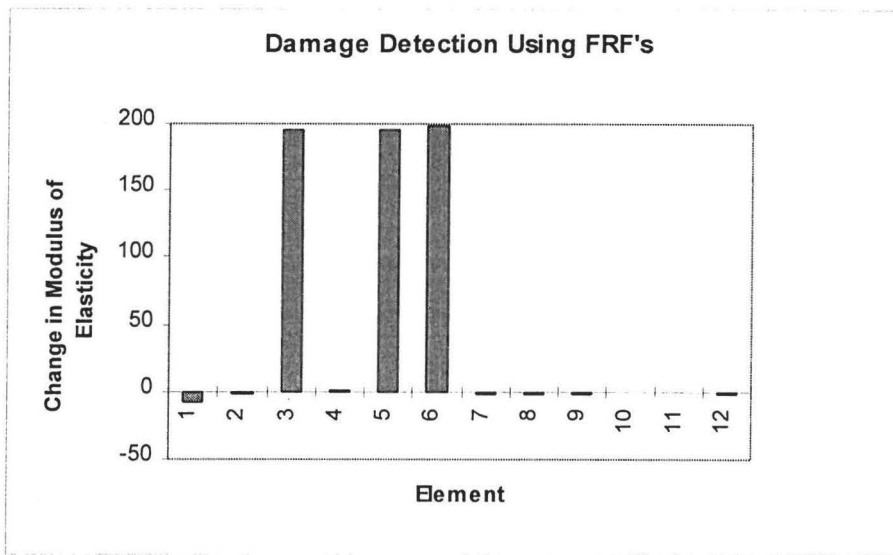


Figure 5.10 Damage detection using DAM approach

The MPM was then used to detect damage. The results may be viewed on figure 5.11.

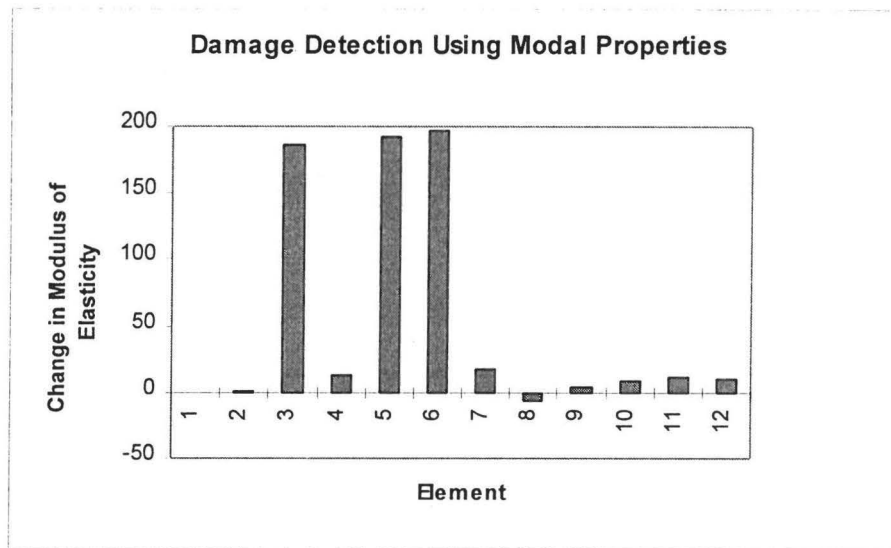


Figure 5.11 Damage detection using MPM (example1, case 3)

Figure 5.11 shows that updating was performed in elements 3, 5 and 6. Therefore damage has occurred in elements 3, 5 and 6 and the extent is approximately $180.0 \times 10^8 \text{MPa}$ for each.

Finally the MCM was implemented to detect damage. The results are shown in figure 5.12.

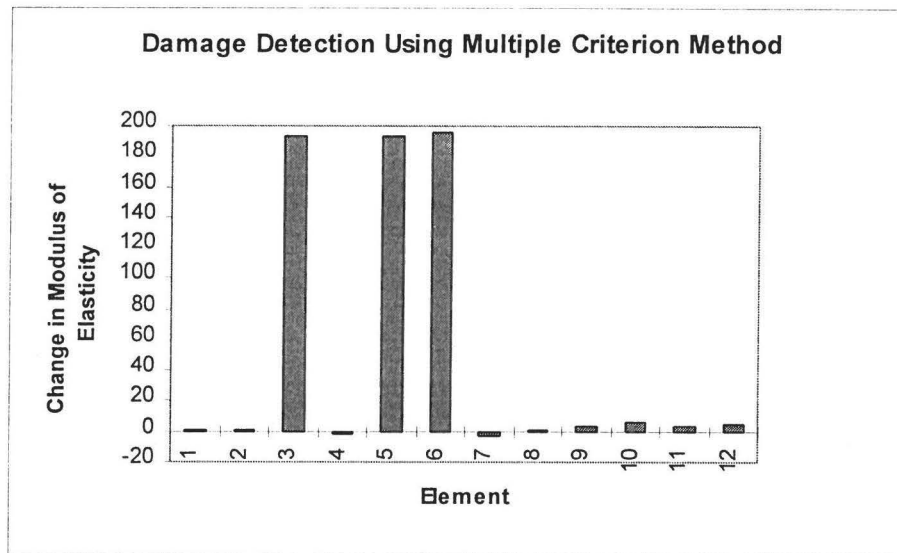


Figure 5.12 Damage detection using MCM (example 1, case 3)

The changes in modulus of elasticity vector when the MCM was used are in elements 3, 5 and 6. From this it may be deduced that damage had occurred in these elements.

The three techniques were able to detect the presence of damage at elements 3, 5 and 6 and its extent to be approximately 180.0×10^8 MPa. As explained in section 5.3 a relationship between the amount of damage that has occurred and changes in modulus of elasticity vector will have to be found and is beyond the scope of this work.

5.3. Example 2

In this example a beam with holes drilled at randomly spaced positions is considered. The picture of the structure may be viewed in Appendix D. The FEM was applied by dividing the beam into 11 elements. Three updating procedures; the DAM, the MPM and the MCM were applied as in example 1. The structure used may be viewed in Figure 5.13.

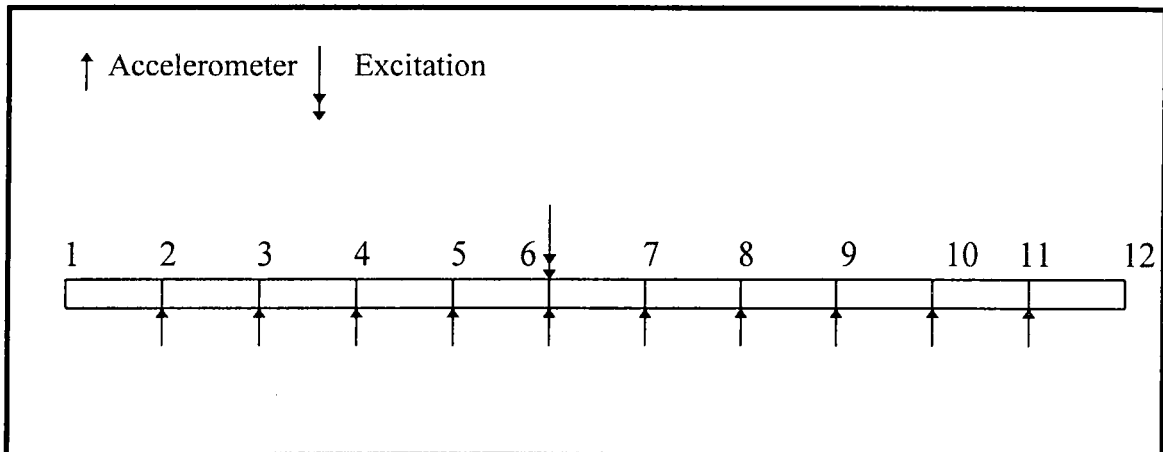


Figure 5.13 The schematic representation of the beam with holes

The accelerometer was placed consecutively from element 2 to 11 and a set of 10 FRFs was obtained. This set FRFs was incorporated into the DAM and was used to update the FEM. The results were stored for later use. Similarly, the MPM and the MCM were used to update the FEM.

5.3.1. Damage Case 1

Damage was introduced at element 2 in the beam depicted in figure 5.13. The set of FRFs measured was used to update the FEM. The modulus of elasticity vector of the FEM before damage was compared to the modulus of elasticity of the newly updated FEM. The changes in modulus of elasticity of each element are illustrated in figure 5.14.

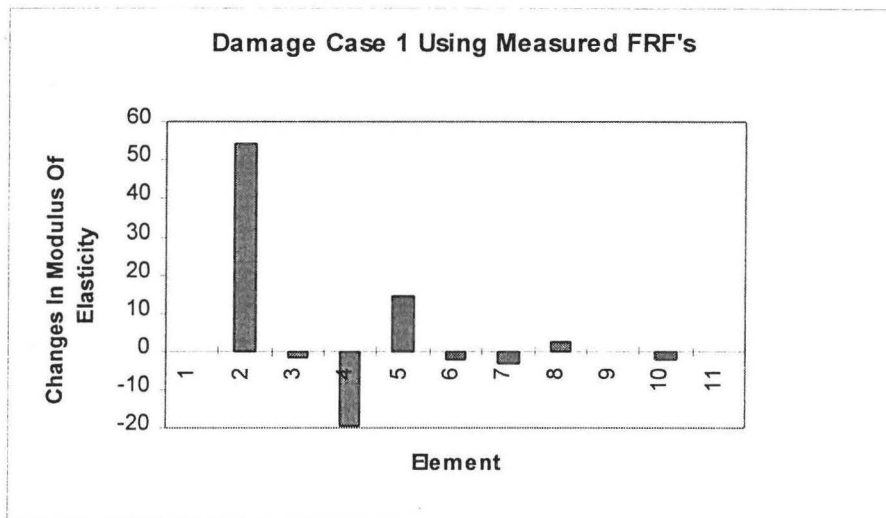


Figure 5.14 Damage detection using DAM (example 2, case1)

Figure 5.14 indicates that updating was performed in elements 2, 4 and 5. However, the most significant updating was performed in element 2. The fact that significant updating was obtained is an indication that damage has occurred its location at element 2 and its extent is 50.0×10^8 MPa.

This approach demonstrated the loss in stiffness at element 3 because of the presence of excessive measurement errors.

The MPM was implemented and the FEM updated. The difference between the modulus of elasticity vector of the updated FEM and the modulus of elasticity before damage was compared. This difference is illustrated in figure 5.15.

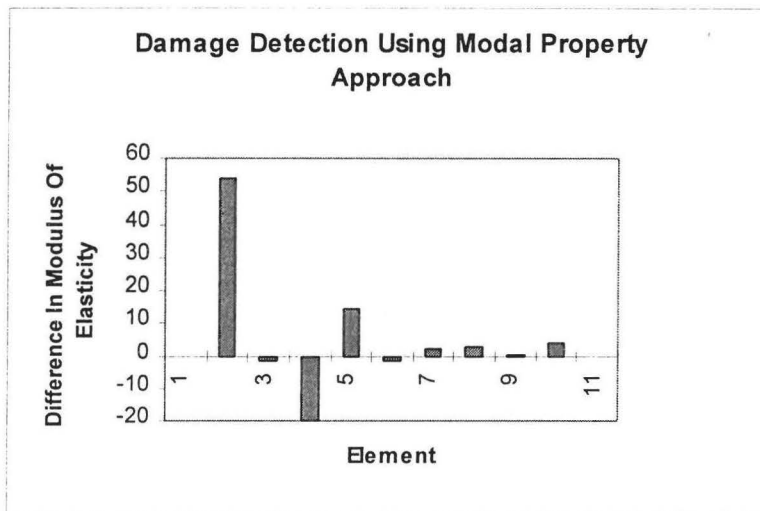


Figure 5.15 Damage detection using MPM (example 2, case 1)

Figure 5.15 indicates that the MPM updated elements 2, 4 and 5 of the FEM. It may also be observed that element 2 was updated more significantly than the other elements. The results indicate that the MPM shows that element 2 to be the location of damage. The extent of damage is about 50.0×10^8 MPa. Figure 5.15 demonstrates that element 4 experienced significant stiffness loss. This is an indication of high noise level in the FRFs which resulted with an error in the measured modes.

When the MCM was applied the difference between the modulus of elasticity vector of the of the updated FEM before and after damage is illustrated in figure 5.16.

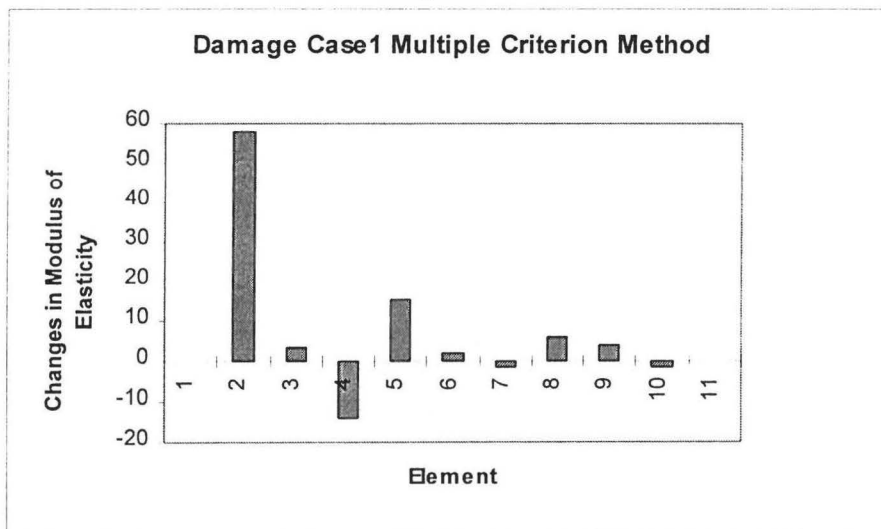


Figure 5.16 Damage detection using MCM (example 2, case 1)

Figure 5.16 indicates that updating was performed in elements 2, 4, 5, 8 and 9. However, the most significant updating was performed in element 2. The MCM shows that damage has occurred in element 2 and its extent is approximately 55.0×10^8 MPa. The FEM obtained from the MCM also experienced loss of stiffness at element 4.

The DAM, the MPM and the MCM were able to detect the presence of damage, its location (element 2) and a factor which can be used to determine its extent (change in modulus of elasticity 55.0×10^8 MPa).

5.3.2. Damage Case 2

In the second case damage was introduced at elements 2 and 3 and the FRF measurements were obtained. These measurements were used to update the FEM. The difference between the newly updated model and the updated model before damage is illustrated in Figure 5.17.

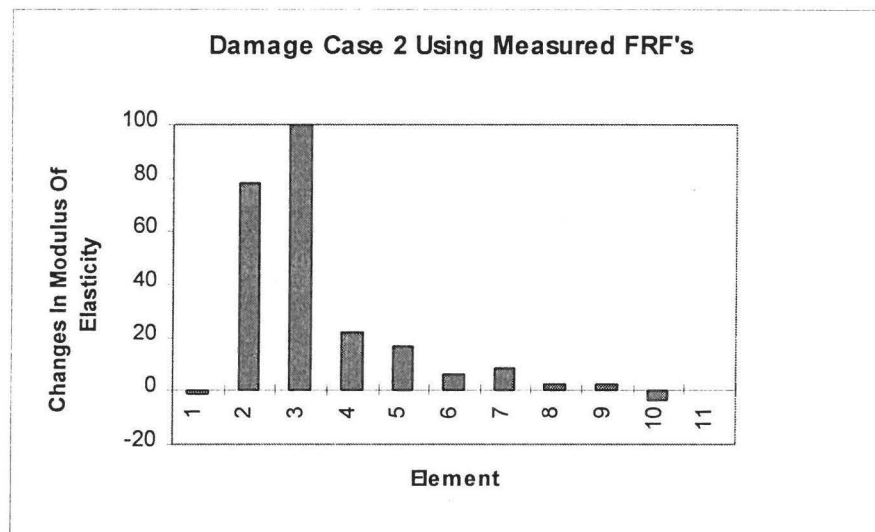


Figure 5.17 Damage detection using DAM (example 2, case 2)

Figure 5.17 indicates that significant updating was performed in elements 2 and 3. The DAM shows that damage has occurred in elements 2 and 3 and the extent of both are 80.0×10^8 MPM and 100.0×10^8 MPM respectively. The modal parameters of the structure were extracted from the measured FRFs. These parameters were used to update the FEM. The difference between the newly updated FEM and the updated FEM before damage is illustrated in Figure 5.18.

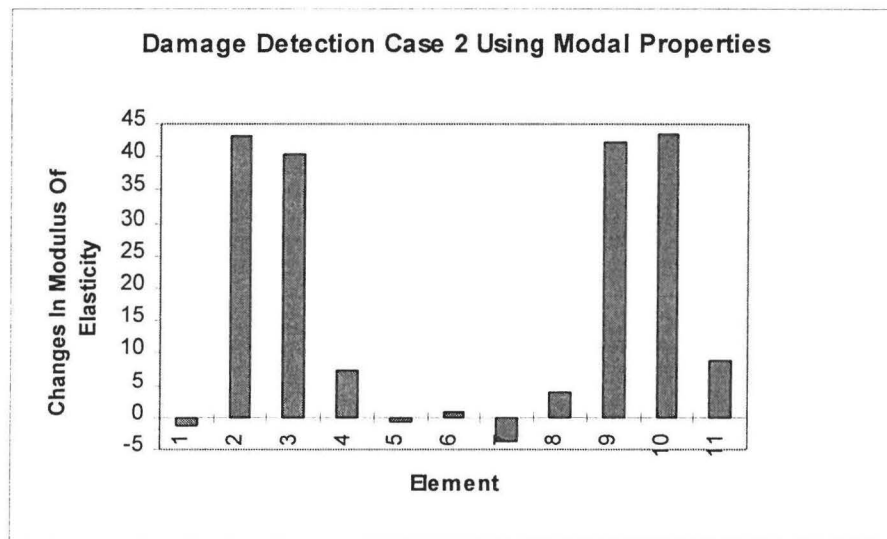


Figure 5.18 Damage detection using MPM (example 2, case 2)

Figure 5.18 indicates that significant damage occurred in elements 2, 3, 9 and 10. This approach was able to detect the presence of damage in the structure (by the virtue of the change in modulus of elasticity). This approach is very weak in locating damage or showing its extent. It should be noted, however, that this approach was able to achieve an updated model. This approach was unable to display any meaningful detection of damage because there is no way to uniquely determine its location.

The MCM was implemented and the results are demonstrated in Figure 5.19.

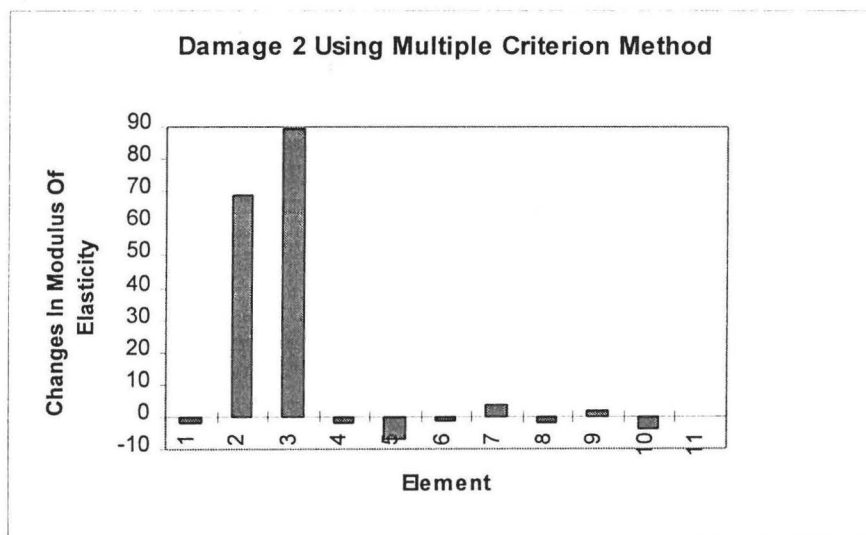


Figure 5.19 Damage detection using MCM (example 2, case 2)

The MCM predicts that damage has occurred in element 2 and 3 and the extent for both are 70.0×10^8 and 90.0×10^8 MPa respectively. The extent of damage in element 2 is closer to damage that was obtained in case 1.

The results demonstrate that the MCM was able to detect the location and the extent of damage better than followed by DAM. The MPM was able to detect the presence of damage but failed to locate its location.

5.3.3. Damage Case 3

In this case damage was introduced in elements 2, 3, and 4. The same procedure as in section 5.3.2 was repeated. The results obtained when the DAM was implemented is illustrated in figure 5.20.

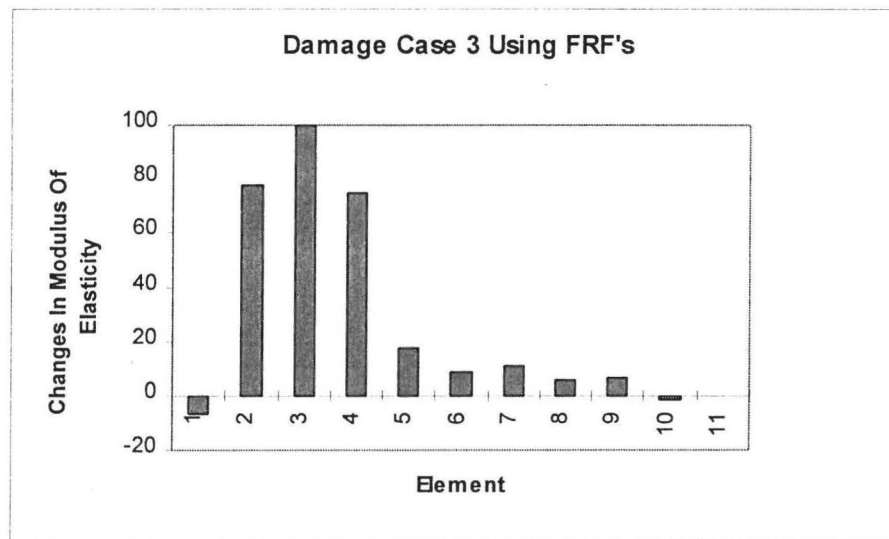


Figure 5.20 Damage detection using DAM (example 2, case 3)

Figure 5.20 demonstrates that damage has occurred in elements 2, 3 and 4. The extent of damage in elements 2, 3 and 4 were 75.0×10^8 , 100.0×10^8 and 70.0×10^8 MPa respectively.

The results obtained when the MPM was implemented are illustrated in Figure 5.21.

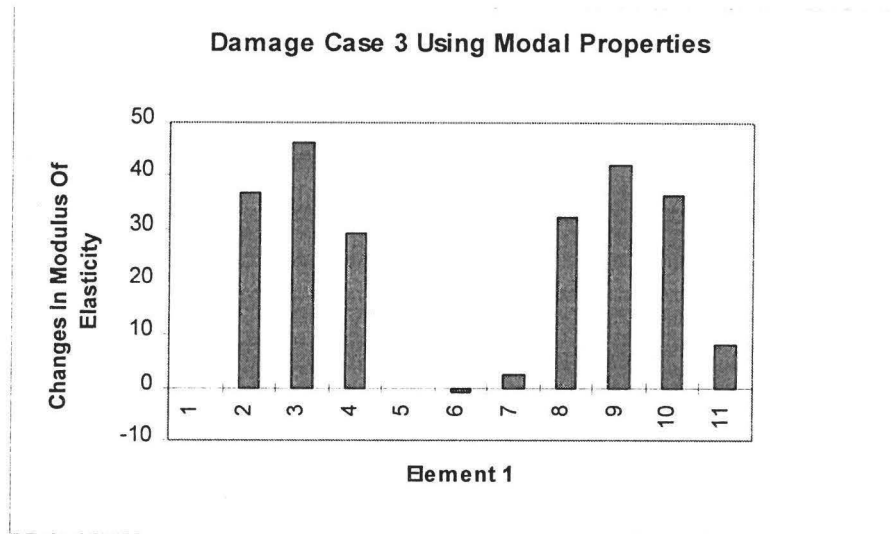


Figure 5.21 Damage detection using MPM (example 2, case 3)

Figure 5.21 shows that updating was performed in elements 2, 3, 8, 9 and 10. These results give the correct location of damage but not uniquely because they also show incorrect locations.

When MCM was implemented the results in figure 5.22 were obtained.

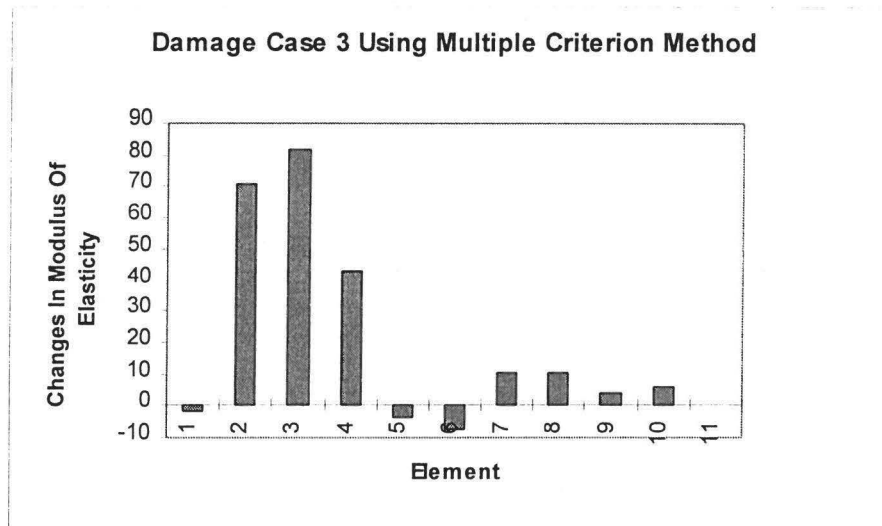


Figure 5.22 Damage detection using the MCM (example 2, case 3)

These results indicate that damage has occurred in elements 2, 3 and 4. The extent of damage are 70.0×10^8 , 80.0×10^8 and 45.0×10^8 MPa.

These results demonstrate that the MCM and the DAM are appropriate for multiple damage detection. The MPM was able to detect the presence of damage but failed to detect the location and extent especially for multiple damages.

5.4. Example 3

The third example is an H-shaped structure which may be viewed in Appendix D and figure 5.23. The accelerometer and excitation were mounted as shown in the figure 5.23. The FRF measurements were taken used to identify the measured modes. The DAM, the MPM and MCM were implemented and the FEM was updated. The results from the three models were stored.

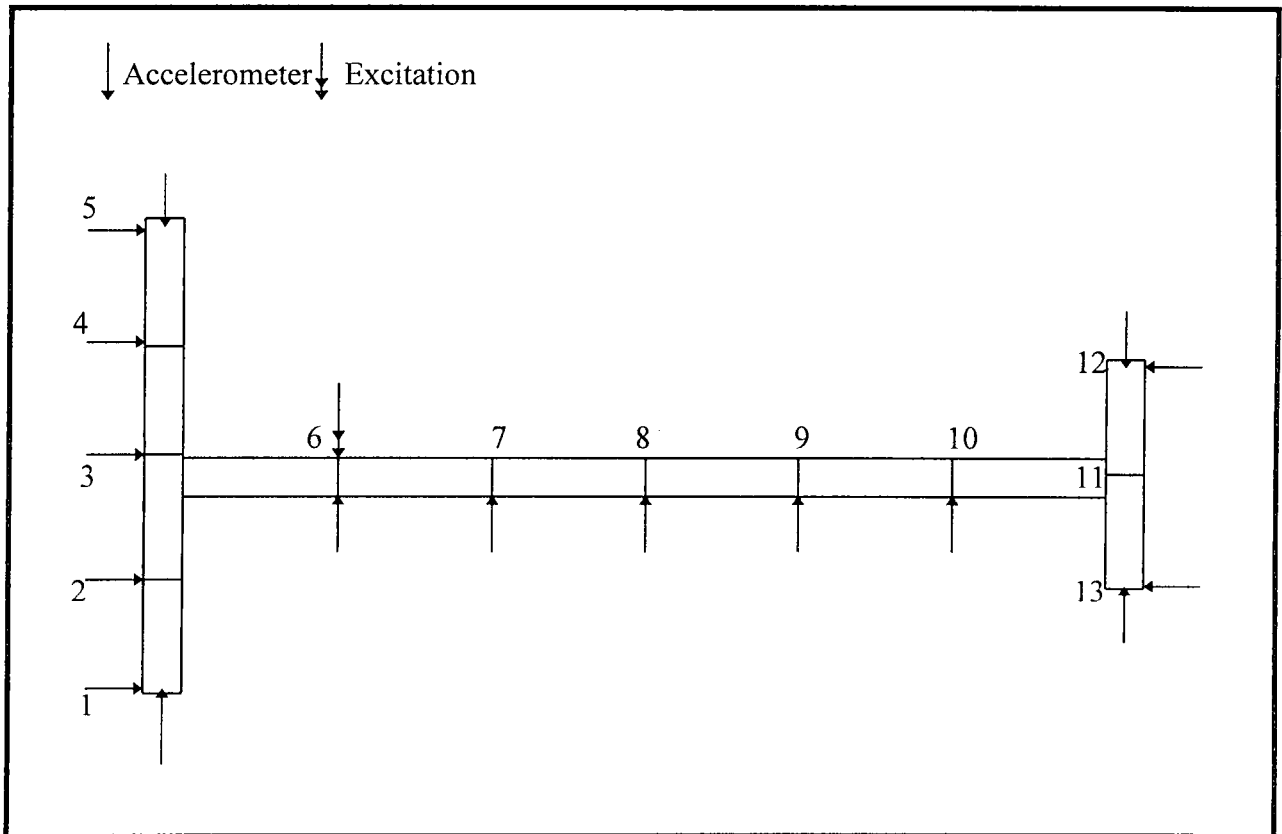


Figure 5.23 The schematic representation of the irregular H-shaped structure

5.4.1. Damage Case 1

In this example damage was introduced in element 3. The measured DAM was used to detect damage on the structure and the results may be viewed in Figure 5.24.

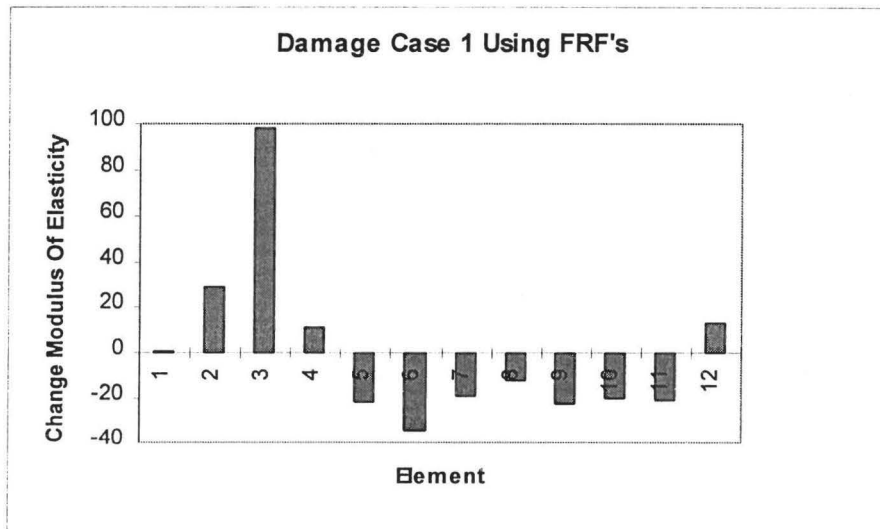


Figure 5.24 Damage detection using DAM (example 3, case 1)

The results indicate that the modulus of elasticity of all the elements were updated. Element 2 was updated most significantly than the other elements. The DAM indicate that damage has occurred in element 3 and its extent was 100.0×10^8 MPa.

The MPM was implemented and the results may be viewed in Figure 5.25.

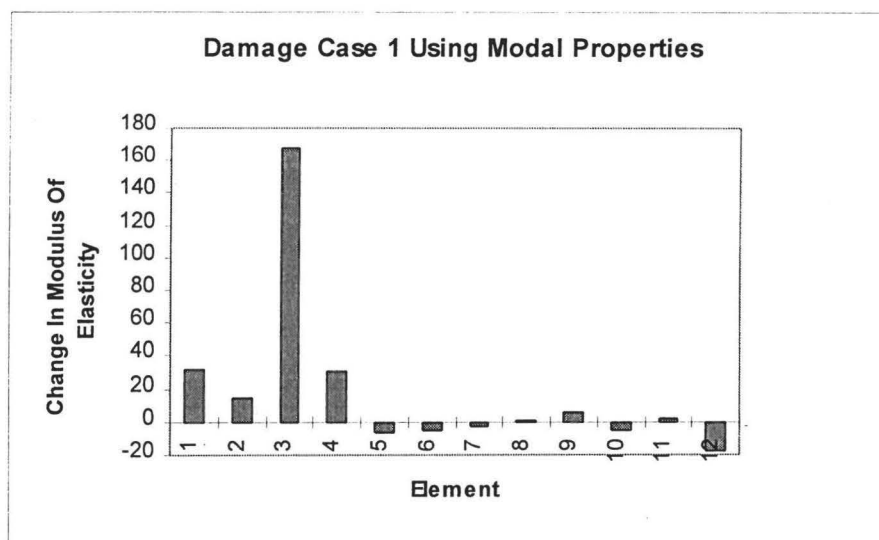


Figure 5.25 Damage detection using MPM (example 3, case 1)

Figure 5.25 indicates that although all elements were updated, element 3 was updated most significantly than other elements. The results indicate that damage of magnitude 160.0×10^8 MPa has occurred in element 3.

The MCM was implemented and the results are displayed in Figure 5.26.

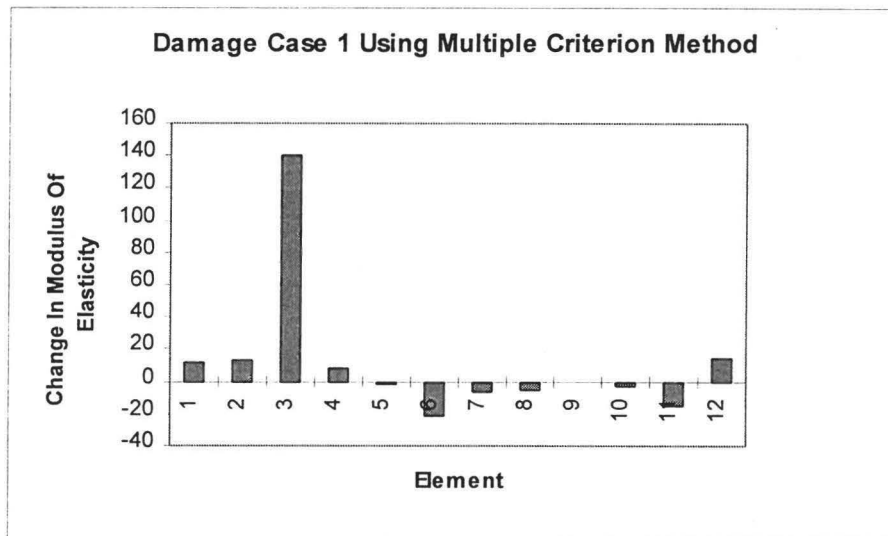


Figure 5.26 Damage detection using MCM (example 3, case 1)

Figure 5.26 indicates that element 3 was most significantly updated. From these results it is concluded that damage has occurred in element 3 and has a magnitude of 140.0×10^8 MPa.

The results from the DAM, MPM and MCM show that the three methods detect damage, its location and its extent at element 3. The magnitudes of the damage given by three methods, however, were not consistent with one another. The MCM gives the magnitude of damage which is more consistent with the level of damage introduced.

5.4.2. Damage Case 2

In this case damage was introduced in elements 3 and 4. The three approaches were applied as discussed before. The results obtained when the DAM was implemented may be viewed figure 5.27.

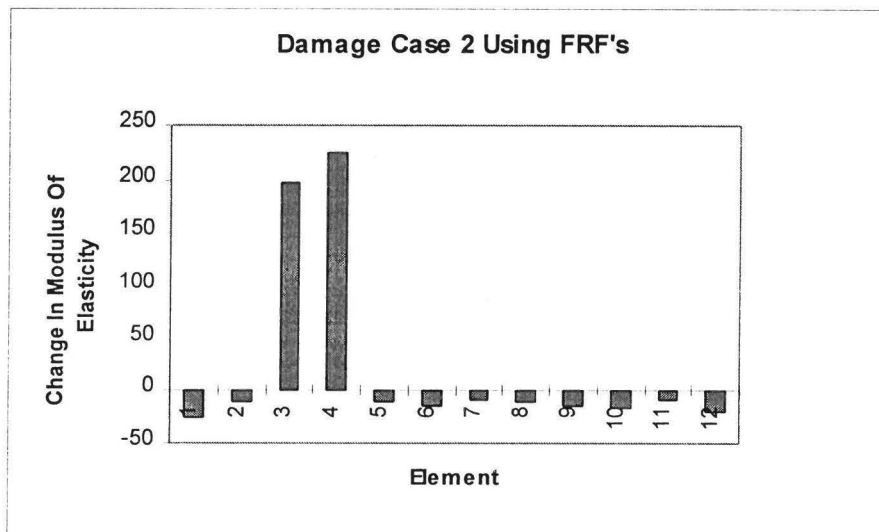


Figure 5.27 Damage detection using DAM (example 3, case 2)

Figure 5.27 indicates that elements 3 and 4 were more significantly updated than the other elements. This approach indicates that damage has occurred in elements 3 and 4 and the respective magnitudes of damage are 200.0×10^8 and 225.0×10^8 MPa's.

The MPM was employed and the results are shown in figure 5.28.

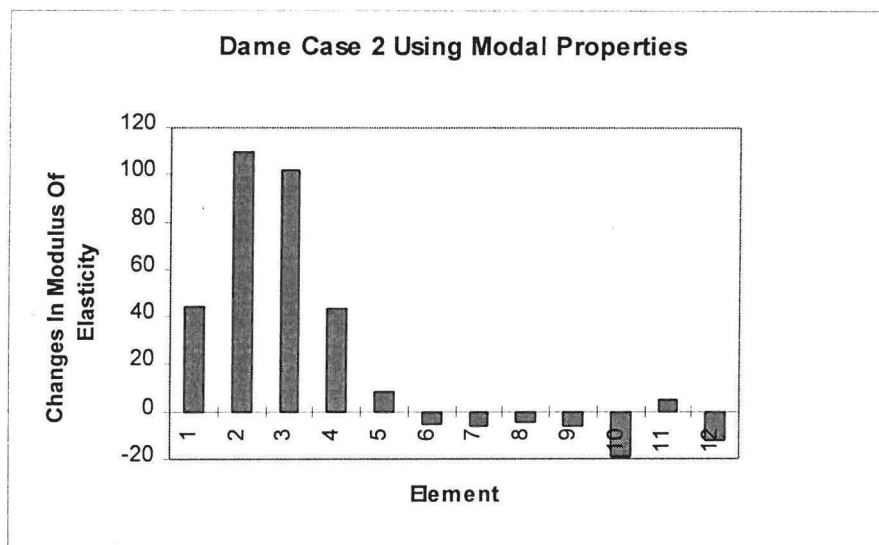


Figure 5.28 Damage detection using MPM (example 3, case 2)

The MPM indicates that elements 2 and 3 were significantly updated. It should be noted, however, that other elements were updated. This method predicts damage to have

occurred in elements 2 and 3 with magnitudes of 110.0×10^8 and 100.0×10^8 MPa respectively.

The MCM was implemented and the results are shown in Figure 5.29.

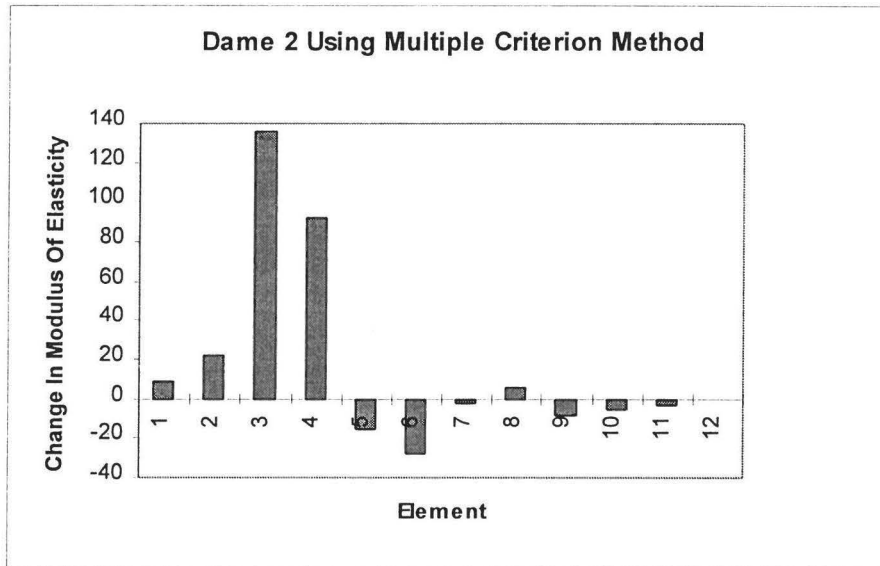


Figure 5.29 Damage detection using MCM (example 3, case 2)

Figure 5.29 indicates that damage has occurred in elements 3 and 4 with 130.0×10^8 MPa and 80.0×10^8 MPa respectively.

The results demonstrate that the DAM and the MCM were able to detect damage on elements 3 and 4. The MPM, though it detected damage on elements 3 and 4, did not explicitly or clearly detect the location of damage as the DAM and MCM (see figure 5.28).

5.4.3. Damage Case 3

In this case damage was introduced in elements 3, 4 and 5 and the same procedure as in the previous section was implemented.

The results obtained when the DAM was implemented are given in figure 5.30.

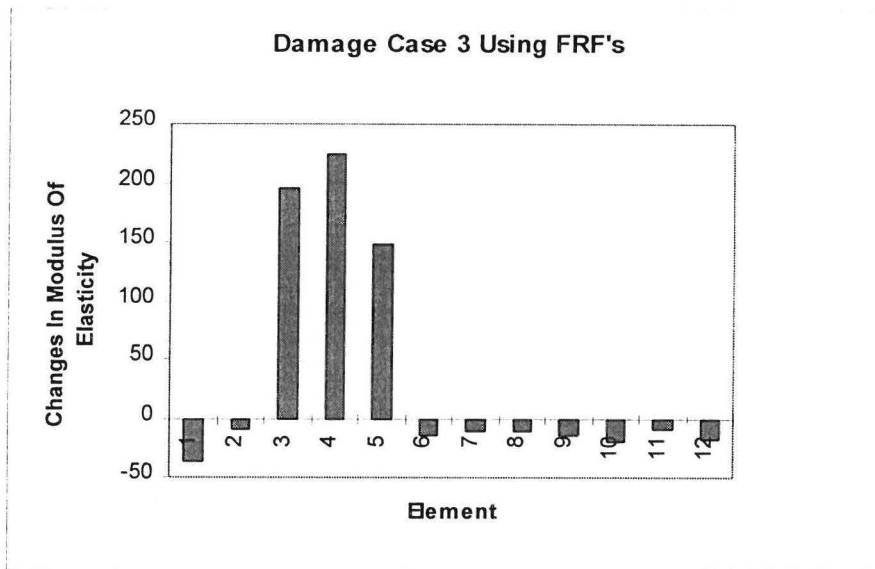


Figure 5.30 Damage detection using DAM (example 3, case 3)

Figure 5.30 indicates that the DAM updated elements 3, 4 and 5 more significantly than the other elements. The magnitudes of damage that have occurred are 200.0×10^8 , 225.0×10^8 and 150.0×10^8 MPa respectively.

The MPM was employed and the results are displayed in Figure 5.31.

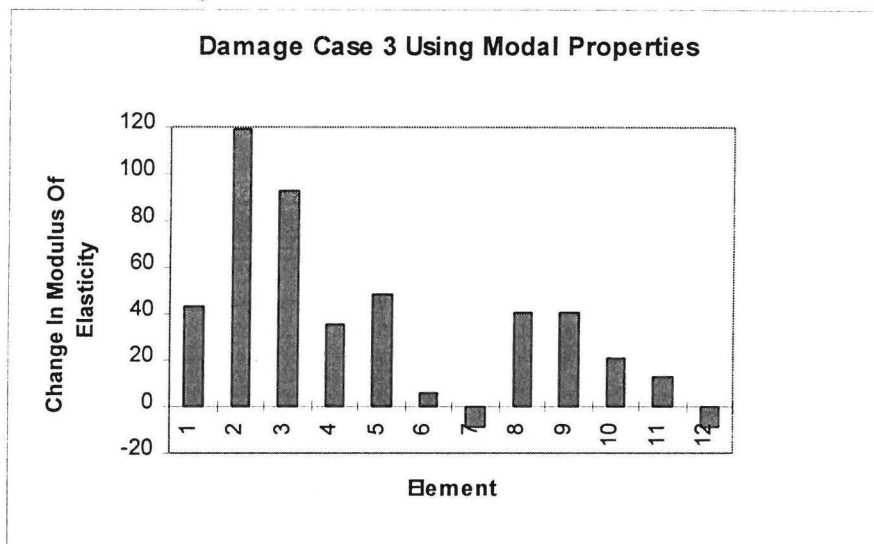


Figure 5.31 Damage detection using MPM (example 3, case 3)

Figure 5.31 seems to indicate that damage has occurred in elements 2 and 3 with magnitudes 120.0×10^8 and 90.0×10^8 MPa respectively. The fact that significant updating was performed is an indication that damage was present.

When the MCM was implemented the results in figure 5.32 were obtained.

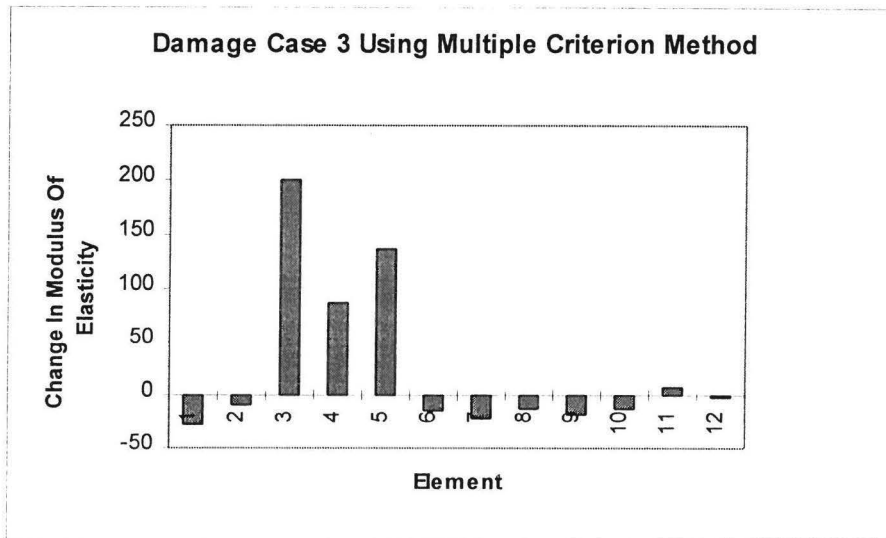


Figure 5.32 Damage detection using MCM (example 3, case 3)

Figure 5.32 indicates that damage has occurred in elements 3, 4 and 5 and has magnitudes of 200.0×10^8 , 100.0×10^8 and 150.0×10^8 MPa respectively.

The results given by the MCM and the DAM were able to show that damage has occurred in elements 3, 4 and 5. The MPM could detect the presence of damage but failed to detect its extent and location.

5.5. Conclusions

In this chapter the new damage detection method was tested using three different results. The results show that the MCM gives the best results followed by the DAM then the MPM. This is because of the fact that the MCM satisfies the measured modal properties and FRF's.

6. Conclusion

In this study a new Multiple Criterion Method (MCM) was proposed and tested using a simple beam, a beam with holes, and an irregular H-shaped structure. The MCM minimises the sum of the Euclidean norm of the error vector obtained from the equation of motion and that obtained from the modified eigenvalue equation. The DAM minimises the Euclidean norm of the error vector from the equation of motion. The MPM minimises the Euclidean norm of the error vector obtained from the modified eigenvalue equation. The results given by the MCM were compared to the results obtained by adding the DAM to the MPM. The three methods were compared using two criteria: the ability to reproduce the measured parameters and the ability to detect damage on the structure. Several issues had to be resolved before the comparisons could be made.

The first issue resolved was how the weighting functions could be chosen. Initially the errors from the DAM and the MPM were added together using variable weighting functions. It was discovered that the optimisation procedure tends to give more weight to the MPM. This is because the MPM tends to give smaller error than the DAM since the DAM has more experimental data than the MPM. It was also discovered that in case of the use of variable weighting functions, the better the accuracy of the FRF data becomes, the more equal the weighting functions become. For the rest of this study it was assumed that the accuracy of the FRF was almost the same as that of the MPM. Because of this assumption it was decided that the DAM and MPM be given equal weights when the MCM was formulated.

The assumption in the previous paragraph worked well, but for future research it is suggested that the rate of convergence be taken into account when the weighting functions are decided upon. In this study it was discovered that the DAM method shows a linear convergence rate, while the MPM shows a quadratic rate of convergence. This may be achieved by computing the sensitivity of the error due to changes in physical

parameters for the MCM and the DAM. This will ensure that the results are not biased towards the MPM results.

The second issue resolved was the problem of the FEM having more degrees of freedom than the measurements taken. Either the FEM had to be reduced or the measured coordinates be expanded. The expansion and reduction methods were programmed. It was found that the time interval per iteration for the expansion method was longer than for the reduction method. Consequently, it was decided that one of the reduction methods would be chosen. In this study it was discovered that the SEREP gives the best accuracy, followed by IRS, then dynamic reduction which is followed by the static reduction. The SEREP method was found to be unstable and consequently, required careful scaling of design variables. Consequently, the IRS method was chosen for the rest of this study. For further research, it is suggested that the application of the SEREP method on an optimisation problem be investigated further, especially with regard to how the design variables must be scaled.

As mentioned in the first paragraph, one of the criteria used to evaluate the effectiveness of the proposed method was its ability to give an updated model. The MAC and the COMAC are the methods that have been proposed before to compare the modes before and after updating. In this study an FRFAC factor was proposed to compare the measured FRFs with analytical ones. It was observed that this factor is a good criterion of comparing FRFs directly. Furthermore, it is suggested that this factor be used to update the FEM. It must also be taken into account that this factor works best when the measured data has a low level of noise. The FRFAC factor was applied selectively in the region with low noise. It was discovered that the presence of high noise level diminishes the significance of this factor as a comparison factor. When the FRFAC was compared with the COMAC and the MAC it was observed that it offered results that are on the same level of accuracy as the other two methods.

The MCM experienced several problems. One of these problems was that it requires too many iterations and is therefore computationally expensive. It was also found that by

scaling the equations of motion in the MCM, the number of iterations may be reduced. In this study the equation of motion was non-dimensionalised by dividing the DAM formulation by the value of the error it gives at the initial design variables. The same was done to the MPM formulation.

The second criterion used to evaluate the MCM was its ability to detect damage on the structures. The method of selective updating in conjunction with the MCM was used to detect damage. In selective updating the structure is divided into two components. Each component is assigned the same physical parameters. The component experiencing the most updating is further divided into smaller elements and the procedure is repeated until damage is located. The ability of the MCM in conjunction with selective updating method to detect damage was compared to the ability of the DAM and MPM. The MCM and DAM methods were generally better able to detect damage than the MPM. For further research, it is suggested that this method of selective updating be investigated.

Furthermore, the nature of the damage introduced to the structure was a saw-cut. In real structures, the main causes of damage include fatigue. In fatigue damage, the presence of damage tends to increase the level of damping on the structure. Because of this, the proportional damping assumption might not hold any longer and consequently complicated modelling of damping may be required and may compromise the effectiveness of the MCM.

The other issue pertaining to damage involves the location of damage. Damage was generally introduced only on one half of the structure. This was done purposefully to destroy the symmetry of the structure, thereby increasing the probability of the updating method detect the presence, location and the extent of damage. However, in reality the presence of damage might not necessarily destroy the symmetry of the structure. Because of this, the proposed updating method needs to be investigated for randomly introduced damage.

In the beginning of this study it was intended that the new method would detect the extent of damage. It was hoped that the extent in which physical parameters would change as a result of damage would correlate well to the extent of damage that occurred. It was discovered, however, that the issue of relating changes in physical parameters to the extent of damage was difficult since it requires highly accurate experimental data which could not be achieved in this study. It was observed that there does exist some relationship between the changes in modulus of elasticity and the amount of damage in the structure. Consequently, it is postulated that the relationship between the changes in modulus of elasticity and the amount of damage that has occurred is a function of the material property of the structure and requires further investigation.

From the two criteria of evaluating the proposed method, it was discovered that the updated model which best approximates the measured parameters is not necessarily the FEM which predicts the position and extent of damage. In concluding this study, it is postulated that for the updated FEM to be unique, it must simultaneously approximate the measured parameters and detect the location of damage. For further research, it is suggested that the updating ability of the FEM be unified with the damage detection ability.

Since this method is a multiple criterion method, other conditions may be added to the MCM equation so that the probability of obtaining a unique solution is increased. In this study it is concluded that the MCM does enhance the probability of getting a unique solution because it was better able to detect damage on the structure when compared with MPM and DAM.

References

- Allemang, R.J. and Brown, D.L. 1982. A correlation coefficient for modal vector analysis, *1st International Modal Analysis Conference*, 110-116.
- Andry, A.N, Shapiro, E.Y. and Chung, J.C. 1983. Eigenstructure assignment for linear systems, *IEEE Transactions on Aerospace and Electronic Systems*, AES-19(5), 711-729.
- Avitabile, P, Foster, T. and O'Callahan, J. 1989. Comparison of reduction vs.expansion for orthogonality checks, *7th International Modal Analysis Conference*, 225-231.
- Avitabile, P, O'Callahan, J. and Milani, J. 1989. Comparison of system characteristics using various model reduction techniques, *7th International Modal Analysis*, 1109-1115.
- Avitabile, P, Pechinsky, F. and O'Callahan, J. 1992. Study of vector correlation using various techniques for model reduction, *10th International Modal Analysis Conference*, 572-583.
- Balmès, E. 1995. Structural Dynamics Toolbox For Use with MATLAB, *Scientific Software*.
- Balmès, E. 1993. Integration of existing methods and user knowledge in a MIMO identification algorithm for structures with high modal densities. *11th International Modal Analysis Conference*, 613-619.
- Baruch, M. 1978. Optimization procedure to correct stiffness and flexibility matrices using vibration data, *AIAA Journal*, 16(11), 1208-1210.
- Baruch, M. and Itzhak, T. 1977. Optimal weighted orthogonalization of measured modes. *TAE Report*. 297.

Bathe, K.J. 1982. Finite Element Procedures In Engineering Analysis, *Prentice-Hall, Inc, Englewood Cliffs*.

Ben-Haim, Y. 1992. Adaptive diagnosis of faults in elastic structures by static displacement measurement: The method of selective sensitivity, *Mechanical Systems and Signal Processing*, **6**, 85-96.

Ben-Haim, Y. 1994. Adaptive model updating by selective sensitivity: Overview and new results, *International Journal of Numerical Methods in Engineering*, in press.

Ben-Haim, Y. and Prells, U. 1993. Selective sensitivity in the frequency domain, -I. Theory, *Mechanical Systems and Signal Processing*, **7**, 461-475.

Berger, H, Chaquin, J.P, and Ohayon, R. 1984. Finite element modal adjustment using experimental modal data, *2nd International Modal Analysis Conference*, 1-5.

Berman, A. and Flannelly, W.G. 1971. Theory of incomplete models of dynamic structures, *AIAA Journal*, **9**(8), 1481.

Berman, A. 1989. Non-unique structural system identification, *7th International Modal Analysis Conference*, 355-359.

Burden, R.L and Faires, J.D. 1993. *Numerical Analysis*, 5th edition, PWS Publishing Company.

Caesar, B. 1987. Updating system matrices using modal test data, *5th International Modal Analysis Conference*, 453-459.

Caesar, B. 1983. Update and Identification of Dynamic Mathematical Models, *1st International Modal Analysis Conference*, 394-401.

Cawley, P. and Adams, D. 1979. The location of defects in structures from measurements of natural frequencies. *I.Mech. E Journal of Strain Analysis*, **14**(2), 49-57.

Chen, J.C, Kuo, C.P, and Garba, J.A. 1983. Direct structural parameter identification by nodal test results, *AIAA/ASME,ASCE/AMS 24th Structural Dynamic and Material Conference*, 44-49.

Collins, J.D, Hart, G.C, Hasselman, T.K, and Kennedy, B. 1974. Statistical identification of structures, *AIAA Journal*, **12**(2), 185-190.

D'Ambrogio, W. and Zobel, P.B. 1990. Damage detection in truss structures using a direct updating technique, *ISMA19 Tools for Noise and Vibration Analysis*, vol II.

Ewins, D.J. 1986. *Modal Testing: Theory and Practice*, Research Studies Press, Letchworth.

Ewins, D.J, He, J. and Lieven, N.A.J. 1988. A review of the error matrix method (emm) for structural dynamic model comparison, *Proceedings of ESA*, The Netherlands.

Friswell, M.I, Garvey, S.D. and Penny, J.E.T. 1994. Model reduction using an iterated IRS technique, *5th International Conference on Recent Advances in Structural Dynamics*, Southampton, UK, July 1994, 879-889.

Friswell, M.I. 1989. Updating physical parameters from frequency response function data. *Transactions of the ASME, Journal of Vibration and Acoustics*, **112**(1), 93-97.

Friswell, M.I. and Mottershead, J.E. 1995. *Finite element model updating in structural dynamics*, Kluwer Academic Publishers.

Friswell, M.I. and Penny, J.E.T. 1992. The effect of close or repeated eigenvalues on the updating of model parameters from FRF data, *Transactions of the ASME, Journal of Vibration and Acoustics*, **114**(4), 514-520.

Fistte, E., Stavrinidis, C. and Ibrahim, S. 1988. Error location and updating of analytical dynamic models using a force balance method, *6th International. Modal Analysis Conference*, 1063-1070.

Foster, C.D. and Mottershead, J.E. 1990. A method for improving finite element models by using experimental data: Application and implications for vibration Monitoring, *International Journal of Mechanical Sciences*, **32**(3), 191-203.

Goh, E.L. and Mottershead, J.E. 1993. On model reduction techniques for finite element updating. *NAFEMS/DTA International Conference on Structural Dynamics, Modelling, Test, Analysis and Correlation*, 421-432.

Grace, A. 1990. *Optimization Toolbox User's Guide*, The Mathworks, Inc.

Guyan, R.J. 1965. Reduction of stiffness and mass matrices, *AIAA Journal*, **3**(2), 380.

Gysin, H.P. 1986. Critical application of the error matrix method of localisation of finite element modelling inaccuracies, *4th International Modal Analysis Conference*, 1339-1351.

Gysin, H.P. 1990. Comparison of expansion methods of fe modelling error localization, *8th International Modal Analysis Conference*, 195-204.

Heylen, W. 1990. Optimization of model matrices by means of experimentally obtained dynamic data. *8th International Modal Analysis Conference*, 32-38.

Heylen, W, and Sas, P, 1987. Review of model optimization techniques. *5th International Modal Analysis Conference*, 1177-1182.

Heylen, W, and Janter, P, 1988. Application of the modal assurance criterion in dynamic model updating, *13th International Modal Analysis Seminar*, 1-18.

Ibrahim, S.R, Stavriniadis, C, Fissette, E. and Brunner, O. 1989. A direct two response approach for updating analytical dynamic models of structures with emphasis on uniqueness, *7th International Modal Analysis Conferencr*, 340-345.

Imregun, M. and Ewins, D.J. 1993. An investigation into mode shape expansion techniques, *11th International Modal Analysis Conference*, 168-175.

Janter, T, Heylen, W, and Sas, P, 1988. A comparison between model optimization procedures based on the model optimization parameter set, *6th International Modal Analysis Conference*, 87-92.

Janter, T. and Sas, P, 1990. Uniqueness aspects of model-updating procedure, *AIAA Journal*, **28**(3), 538-543.

Ju, F.D. and Mimovitch, M.E. 1988 Experimental diagnosis of fracture damage in structures by modal frequency method, *ASME Journal of Vibration, Acoustics, Stress and Reliability in Design*, **110**, 456-463.

Jung, H., 1990 Sensitivity analysis using macro elements, *15th International Modal Analysis Seminar*, K.U. Leuven.

Kabè, A.M. 1985. Stiffness matrix adjustment using modal data, *AIAA Journal*, **23**(9), 1431-1436.

Lim, T.W. and Kashangaki, T.A. Structural damage detection of space truss structures using best achievable eigenvectors, *AIAA Journal*, 32(5), 1049-1057.

Link, M. 1986 Identification of physical system matrices using incomplete vibration test data, *4th International Modal Analysis Conference*, 386-393.

Lallement, G. and Piranda, J. 1990 Localization methods for parametric updating of FE models, *8th International Modal Analysis Conference*, 579-585.

Lawrence, C. 1993. Identification of differences between finite element analysis and experimental vibration data, *11th International Modal Analysis Conference*, 1681-1691.

Leung, A.Y.T. 1987. An accurate method of dynamic condensation in structural analysis, *International Journal of Numerical Methods in Engineering*, 1705-1715.

Lieven, N.A.J. and Ewins, D.J. 1988. Spatial correlation of mode shapes, the coordinate modal assurance criterion, *6th International Modal Analysis Conference*, 690-695.

Lieven, N.A.J. and Ewins, D.J. 1990, Expansion of modal data for correction, *8th International Modal Analysis Conference*, 605-609.

Lieven, N.A.J. and Ewins, D.J. 1990, Error location and updating the finite element model using singular value decomposition technique (SVD), *8th International Modal Analysis Conference*, 769-773.

Link, M. and Santiago, O.F. 1991. Updating and localizing structural errors based on minimisation of equation errors, *International Conference on Spacecraft Structures and Mechanical Testing*, ESA/ESTEC, Noordwijk, Holland.

Lin, R.M. and Ewins, D.J. 1990. Model updating using FRF data, *15th International Modal Analysis Seminar*, 141-163.

Minus, C. and Inman, D.J. 1988. Correcting finite element models with measured modal results using eigenstructure assignment methods, *6th International Modal Analysis Conference*, 583-587.

Minus, C. and Inman, D.J. 1990. Matching finite element models to modal data, *Transactions of the ASME, Journal of Vibration and Acoustics*, **112**(1), 84-92.

Mottershead, J.E. 1990. Theory for the estimation of structural vibration parameters from incomplete data, *AIAA Journal*, **28**(3), 559-561.

Nobari, A.S, Imregun, M. and Ziaei Rad, S. 1990 On the uniqueness of updated models. ISMA19, Tools for Noise and Vibration Analysis, vol 1, 151-163.

O'Callahan, J.C. 1989. A procedure for an Improved Reduced System (IRS) model, *7th International Modal Analysis Conference*, 17-21.

O'Callahan, J, Avitabile, P. and Riemer, R. 1989. System equivalent reduction expansion process, *7th International Modal Analysis Conference*, 29-37.

Paz, M. 1984. Dynamic condensation, *AIAA Journal*, **22**(5), 724-727.

Penny, J.E.T, Friswell, M.I. and Garvey, S.D. 1994. Automatic choice of measurement locations for dynamic testing, *AIAA Journal*, **32**(2), 407-414.

Rizos, P.F. *et al.* 1990 Identification of crack location and magnitude in a cantilever beam from vibration modes, *Journal of Sound & Vibration*, **138**(3), 381-388.

Sestieri, A. and D'Ambrogio, W. 1989. Why be modal: how to avoid the use of modes in the modification of vibrating systems, *7th International Modal Analysis Conference*, **4**(1), 25-30.

Sidhu, J. and Ewins, D.J, 1984. Correction of finite element and modal test studies of a practical structure, *2nd International Modal Analysis Conference*, 756-762.

Slater, J.C, Johnson, A.R, Fatemi, B, and Wiederrich, J.L, 1988. Model refinement through a statistical analysis of a mode shape difference vector, *6th International Modal Analysis Conference*, 93-99.

The Mathworks. 1992. *MATLAB Reference guide*.

Urgeueira, A.P.V, Lieven, N, and Ewins, D.J. 1990. A generalized reduction method for spatial models. *8th International Modal Analysis Conference*, 22-27.

Zimmerman, D.C. and Kaouk, M. 1992 Eigenstructure assignment approach for structural damage detection, *AIAA Journal*, **30**(7), 1848-1855.

Zimmerman, D.C. and Widengren, M. 1990. Correcting finite element models using a symmetric eigenstructure assignment technique, *AIAA Journal*, **28**(9), 1670-1676.

Wei, J.J.C, Zhang, Q, Allemang, R.J, and Wei, M.L, 1988. Correction of finite element model via selected physical parameters, *13th International Modal Analysis Seminar*, K.U.Leuven C-12.

Wei, M.L. and Janter, T. 1988 Optimization of mathematical model via selected physical parameters, *6th International Modal Analysis Conference*, 73-79.

Wolff, T. and Richardson, M.H. 1989 Fault detection in structures from changes in their modal parameters, *7th International Modal Analysis Conference*, 87-94.

Appendix A: The Expansion and Reduction Programs

These programs are for investigating the expansion and reduction methods in order to determine which ones are appropriate for this type of work.

The programs listed in this appendix apply the Guyan reduction, dynamic reduction, improved reduced system (IRS), the System Equivalent Reduction Expansion Process (SEREP), Expansion Using Mass and Stiffness Matrices and Expansion Using Modal Data. These methods were tested using the DAM, MPM and MCM.

```
% WRITTEN BY TSHILIDZI MARWALA
% 24 JANUARY 1997
clear all;
% initial values
for i=1:10;
    E(i)=30.0;
end;
% DAMPING MATRIX
E(11)=0; E(12)=0;

% LOWER BOUNDS
for i=1:10;
    vlb(i)=60.0;
end;
vlb(11)=0; vlb(12)=0;

% UPPER BOUNDS
for i=1:10;
    vub(i)=80.0;
end;
vub(11)=50; vub(12)=50;

options(1)=1; % DISPLAY TABULAR FORM
options(14)=4000; % MAXIMUM NUMBER OF ITERATIONS
options(18)=1; % STEP SIZE
options(3)=1e-2; % CONVERGENCE PARAMETER

%THIS PART CALLS THE OPTIMIZATION ROUTINES WHICH HAVE IMPLEMENTED ALL THE
%REDUCTION AND EXPANSION METHOD
E=constr('fun_irs',E,options,vlb,vub);
% E=constr('fun_irs',E,options,vlb,vub);
% E=constr('fun_guy',E,options,vlb,vub); % guyan reduction
% E=constr('fun_dyn',E,options,vlb,vub); % dynamic reduction
% E=constr('fun_egu',E,options,vlb,vub); % expansion based on guyan reduction
% E=constr('fun_ser',E,options,vlb,vub); % serep method
% E=constr('fun_sta',E,options,vlb,vub); % static reduction
% E=constr('fun_ese',E,options,vlb,vub); % serep expansion
```

(a) Reduction Using Guyan Reduction

```

%fun_guy.m
function [func,g]=fun(E);
% load FRF
load frf;
dof=size(IIf);
dof_f=dof(2);
dof_w=dof(1);
% LOAD COMPUTED MODES
load mod_gu_r;
% DEFINITION OF GEOMETRY
% Length (x) L [m]
L=0.9;
% Width (y) b [m]
b=0.0292;
% Thickness (z) h [m]
h=0.0096;
% CONSIDER BEAM WITH 10 ELEMENTS
d=L/10;
Iz=(1/12)*b*h^3;
Iy=(1/12)*h*b^3;
Jx=(1/12)*b*h*(b^2 + h^2);
Area =b*h;
% CO-ORDINATES OF NODES
% node# unused x y z
node=[ 10 0 0 0 0 0
       2 0 0 0 d 0 0
       3 0 0 0 2*d 0 0
       4 0 0 0 3*d 0 0
       5 0 0 0 4*d 0 0
       6 0 0 0 5*d 0 0
       7 0 0 0 6*d 0 0
       8 0 0 0 7*d 0 0
       9 0 0 0 8*d 0 0
      10 0 0 0 9*d 0 0
      11 0 0 0 10*d 0 0
      12 0 0 0 0 1 0];
% USE BEAM ELEMENTS
elt=[ Inf abs('beam1')
% n#1 n#2 pl# il# nr 0
  1 2 1 1 12 0
  2 3 2 1 12 0
  3 4 3 1 12 0
  4 5 4 1 12 0
  5 6 5 1 12 0
  6 7 6 1 12 0
  7 8 7 1 12 0
  8 9 8 1 12 0
  9 10 9 1 12 0
 10 11 10 1 12 0];

% MATERIAL PROPERTIES FOR ALUMINIUM
% MatId MatType E [N/m^2] nu rho [kg/m^3]
pl=[ 1 1 E(1)*1E8 0.35 2700
     2 1 E(2)*1E9 0.35 2700
     3 1 E(3)*1E9 0.35 2700

```

```

4      1      E(4)*1E9      0.35      2700
5      1      E(5)*1E9      0.35      2700
6      1      E(6)*1E9      0.35      2700
7      1      E(7)*1E9      0.35      2700
8      1      E(8)*1E9      0.35      2700
9      1      E(9)*1E9      0.35      2700
10     1      E(10)*1E9     0.35      2700];
% SECTION PROPERTIES
% SecId SecType Jx [kgm^2] Iz [kgm^2] Iy [kgm^2] A [m^2]
il=[ 1 1 Jx Iy Iz Area];
% ASSEMBLE MASS AND STIFFNESS MATRIX
[M,K,mdof]=fe_mk(node,elt,pl,il);
% "ACTIVE" DEGREES OF FREEDOM CONSIDER y, z, Ty and Tz degrees of freedom
% Node 1 is fixed in translation and rotation
[adof,ind]=fe_c(mdof,[.02 .06]);
mr=M(ind,ind);kr=K(ind,ind);
[adof,ind]=fe_c(adof,[1],[,],2);
Ms=mr(ind,ind);Ks=kr(ind,ind);
% COMPUTE MASS NORMALISED NORMAL MODES
[modeq,freq]=fe_eig(Ms,Ks,[0],adof,adof);
% CONDENSING THE DYNAMIC STIFFNESS MATRIX GUYAN STATIC REDUCTION
master=[1 3 5 7 9 11 13 15 17 19];
slave=[2 4 6 8 10 12 14 16 18 20];
% PARTITION STIFFNESS AND MASS MATRICES
kmm=Ks(master,master);kms=Ks(master,slave);
ksm=Ks(slave,master);kss=Ks(slave,slave);
mmm=Ms(master,master);mms=Ms(master,slave);
msm=Ms(slave,master);mss=Ms(slave,slave);
% REARRANGE THE MASS AND STIFFNESS MATRICES
Ms=[mmm mms;msm mss];
Ks=[kmm kms;ksm kss];
% COMPUTING THE T VECTOR
dof=size(mmm);
dof=dof(1);
identity=zeros(size(mmm));
for n=1:dof;
    identity(n,n)=1;
end;
Ts=[identity;-inv(kss)*ksm];
% REDUCED MASS AND STIFFNESS
mrr=Ts'*Ms*Ts;krr=Ts'*Ks*Ts;
%THIS PART OF THE PROGRAM COMPUTES THE ERROR USING MEASURED MODAL
PROPERTIES
dof=size(mode); dof_m=dof(2);
for n=1:dof_m;
    e_rror=-(freqw(n).^2*mrr*mode(:,n));
    error=e_rror+ (krr*mode(:,n));
end;
func1=sqrt(sum(error.^2));
% DEFINING THE FORCE VECTOR
Force=zeros(dof_f,1);
Force(3)=1;
% DAMPING FACTOR
alfa=E(11)/100;
beta=E(12)/100;
for n=1:dof_w;
    crr=j*(alfa*mrr+beta*krr)*I/w(n);

```

```

er_ror= (-Ilw(n)^2*mrr+crr+krr)*Ilxf(n,:)-Force;
error(n)=sum(er_ror.^2);
end;
func2=sqrt(sum(error));
% THIS PART OF THE PROGRAM ADDS THE ERROR
func=func1+func2;

```

(b) Using Dynamic Reduction

```

%fun_dyn
function [func,g]=fun(E);
load frf;
dof=size(Ilxf);
dof_f=dof(2);
dof_w=dof(1);
load modek;
% DEFINITION OF GEOMETRY
% Length (x) L [m]
L=0.9;
% Width (y) b [m]
b=0.0292;
% Thickness (z) h [m]
h=0.0096;
% CONSIDER BEAM WITH 10 ELEMENTS
d=L/10;
Iz=(1/12)*b*h^3;
Iy=(1/12)*h*b^3;
Jx=(1/12)*b*h*(b^2 + h^2);
Area =b*h;
% COORDINATES OF NODES
% node# unused x y z
node=[ 1 0 0 0 0 0
      2 0 0 0 d 0 0
      3 0 0 0 2*d 0 0
      4 0 0 0 3*d 0 0
      5 0 0 0 4*d 0 0
      6 0 0 0 5*d 0 0
      7 0 0 0 6*d 0 0
      8 0 0 0 7*d 0 0
      9 0 0 0 8*d 0 0
     10 0 0 0 9*d 0 0
     11 0 0 0 10*d 0 0
     12 0 0 0 0 1 0];
% USE BEAM ELEMENTS
elt=[ Inf abs('beam1')
% n#1 n#2 pl# il# nr 0
  1 2 1 1 12 0
  2 3 2 1 12 0
  3 3 3 1 12 0
  4 4 4 1 12 0
  5 6 5 1 12 0
  6 7 6 1 12 0
  7 8 7 1 12 0
  8 9 8 1 12 0
  9 10 9 1 12 0
 10 11 10 1 12 0];

```

```

% MATERIAL PROPERTIES FOR ALUMINIUM
% MatId MatType E [N/m^2] nu rho [kg/m^3]
pl=[ 1 1 E(1)*1E8 0.35 2700
2 1 E(2)*1E9 0.35 2700
3 1 E(3)*1E9 0.35 2700
4 1 E(4)*1E9 0.35 2700
5 1 E(5)*1E9 0.35 2700
6 1 E(6)*1E9 0.35 2700
7 1 E(7)*1E9 0.35 2700
8 1 E(8)*1E9 0.35 2700
9 1 E(9)*1E9 0.35 2700
10 1 E(10)*1E9 0.35 2700];
% SECTION PROPERTIES
% SecId SecType Jx [kgm^2] Iz [kgm^2] Iy [kgm^2] A [m^2]
il=[ 1 1 Jx Iy Iz Area];
% ASSEMBLE MASS AND STIFFNESS MATRIX
[M,K,mdof]=fe_mk(node,elt,pl,il);
% "ACTIVE" DEGREES OF FREEDOM
% Node 1 is fixed in translation and rotation
% Consider y, z, Ty and Tz degrees of freedom
[adof,ind]=fe_c(mdof,[.02 .06]);
mr=M(ind,ind);kr=K(ind,ind);
[adof,ind]=fe_c(adof,[1],[,],2);
Ms=mr(ind,ind);Ks=kr(ind,ind);
% COMPUTE MASS NORMALISED NORMAL MODES
[modeq,freq]=fe_eig(Ms,Ks,[0],adof,adof);
% CONDENSING THE DYNAMIC STIFFNESS MATRIX
% GUYAN DYNAMIC REDUCTION
master=[1 3 5 7 9 11 13 15 17 19];
slave=[2 4 6 8 10 12 14 16 18 20];
% PARTITION STIFFNESS AND MASS MATRICES
kmm=Ks(master,master); kms=Ks(master,slave);
ksm=Ks(slave,master); kss=Ks(slave,slave);
mmm=Ms(master,master); mms=Ms(master,slave);
msm=Ms(slave,master); mss=Ms(slave,slave);
% REARRANGE THE MASS AND STIFFNESS MATRICES
Ms=[mmm mms;msm mss];
Ks=[kmm kms;ksm kss];
% COMPUTING THE T VECTOR
dof=size(mmm);
dof=dof(1);
identity=zeros(size(mmm));
for n=1:dof;
    identity(n,n)=1;
end;
w0=2*pi*250;
Ts=[identity;-inv(kss-w0^2*mss)*(ksm-w0^2*msm)];
% REDUCED MASS AND STIFFNESS
mrr=Ts'*Ms*Ts;kr=Ts'*Ks*Ts;
% THIS PART OF THE PROGRAM COMPUTES THE ERROR BY USING MEASURED MODEAL
PROPERTIES
dof=size(mode);
dof_m=dof(2);
for n=1:dof_m;
    e_rror=-freqw(n)^2*mrr*mode(:,n);
    error=e_rror+(kr*mode(:,n));
end;

```



```

func1=sqrt(sum(error.^2));
% THIS PART OF THE PROGRAM COMPUTES THE ERROR BY USING THE MEASURED FRF
% DEFINING THE FORCE VECTOR
Force=zeros(dof_f,1);
Force(3)=1;
% damping factor
alfa=E(11)/100;
beta=E(12)/100;
for n=1:dof_w;
    crr=j*(alfa*mrr+beta*krr)*llw(n);
    er_ror= (-llw(n)^2*mrr+crr+krr)*llxf(n,:)-Force;
    error(n)=sum(er_ror.^2);
end;
func2=sqrt(sum(error));
% THIS PART OF THE PROGRAM ADDS THE ERROR
func=func1+func2;

```

(c) Using Improved Reduced System

```

%fun_irs
function [func,g]=fun(E);
load frf;
dof=size(llxf);
dof_f=dof(2);
dof_w=dof(1);
load modek;
% DEFINITION OF GEOMETRY
% Length (x) L [m]
L=0.9;
% Width (y) b [m]
b=0.0292;
% Thickness (z) h [m]
h=0.0096;
% CONSIDER BEAM WITH 10 ELEMENTS
d=L/10;
Iz=(1/12)*b*h^3;
Iy=(1/12)*h*b^3;
Jx=(1/12)*b*h*(b^2 + h^2);
Area =b*h;
% COORDINATES OF NODES
% node# unused x y z
node=[ 1 0 0 0 0 0
       2 0 0 0 d 0 0
       3 0 0 0 2*d 0 0
       4 0 0 0 3*d 0 0
       5 0 0 0 4*d 0 0
       6 0 0 0 5*d 0 0
       7 0 0 0 6*d 0 0
       8 0 0 0 7*d 0 0
       9 0 0 0 8*d 0 0
      10 0 0 0 9*d 0 0
      11 0 0 0 10*d 0 0
      12 0 0 0 0 1 0];
% USE BEAM ELEMENTS
elt=[ Inf abs('beam1')
% n#1 n#2 pl# il# nr 0
1 2 1 1 12 0

```

```

2 3 2 1 12 0
3 4 3 1 12 0
4 5 4 1 12 0
5 6 5 1 12 0
6 7 6 1 12 0
7 8 7 1 12 0
8 9 8 1 12 0
9 10 9 1 12 0
10 11 10 1 12 0];
% MATERIAL PROPERTIES FOR ALUMINIUM
% MatId MatType E [N/m^2] nu rho [kg/m^3]
pl=[ 1 1 E(1)*1E8 0.35 2700
2 1 E(2)*1E9 0.35 2700
3 1 E(3)*1E9 0.35 2700
4 1 E(4)*1E9 0.35 2700
5 1 E(5)*1E9 0.35 2700
6 1 E(6)*1E9 0.35 2700
7 1 E(7)*1E9 0.35 2700
8 1 E(8)*1E9 0.35 2700
9 1 E(9)*1E9 0.35 2700
10 1 E(10)*1E9 0.35 2700];
% SECTION PROPERTIES
% SecId SecType Jx [kgm^2] Iz [kgm^2] Iy [kgm^2] A [m^2]
il=[ 1 1 Jx Iy Iz Area];
% ASSEMBLE MASS AND STIFFNESS MATRIX
[M,K,mdof]=fe_mk(node,elt,pl,il);
% "ACTIVE" DEGREES OF FREEDOM
% NODE 1 IS FIXED IN TRANSLATION AND ROTATION
% Consider y, z, Ty and Tz degrees of freedom
[adof,ind]=fe_c(mdof,[.02 .06]);
mr=M(ind,ind);kr=K(ind,ind);
[adof,ind]=fe_c(adof,[1],[,],2);
Ms=mr(ind,ind);Ks=kr(ind,ind);
% COMPUTE MASS NORMALISED NORMAL MODES
[modeq,freq]=fe_eig(Ms,Ks,[0],adof,adof);
% CONDENSING THE DYNAMIC STIFFNESS MATRIX
% IMPROVED REDUCED SYSTEM
master=[1 3 5 7 9 11 13 15 17 19];
slave=[2 4 6 8 10 12 14 16 18 20];
% PARTITION STIFFNESS AND MASS MATRICES
kmm=Ks(master,master);
kms=Ks(master,slave);
ksm=Ks(slave,master);
kss=Ks(slave,slave);
mmm=Ms(master,master);
mms=Ms(master,slave);
msm=Ms(slave,master);
mss=Ms(slave,slave);
% REARRANGE THE MASS AND STIFFNESS MATRICES
Ms=[mmm mms;msm mss];
Ks=[kmm kms;ksm kss];
% COMPUTING THE T VECTOR
dof=size(mmm);
dof=dof(1);
identity=zeros(size(mmm));
for n=1:dof;
    identity(n,n)=1;

```

```

end;
Ts=[identity;-inv(kss)*(ksm)];
% REDUCED MASS AND STIFFNESS
mrr=Ts'*Ms*Ts;krr=Ts'*Ks*Ts;
s1=[zeros(size(kmm));s2=[zeros(size(kms))]];
s3=[zeros(size(ksm));s4=inv(kss);
S=[s1 s2;s3 s4];
Ti=Ts+S*Ms*Ts*inv(mrr)*krr;
mrr=Ti'*Ms*Ti;krr=Ti'*Ks*Ti;
% THIS PART OF THE PROGRAM COMPUTES THE ERROR BY USING MEASURED %MODEAL
PROPERTIES
dof=size(mode);
dof_m=dof(2);
for n=1:dof_m;
    e_rror=-freqw(n).^2*mrr*mode(:,n);
    error=e_rror+krr*mode(:,n);
end;
func1=sqrt(sum(error.^2));
% THIS PART OF THE PROGRAM COMPUTES THE ERROR BY USING THE %MEASURED FRF
% DEFINING THE FORCE VECTOR
Force=zeros(dof_f,1);
Force(3)=1;
% DAMPING FACTOR
alfa=E(11)/100;
beta=E(12)/100;
for n=1:dof_w;
    crr=j*(alfa*mrr+beta*krr)*Iiw(n);
    er_ror=(-Iiw(n)^2*mrr+crr+krr)*Iixf(n,:)-Force;
    error(n)=sum(er_ror.^2);
end;
func2=sqrt(sum(error));
% This part of the program adds the error
func=func1+func2;

```

(d) System Equivalent Reduction Expansion Process (SEREP)

```

%fun_ser
function [func,g]=fun(E);
load modek;
load frf;
dof=size(Iixf);
dof_w=dof(1); % number of frequency measured
dof_f=dof(2); % number of FRF measured
% DEFINITION OF GEOMETRY
% Length (x) L [m]
L=0.9;
% Width (y) b [m]
b=0.0292;
% Thickness (z) h [m]
h=0.0096;
% CONSIDER BEAM WITH 10 ELEMENTS
d=L/10;
Iz=(1/12)*b*h^3;
Iy=(1/12)*h*b^3;
Jx=(1/12)*b*h*(b^2 + h^2);
Area =b*h;
% COORDINATES OF NODES

```

```

% node# unused x y z
node=[ 1 0 0 0 0 0 0
      2 0 0 0 d 0 0
      3 0 0 0 2*d 0 0
      4 0 0 0 3*d 0 0
      5 0 0 0 4*d 0 0
      6 0 0 0 5*d 0 0
      7 0 0 0 6*d 0 0
      8 0 0 0 7*d 0 0
      9 0 0 0 8*d 0 0
     10 0 0 0 9*d 0 0
     11 0 0 0 10*d 0 0
     12 0 0 0 0 1 0];
% USE BEAM ELEMENTS
elt=[ Inf abs('beam1')
% n#1 n#2 pl# il# nr 0
  1 2 1 1 12 0
  2 3 2 1 12 0
  3 4 3 1 12 0
  4 5 4 1 12 0
  5 6 5 1 12 0
  6 7 6 1 12 0
  7 8 7 1 12 0
  8 9 8 1 12 0
  9 10 9 1 12 0
 10 11 10 1 12 0];
% MATERIAL PROPERTIES FOR ALUMINIUM
% MatId MatType E [N/m^2] nu rho [kg/m^3]
pl=[ 1 1 E(1)*1E8 0.35 2700
     2 1 E(2)*1E9 0.35 2700
     3 1 E(3)*1E9 0.35 2700
     4 1 E(4)*1E9 0.35 2700
     5 1 E(5)*1E9 0.35 2700
     6 1 E(6)*1E9 0.35 2700
     7 1 E(7)*1E9 0.35 2700
     8 1 E(8)*1E9 0.35 2700
     9 1 E(9)*1E9 0.35 2700
    10 1 E(10)*1E9 0.35 2700];
% SECTION PROPERTIES
% SecId SecType Jx [kgm^2] Iz [kgm^2] Iy [kgm^2] A [m^2]
il=[ 1 1 Jx Iy Iz Area];
% ASSEMBLE MASS AND STIFFNESS MATRIX
[M,K,mdof]=fe_mk(node,elt,pl,il);
% "Active" degrees of freedom
% Node 1 is fixed in translation and rotation
% Consider y, z, Ty and Tz degrees of freedom
[adof,ind]=fe_c(mdof,[.02 .06]);
mr=M(ind,ind);kr=K(ind,ind);
[adof,ind]=fe_c(adof,[1],[,],2);
Ms=mr(ind,ind);Ks=kr(ind,ind);
% COMPUTE MASS NORMALISED NORMAL MODES
[mod_e,freq]=fe_eig(Ms,Ks,[0],adof,adof);
% CONDENSING THE DYNAMIC STIFFNESS MATRIX
% SEREP REDUCTION
% DEFINE MASTER AND SLAVE COORDINATES
master=[1 3 5 7 9 11 13 15 17 19];
slave=[2 4 6 8 10 12 14 16 18 20];

```

```

% PARTITION STIFFNESS AND MASS MATRICES
kmm=Ks(master,master);
kms=Ks(master,slave);
ksm=Ks(slave,master);
kss=Ks(slave,slave);
mmm=Ms(master,master);
mms=Ms(master,slave);
msm=Ms(slave,master);
mss=Ms(slave,slave);
% REARRANGE MASS AND STIFFNESS MATRICES
Ms=[mmm mms;msm mss];
Ks=[kmm kms;ksm kss];
% SELECT MODES TO BE CONSIDERED
mi=1:4; % number of modes measured
mod_mas=mod_e(master,mi);
mod_sla=mod_e(slave,mi);
mode_r=[mod_mas;mod_sla];
% CALCULATE PSEUDO INVERSE
A=mod_mas'*mod_mas;
p_inverse=inv(A)*mod_mas';
% FIND T TRANSFORMATION
T=mode_r*p_inverse;
% REDUCED MASS AND STIFFNESS
mrr=T'*Ms*T;krr=T'*Ks*T;
% USING MODE SHAPES
dof=size(mode);
dof_m=dof(2);
for n=1:dof_m;
    e_rror=-freqw(n).^2*mrr*mode(:,n);
    error=e_rror+krr*mode(:,n);
end;
func1=sqrt(sum(error.^2));
% THIS PART OF THE PROGRAM USES THE MEASURED FRF
% DEFINING THE FORCE VECTOR
Force=zeros(dof_f,1);
Force(3)=1;
% DEFINING THE DAMPING COEFFICIENTS
alfa=E(11)/100;
beta=E(12)/100;
for n=1:dof_w;
    crr=j*(alfa*mrr+beta*krr)*llw(n);
    er_ror=-llw(n)^2*mrr+crr+krr)*llxf(n,:)-Force;
    error(n)=sum(er_ror.^2);
end;
func2=sqrt(sum(error));
% THIS PART OF THE PROGRAM COMBINES THE TWO METHODS WITH
% EQUAL WEIGHTING FUNCTIONS
func=func1+func2;

```

(e) Expansion Using Mass and Stiffness Matrices

```

%fun_sta
function [func,g]=fun(E);
load frf;
dof=size(IIf);
dof_f=dof(2);
dof_w=dof(1);
load modek;
% DEFINITION OF GEOMETRY
% Length (x) L [m]
L=0.9;
% Width (y) b [m]
b=0.0292;
% Thickness (z) h [m]
h=0.0096;
% CONSIDER BEAM WITH 10 ELEMENTS
d=L/10;
Iz=(1/12)*b*h^3;
Iy=(1/12)*h*b^3;
Jx=(1/12)*b*h*(b^2 + h^2);
Area =b*h;
% COORDINATES OF NODES
% node# unused x y z
node=[ 1 0 0 0 0 0
      2 0 0 0 d 0 0
      3 0 0 0 2*d 0 0
      4 0 0 0 3*d 0 0
      5 0 0 0 4*d 0 0
      6 0 0 0 5*d 0 0
      7 0 0 0 6*d 0 0
      8 0 0 0 7*d 0 0
      9 0 0 0 8*d 0 0
     10 0 0 0 9*d 0 0
     11 0 0 0 10*d 0 0
     12 0 0 0 0 1 0];
% USE BEAM ELEMENTS
elt=[ Inf abs('beam1')
% n#1 n#2 pl# il# nr 0
  1 2 1 1 12 0
  2 3 2 1 12 0
  3 4 3 1 12 0
  4 5 4 1 12 0
  5 6 5 1 12 0
  6 7 6 1 12 0
  7 8 7 1 12 0
  8 9 8 1 12 0
  9 10 9 1 12 0
 10 11 10 1 12 0];
% MATERIAL PROPERTIES FOR ALUMINIUM
% MatId MatType E [N/m^2] nu rho [kg/m^3]
pl=[ 1 1 E(1)*1E8 0.35 2700
  2 1 E(2)*1E9 0.35 2700
  3 1 E(3)*1E9 0.35 2700
  4 1 E(4)*1E9 0.35 2700
  5 1 E(5)*1E9 0.35 2700
  6 1 E(6)*1E9 0.35 2700

```

```

7 1 E(7)*1E9 0.35 2700
8 1 E(8)*1E9 0.35 2700
9 1 E(9)*1E9 0.35 2700
10 1 E(10)*1E9 0.35 2700];
% SECTION PROPERTIES
% SecId SecType Jx [kgm^2] Iz [kgm^2] Iy [kgm^2] A [m^2]
il=[ 1 1 Jx Iy Iz Area];
% ASSEMBLE MASS AND STIFFNESS MATRIX
[M,K,mdof]=fe_mk(node,elt,pl,il);
% "Active" degrees of freedom
% Node 1 is fixed in translation and rotation. Consider y, z, Ty and Tz degrees of freedom
[adof,ind]=fe_c(mdof,[.02 .06]);
mr=M(ind,ind);kr=K(ind,ind);
[adof,ind]=fe_c(adof,[1],[],2);
Ms=mr(ind,ind);Ks=kr(ind,ind);
% COMPUTE MASS NORMALISED NORMAL MODES
[modeq,freq]=fe_eig(Ms,Ks,[0],adof,adof);
% EXPANDING USING MASS AND STIFFNESS MATRIX
master=[1 3 5 7 9 11 13 15 17 19];
slave=[2 4 6 8 10 12 14 16 18 20];
% PARTITION STIFFNESS AND MASS MATRICES
kmm=Ks(master,master);
kms=Ks(master,slave);
ksm=Ks(slave,master);
kss=Ks(slave,slave);
mmm=Ms(master,master);
mms=Ms(master,slave);
msm=Ms(slave,master);
mss=Ms(slave,slave);
Ms=[mmm mms;msm mss];Ks=[kmm kms;ksm kss];
% COMPUTING THE MODES AT UNMEASURED COORDINATES
dof=size(mode);
dof=dof(2);
for n=1:dof;
unmeasured_mode(:,n)=-inv(freqw(n).^2*mss+kss)*(freqw(n).^2*msm+ksm)*mode(:,n);
end;
mode=[mode;unmeasured_mode];
% THIS PART OF THE PROGRAM COMPUTES THE ERROR BY USING MEASURED %MODAL
PROPERTIES
dof=size(mode);
dof=dof(2);
for n=1:dof;
e_rror=-freq(n)^2*Ms*mode(:,n);
error=e_rror+ Ks*mode(:,n);
end;
func1=sqrt(sum(error.^2));
% THIS PART OF THE PROGRAM COMPUTES THE ERROR BY USING THE %MEASURED FRF
% DEFINING THE FORCE VECTOR
Force=zeros(20,1);
Force(3)=1;
% DAMPING FACTOR
alfa=E(11)/100;
beta=E(12)/100;
% EXPANDING THE MEASURED FRF
dof=size(I1xf);
dof=dof(1);
for n=1:dof;

```

```

unmeasured_FRF(:,n)=-inv(-IIw(n).^2*mss+kss)*(-IIw(n).^2*msm+ksm)*IIxf(n,:);
end;
IIxf=[IIxf;unmeasured_FRF'];
for n=1:dof_w;
    crr=j*(alfa*Ms+beta*Ks)*IIw(n);
    er_ror=-IIw(n).^2*Ms+crr+Ks)*IIxf(n,:)-Force;
    error(n)=sum(er_ror.^2);
end;
func2=sqrt(sum(error));
% THIS PART OF THE PROGRAM ADDS THE ERROR
func=func1+func2;

```

(f) Expansion Using Modal Data

```

%fun_ese
function [func,g]=fun(E);
load frf;
dof=size(IIxf);
dof_f=dof(2);
dof_w=dof(1);
load modek;
% DEFINITION OF GEOMETRY
% Length (x) L [m]
L=0.9;
% Width (y) b [m]
b=0.0292;
% Thickness (z) h [m]
h=0.0096;
% CONSIDER BEAM WITH 10 ELEMENTS
d=L/10;
Iz=(1/12)*b*h^3;
Iy=(1/12)*h*b^3;
Jx=(1/12)*b*h*(b^2 + h^2);
Area =b*h;
% COORDINATES OF NODES
% node# unused x y z
node=[ 1 0 0 0 0 0 0
      2 0 0 0 d 0 0
      3 0 0 0 2*d 0 0
      4 0 0 0 3*d 0 0
      5 0 0 0 4*d 0 0
      6 0 0 0 5*d 0 0
      7 0 0 0 6*d 0 0
      8 0 0 0 7*d 0 0
      9 0 0 0 8*d 0 0
     10 0 0 0 9*d 0 0
     11 0 0 0 10*d 0 0
     12 0 0 0 0 1 0];
% USE BEAM ELEMENTS
elt=[ Inf abs('beam1')
% n#1 n#2 pl# il# nr 0
  1 2 1 1 12 0
  2 3 2 1 12 0
  3 4 3 1 12 0
  4 5 4 1 12 0
  5 6 5 1 12 0
  6 7 6 1 12 0

```



```

7 8 7 1 12 0
8 9 8 1 12 0
9 10 9 1 12 0
10 11 10 1 12 0];
% MATERIAL PROPERTIES FOR ALUMINIUM
% MatId MatType E [N/m^2] nu rho [kg/m^3]
pl=[ 1 1 E(1)*1E8 0.35 2700
2 1 E(2)*1E9 0.35 2700
3 1 E(3)*1E9 0.35 2700
4 1 E(4)*1E9 0.35 2700
5 1 E(5)*1E9 0.35 2700
6 1 E(6)*1E9 0.35 2700
7 1 E(7)*1E9 0.35 2700
8 1 E(8)*1E9 0.35 2700
9 1 E(9)*1E9 0.35 2700
10 1 E(10)*1E9 0.35 2700];
% SECTION PROPERTIES
% SecId SecType Jx [kgm^2] Iz [kgm^2] Iy [kgm^2] A [m^2]
il=[ 1 1 Jx Iy Iz Area];
% ASSEMBLE MASS AND STIFFNESS MATRIX
[M,K,mdof]=fe_mk(node,elt,pl,il);
% "Active" degrees of freedom
% Node 1 is fixed in translation and rotation
% Consider y, z, Ty and Tz degrees of freedom
[adof,ind]=fe_c(m dof,[.02 .06]);
mr=M(ind,ind);kr=K(ind,ind);
[adof,ind]=fe_c(adof,[1],[,],2);
Ms=mr(ind,ind);Ks=kr(ind,ind);
% COMPUTE MASS NORMALISED NORMAL MODES
[modeq,freq]=fe_eig(Ms,Ks,[0],adof,adof);
% EXPANSION USING MODAL DATA
master=[1 3 5 7 9 11 13 15 17 19];
slave=[2 4 6 8 10 12 14 16 18 20];
% PARTITION STIFFNESS AND MASS MATRICES
kmm=Ks(master,master);
kms=Ks(master,slave);
ksm=Ks(slave,master);
kss=Ks(slave,slave);
mmm=Ms(master,master);
mms=Ms(master,slave);
msm=Ms(slave,master);
mss=Ms(slave,slave);
Ms=[mmm mms;msm mss];Ks=[kmm kms;ksm kss];
% THIS METHOD IS THE EXPANSION VERSION OF SEREP
% ANALYTICAL MODE AT MEASURED AND UNMEASURED CO_ORDINATES
modeq_m=modeq(master,1:4);
modeq_s=modeq(slave,1:4);
% PSEUDO INVERSE
p_modeq=inv(modeq_m'*modeq_m)*modeq_m';
T=p_modeq*modeq_m;
mode_un=modeq_s*T;
mode=[mode;full(mode_un)];
%THIS PART COMPUTES THE ERROR USING MEASURED MODAL PROPERTIES
dof=size(mode);
dof=dof(2);
for n=1:dof;
e_rror=- freq(n)^2*Ms*mode(:,n);

```

```

    error=e_rror+Ks*mode(:,n);
end;
func=sqrt(sum(error.^2));
% THIS PART OF THE PROGRAM COMPUTES THE ERROR BY USING THE %MEASURED FRF
% DEFINING THE FORCE VECTOR
% Force=zeros(20,1);
% Force(3)=1;
% DAMPING FACTOR
alfa=E(11)/100;
beta=E(12)/100;
% EXPANDING THE MEASURED FRF
dof=size(IIf);
dof=dof(1);
for n=1:dof;
    unmeasured_FRF(:,n)=-inv(-IIfw(n)*mss+kss)*(-IIfw(n)*msm+ksm)*IIf(n,:);
end;
IIf=[IIf unmeasured_FRF'];
for n=1:dof_w;
    crr=j*(alfa*Ms+beta*Ks)*IIfw(n);
    er_ror=(- IIfw(n)^2*Ms+crr+Ks)*IIf(n,:)-Force;
    error(n)=sum(er_ror.^2);
end;
func2=sqrt(sum(error));
% THIS PART OF THE PROGRAM ADDS THE ERROR
func=func1+func2;

```

Appendix B: The Expansion of Measured FRFs

Expansion using Mass and Stiffness Matrices

This method is the inverse of the Guyan reduction method. Suppose ω_m and H_m are the frequencies and their corresponding frequency response functions (FRF's). Then the mass and the stiffness matrices from the finite element analysis may be partitioned into measured and unmeasured co-ordinates. The equation of motion may then be written as follows:

$$\left(-\omega_m^2 \begin{bmatrix} [M_{mm}] & [M_{ms}] \\ [M_{ms}] & [M_{ss}] \end{bmatrix} + \begin{bmatrix} [K_{mm}] & [K_{ms}] \\ [K_{ms}] & [K_{ss}] \end{bmatrix} \right) \begin{Bmatrix} H_m \\ H_s \end{Bmatrix} = \begin{Bmatrix} F \\ 0 \end{Bmatrix} \quad (\text{b.1})$$

where H_s represents the FRF's at the slave or the unmeasured co-ordinates. By rearranging the lower part of the matrix equation produces a solution for the unknown part of the measured mode shape vector. Thus

$$\{H_s\} = -(-\omega^2 [M_{ss}] + [K_{ss}])^{-1} (-\omega^2 [M_{sm}] + [K_{sm}]) \{H_m\} \quad (\text{b.2})$$

Other estimates of the unmeasured degrees of freedom may be obtained by using the upper part of equation b.1. This calculation will involve the pseudo inverse; using the upper part is satisfactory if the number of measured degrees of freedom exceeds the number of unmeasured degrees of freedom

Appendix C: Programs used for the examples

In this appendix the IRS is chosen in the implementation of the DAM, MPM and MCM. The programs are written to test the MCM, DAM, and MPM on the three examples.

(c.1) Example 1 (Freely suspended beam)

(C.1.1) This Program Uses Measured FRFs And Modal Properties

This program calls program funa_bim which is listed in section c.1.2.

```
% Written by Tshilidzi Marwala
% 24 March 1997
clear all;
for n=1:14;
    E(n)=700; % initial design
end;
% Bounds
for n=1:14;
    vlb(n)=300; % lower bounds
end;
vlb(13)=0;
vlb(14)=0;
for n=1:14;
    vub(n)=800; % upper bounds
end;
vlb(13)=0;
vlb(14)=0;
options(1)=1;
options(2)=0.1; % accuracy of the design
options(3)=0.00001; % accuracy of the objective functions
options(14)=100000; % maximum number of iterations
%OPTIMISATION ROUTINE IMPLEMENTING THE DAM, MPM and MCM
E=constr('funa_bim',E,options,vlb,vub);
```

(C.1.2) Program funa_bim

```
%funa_bim
function [func,g]=fun(E);
load f_dame3;
llw=llw;
dof=size(llxe);
dof_f=dof(2);
dof_w=dof(1);
% DEFINITION OF GEOMETRY
% Length (x) L [m] Adjust L as required
L=1.0;
% Width (y) b [m] Adjust b as required
b=0.0254;
% Thickness (z) h [m] Adjust h as required
h=0.0134;
% CONSIDER BEAM WITH 10 ELEMENTS
Iz=(1/12)*b*h^3; % See Meriam & Kraige p706
```

```

Iy=(1/12)*h*b^3;
Jx=(1/12)*b*h*(b^2 + h^2);
Area =b*h;
% COORDINATES OF NODES
% node# unused x y z
node=[ 1 0 0 0 0 0 0
      2 0 0 0 0.087 0 0
      3 0 0 0 0.177 0 0
      4 0 0 0 0.26 0 0
      5 0 0 0 0.337 0 0
      6 0 0 0 0.42 0 0
      7 0 0 0 0.504 0 0
      8 0 0 0 0.586 0 0
      9 0 0 0 0.67 0 0
     10 0 0 0 0.752 0 0
     11 0 0 0 0.835 0 0
     12 0 0 0 0.917 0 0
     13 0 0 0 1.0 0 0
     14 0 0 0 0 1 0];
% USE BEAM ELEMENTS
elt=[ Inf abs('beam1')
% n#1 n#2 pl# il# nr 0
  1 2 1 1 14 0
  2 3 2 1 14 0
  3 4 3 1 14 0
  4 5 4 1 14 0
  5 6 5 1 14 0
  6 7 6 1 14 0
  7 8 7 1 14 0
  8 9 8 1 14 0
  9 10 9 1 14 0
 10 11 10 1 14 0
 11 12 11 1 14 0
 12 13 12 1 14 0];
% MATERIAL PROPERTIES FOR ALUMINIUM
% MatId MatType E [N/m^2] nu rho [kg/m^3]
pl=[ 1 1 E(1)*1e8 0.35 2700
    2 1 E(2)*1e8 0.35 2700
    3 1 E(3)*1e8 0.35 2700
    4 1 E(4)*1e8 0.35 2700
    5 1 E(5)*1e8 0.35 2700
    6 1 E(6)*1e8 0.35 2700
    7 1 E(7)*1e8 0.35 2700
    8 1 E(8)*1e8 0.35 2700
    9 1 E(9)*1e8 0.35 2700
   10 1 E(10)*1e8 0.35 2700
   11 1 E(11)*1e8 0.35 2700
   12 1 E(12)*1e8 0.35 2700];
% SECTION PROPERTIES
% SecId SecType Jx [kgm^2] Iz [kgm^2] Iy [kgm^2] A [m^2]
il=[ 1 1 Jx Iy Iz Area];
% ASSEMBLE MASS AND STIFFNESS MATRIX
[m,k,mdof]=fe_mk(node,elt,pl,il);
% "Active" degrees of freedom
% Node 1 is fixed in translation and rotation
% Consider x, y, Tx and Ty degrees of freedom
[adof,ind]=fe_c(mdof,[.02 .06]);

```

```

% COMPUTE MASS NORMALISED NORMAL MODES
[mode,freq]=fe_eig(m,k,[0],mdof,adof);
master=[3 5 7 9 11 13 15 17 19 21 23];
slave=[1 2 4 6 8 10 12 14 16 18 20 22 24 25 26];
Ks=k(ind,ind);Ms=m(ind,ind);
% PARTITION STIFFNESS AND MASS MATRICES
kmm=Ks(master,master);
kms=Ks(master,slave);
ksm=Ks(slave,master);
kss=Ks(slave,slave);
mmm=Ms(master,master);
mms=Ms(master,slave);
msm=Ms(slave,master);
mss=Ms(slave,slave);
% REARRANGE THE MASS AND STIFFNESS MATRICES
Ms=[mmm mms;msm mss];
Ks=[kmm kms;ksm kss];
% COMPUTING THE T VECTOR
dof=size(mmm);
dof=dof(1);
identity=zeros(size(mmm));
for n=1:dof;
    identity(n,n)=1;
end;
Ts=[identity;-inv(kss)*(ksm)];
% REDUCED MASS AND STIFFNESS
mrr=Ts'*Ms*Ts;krr=Ts'*Ks*Ts;
s1=[zeros(size(kmm))];s2=[zeros(size(kms))];
s3=[zeros(size(ksm))];s4=inv(kss);
S=[s1 s2;s3 s4];
Ti=Ts+S*Ms*Ts*inv(mrr)*krr;
mrr=Ti'*Ms*Ti;krr=Ti'*Ks*Ti;
dof_f=size(I1xe);
dof_w=dof_f(1);
dof=dof_f(2);
ZERO=zeros(dof,1);
ZERO(5)=1;
alfa=E(13)/1000;beta=E(14)/1000;
alfa=0;beta=0;
for n=1:dof_w;
    crr=j*(alfa*mrr+beta*krr)*I1w(n);
    er_ror1=real(-I1w(n).^2*mrr+crr+krr)*I1xe(n,:)+ZERO;
    error(n)=sum((abs(er_ror1)).^2);
end;
func=sqrt(sum(error))/60.2983; % the function was normalised by using sqrt(sum(error(at initial design)))
% func=0;
% USING MODAL APPROACH
% COMPUTE MASS NORMALISED NORMAL MODES
[mode1,freq1]=fe_eig(mrr,krr);
mode1=mode1(:,3:5);
load m_dame3;
mode=fe_norm(mode,mrr);
for n=1:3;
    error1(n)=mode1(:,n)*(-freqw(n).^2*mrr+krr)*mode(:,n);
end;
func=sqrt(sum(error1.^2))/697976+func; % the function was normalised by using

```

(C.1.3) Program For Identifying The Measured Modes

```

% Tshilidzi Marwala
% 15 March 1997
clear all;
% THIS FUNCTION TAKES THE MEASURED FRF'S AND CONVERT THEM INTO
% MODE SHAPES AND NATURAL FREQUENCIES AND THEN SAVES THEM
% LOAD IHW, IIXF
load c:\final\ff_dame3;
Iixf=Iixe;
% DEFINE OPTIONS
IDopt=[3 0 22 1 size(Iixf,1) 1 10 1 0 0 0 1 3];
iigui
idcom
% cps=output shape matrix (describing sensors p 1-53)
% pbs=input shape matrix (Describing actuators)
% Note error p2-91
[freqw,ga,pbs,cps]=res2nor(Iires,Iipo,IDopt)
% DEFINITION OF GEOMETRY
% Lengte (x) L [m]
L=1.0;
% DIVIDE THE BEAM INTO 10 ELEMENTS
d=L/12;
% COORDINATES OF NODES
% node# unused x y z
node=[ 1 0 0 0 0 0 0
      2 0 0 0 0.087 0 0
      3 0 0 0 0.177 0 0
      4 0 0 0 0.26 0 0
      5 0 0 0 0.337 0 0
      6 0 0 0 0.42 0 0
      7 0 0 0 0.504 0 0
      8 0 0 0 0.586 0 0
      9 0 0 0 0.67 0 0
     10 0 0 0 0.752 0 0
     11 0 0 0 0.835 0 0
     12 0 0 0 0.917 0 0
     13 0 0 0 1.0 0 0
     14 0 0 0 0 1 0];
mdof=[2.02 3.02 4.02 5.02 6.02 7.02 8.02 9.02 10.02 11.02 12.02];
figure(2)
LDraw(1,1)=[10];
LDraw(1,82+[1:LDraw(1)])=[2 3 4 5 6 7 8 9 10 11];
mode=[cps];
opt=[2 2 40 0 0 11]
feplot(node,LDraw,mode,mdof,opt)
fecom NodeText
f=freqw/(2*pi)
save c:\final\fm_dame3 mode freqw

```

(C.1.4) Implementation of The Comparison Methods

```

% MAC.M
% Tshilidzi Marwala
% 13 March 1997
% This program takes 2 FRF's compute modes compare using MAC and COMAC
% as well as COFRF
clear all;

```

```

% LOAD A PROCEDURE THAT CALCULATES THE MODES
load f_dame2;
IIf=IIfx;
get_mode;
mode1=mode;
freqw1=freqw;
save c:\final\modek1 freqw1 mode1;

clear all;
% load the second set of FRF, compute modes and save them
load frfc; % Original FRF which were used for updating
IIf=IIfx;
get_mode;
mode2=mode;
freqw2=freqw;
save c:\final\modek2 freqw2 mode2;
clear all
load uf_dame02;
IIf=IIfx;
get_mode;
mode3=mode;
freqw3=freqw;
save c:\final\modek3 freqw3 mode3;

clear all;
load modek1;
load modek2;
load modek3;
% COMPUTING THE "MAC" AND THE COMAC
MAC1=ii_mac(mode1,mode2);
MAC=ii_mac(mode1,mode2,'plot');
COMAC1=ii_comac(mode1,mode2);
% COMPUTING THE "MAC" AND THE "COMAC"
MAC2=ii_mac(mode1,mode3);
MAC=ii_mac(mode1,mode2,'plot');
COMAC2=ii_comac(mode1,mode3);

% PRODUCT OF "COMAC"
b1=prod(COMAC1)
b2=prod(COMAC2)
% REDUCING THE "MAC"
dof=size(MAC1);
mac=zeros(dof);
dof=dof(1);
for i=1:dof;
    mac(i,i)=1;
end;
a=MAC1-mac;
a=a.^2;
a1=sum(sum(a)) % The mac based scalar factor before updating
% REDUCING THE "MAC"
dof=size(MAC2);
mac=zeros(dof);
dof=dof(1);
for i=1:dof;
    mac(i,i)=1;
end;

```



```

a=MAC2-mac;
a=a.^2;
a2=sum(sum(a)) % The mac based scalar factor after updating
% COMPARISON OF THE FRF'S
load uf_dame02;
Ixf=Ixe;
load frfc;
load f_dame2;
nume=sum(abs(Ixe));
nume=sum(nume);
deno=sum(abs(Ixh));
deno=sum(deno);
COFRF1=nume*deno/(deno*deno) % before updating
deno=sum(abs(Ixf));
deno=sum(deno);
COFRF2=nume*deno/(deno*deno) % after updating
[freqw1 freqw2 freqw3]

```

(C.1.5) The Program Used for Downloading the Data

```

% BEAM.M
% Tshilidzi Marwala 20 March 1997
clear all;
% Definition of geometry
% Length (x) L [m] Adjust L as required
L=1.0;
% Width (y) b [m] Adjust b as required
b=0.0254;
% Thickness (z) h [m] Adjust h as required
h=0.0134;
% CONSIDER BEAM WITH 10 ELEMENTS
Iz=(1/12)*b*h^3; % See Meriam & Kraige p706
Iy=(1/12)*h*b^3;
Jx=(1/12)*b*h*(b^2 + h^2);
Area =b*h;
% COORDINATES OF NODES
% node# unused x y z
node=[ 1 0 0 0 0 0 0
      2 0 0 0 0.087 0 0
      3 0 0 0 0.177 0 0
      4 0 0 0 0.26 0 0
      5 0 0 0 0.337 0 0
      6 0 0 0 0.42 0 0
      7 0 0 0 0.504 0 0
      8 0 0 0 0.586 0 0
      9 0 0 0 0.67 0 0
     10 0 0 0 0.752 0 0
     11 0 0 0 0.835 0 0
     12 0 0 0 0.917 0 0
     13 0 0 0 1.0 0 0
     14 0 0 0 0 1 0];
% USE BEAM ELEMENTS
elt=[ Inf abs('beam1')
% n#1 n#2 pl# il# nr 0
  1 2 1 1 14 0
  2 3 1 1 14 0
  3 4 1 1 14 0

```

```

4 5 1 1 14 0
5 6 1 1 14 0
6 7 1 1 14 0
7 8 1 1 14 0
8 9 1 1 14 0
9 10 1 1 14 0
10 11 1 1 14 0
11 12 1 1 14 0
12 13 1 1 14 0];
% MATERIAL PROPERTIES FOR ALUMINIUM
% MatId MatType E [N/m^2] nu rho [kg/m^3]
pl=[ 1 1 7.0e10 0.35 2700];
% SECTION PROPERTIES
% SecId SecType Jx [kgm^2] Iz [kgm^2] Iy [kgm^2] A [m^2]
il=[ 1 1 Jx Iy Iz Area];
% ASSEMBLE MASS AND STIFFNESS MATRIX
[m,k,mdof]=fe_mk(node,elt,pl,il);
% "Active" degrees of freedom
% Consider x, y, Tx and Ty degrees of freedom
[adof,ind]=fe_c(mdof,[.02 .06]);
% COMPUTE MASS NORMALISED NORMAL MODES
[mode,freq]=fe_eig(m,k,[0],mdof,adof);
% LOADING EXPERIMENTAL DATA
load t002.tra;
a1=t002(5:201,1);
Ilw=t002(5:201,2);
load t002.trb;
a1l=t002(5:201,1);
FRF2=a1.*exp(i*a1l*pi/180);
load t003.tra;
a1=t003(5:201,1);
load t003.trb;
a1l=t003(5:201,1);
FRF3=a1.*exp(i*a1l*pi/180);
load t004.tra;
a1=t004(5:201,1);
load t004.trb;
a1l=t004(5:201,1);
FRF4=a1.*exp(i*a1l*pi/180);

load t005.tra;
a1=t005(5:201,1);
load t005.trb;
a1l=t005(5:201,1);
FRF5=a1.*exp(i*a1l*pi/180);

load t006.tra;
a1=t006(5:201,1);
load t006.trb;
a1l=t006(5:201,1);
FRF6=a1.*exp(i*a1l*pi/180);

load t007.tra;
a1=t007(5:201,1);
load t007.trb;
a1l=t007(5:201,1);
FRF7=a1.*exp(i*a1l*pi/180);

```

```

load t008.tra;
a1=t008(5:201,1);
load t008.trb;
a11=t008(5:201,1);
FRF8=a1.*exp(i*a11*pi/180);

load t009.tra;
a1=t009(5:201,1);
load t009.trb;
a11=t009(5:201,1);
FRF9=a1.*exp(i*a11*pi/180);

load t010.tra;
a1=t010(5:201,1);
load t010.trb;
a11=t010(5:201,1);
FRF10=a1.*exp(i*a11*pi/180);

load t001.tra;
a1=t001(5:201,1);
load t001.trb;
a11=t001(5:201,1);
FRF1=a1.*exp(i*a11*pi/180);

load t011.tra;
a1=t011(5:201,1);
load t011.trb;
a11=t011(5:201,1);
FRF11=a1.*exp(i*a11*pi/180);

IIw=2*pi*IIw;
FRF_1=FRF1./(-IIw.^2);FRF_2=FRF2./(-IIw.^2);FRF_3=FRF3./(-IIw.^2);
FRF_4=FRF4./(-IIw.^2);FRF_5=FRF5./(-IIw.^2);FRF_6=FRF6./(-IIw.^2);
FRF_7=FRF7./(-IIw.^2);FRF_8=FRF8./(-IIw.^2);FRF_9=FRF9./(-IIw.^2);
FRF_10=FRF10./(-IIw.^2);FRF_11=FRF11./(-IIw.^2);
IIxe=[FRF_1 FRF_2 FRF_3 FRF_4 FRF_5 FRF_6 FRF_7 FRF_8 FRF_9 FRF_10 FRF_11];
% INPUT/OUTPUT MATRIX
b=fe_c(m dof,[6.08]);
cd=fe_c(m dof,[2.02 3.02 4.02 5.02 6.02 7.02 8.02 9.02 10.02 11.02 12.02]);
pb=mode'*b; % actuator
cp=cd*mode; % mode shapes from sensors
IIxf=norm2xf(freq,0.01,pb,cp,IIw); % FE normal 2 complex data file
save c:\final\l_dame02 IIw IIxe
IIw=(IIw/2/pi);
% PLOTTING THE FRF'S TOGETHER
IDopt = [3 0 22 1 size(IIxf,1) 1 9 1 0 0 0 1 7];
iigui
iicom('IIxeOn'); % commode('iicom','IIxeOn');
if exist('legend')==2 legend('Toolbox','Alternatief');iimouse; end

```

(C.2) Example 2: Freely Suspended Beam With Holes

(C.2.1) Program Used For Example 2

```

% This program takes the measured FRF and use them to update
% the FEA
% Written by Tshilidzi Marwala

```

```

% 1 April 1997
clear all;
for n=1:11;
    E(n)=700;      % initial design
end;
for n=1:11;
    vlb(n)=600;   % upper bounds
end;
for n=1:11;
    vub(n)=720;   % upper bounds
end;
options(1)=1;
options(2)=1;
options(3)=1e-2;
options(14)=100000;
%OPTIMISATION ROUTINE IN SECTION C.22
E=constr('funa_bim',E,options,vlb,vub);

```

(C.2.2) Program funa_bim

```

function [func,g]=fun(E);
load f_dame2;
Hxf=Hxe;
% DEFINITION OF GEOMETRY
% Length (x) L [m]          Adjust L as required
L=1.1;
% Width (y) b [m]          Adjust b as required
b=0.0292;
% Thickness (z) h [m]      Adjust h as required
h=0.0096;
% CONSIDER BEAM WITH 11 ELEMENTS
d=L/11;
Iz=(1/12)*b*h^3;          % See Meriam & Kraige p706
Iy=(1/12)*h*b^3;
Jx=(1/12)*b*h*(b^2 + h^2);
Area =b*h;
% COORDINATES OF NODES
% node# unused x y z
node=[ 1  0  0  0  0  0  0
       2  0  0  0      d  0  0
       3  0  0  0     2*d  0  0
       4  0  0  0     3*d  0  0
       5  0  0  0     4*d  0  0
       6  0  0  0     5*d  0  0
       7  0  0  0     6*d  0  0
       8  0  0  0     7*d  0  0
       9  0  0  0     8*d  0  0
      10  0  0  0     9*d  0  0
      11  0  0  0    10*d  0  0
      12  0  0  0    11*d  0  0
      13  0  0  0      0  1  0];
% USE BEAM ELEMENTS
elt=[ Inf abs('beam1')
% n#1 n#2 pl# il# nr 0
  1  2  1  1  13  0
  2  3  2  1  13  0
  3  4  3  1  13  0

```

```

4 5 4 1 13 0
5 6 5 1 13 0
6 7 6 1 13 0
7 8 7 1 13 0
8 9 8 1 13 0
9 10 9 1 13 0
10 11 10 1 13 0
11 12 11 1 13 0];
% MATERIAL PROPERTIES FOR ALUMINIUM
% MatId MatType E [N/m^2] nu rho [kg/m^3]
pl=[ 1 1 E(1)*1e8 0.35 2700
2 1 E(2)*1e8 0.35 2700
3 1 E(3)*1e8 0.35 2700
4 1 E(4)*1e8 0.35 2700
5 1 E(5)*1e8 0.35 2700
6 1 E(6)*1e8 0.35 2700
7 1 E(7)*1e8 0.35 2700
8 1 E(8)*1e8 0.35 2700
9 1 E(9)*1e8 0.35 2700
10 1 E(10)*1e8 0.35 2700
11 1 E(11)*1e8 0.35 2700];
% SECTION PROPERTIES
% SecId SecType Jx [kgm^2] Iz [kgm^2] Iy [kgm^2] A [m^2]
il=[ 1 1 Jx Iy Iz Area];
% ASSEMBLE MASS AND STIFFNESS MATRIX
[m,k,mdof]=fe_mk(node,elt,pl,il);
% "Active" degrees of freedom
% Consider y, z, Ty and Tz degrees of freedom
[adof,ind]=fe_c(mdof,[.02 .06]);
% COMPUTE MASS NORMALISED NORMAL MODES
[mode,freq]=fe_eig(m,k,[0],mdof,adof);
% Condensing the dynamic stiffness matrix
% IRS
master=[3 5 7 9 11 13 15 17 19 21];
slave=[1 2 4 6 8 10 12 14 16 18 20 22 23 24];
Ks=k(ind,ind);Ms=m(ind,ind);
% PARTITION STIFFNESS AND MASS MATRICES
kmm=Ks(master,slave);
kms=Ks(master,slave);
ksm=Ks(slave,slave);
kss=Ks(slave,slave);
mmm=Ms(master,slave);
mms=Ms(master,slave);
msm=Ms(slave,slave);
mss=Ms(slave,slave);
% REARRANGE THE MASS AND STIFFNESS MATRICES
Ms=[mmm mms;msm mss];
Ks=[kmm kms;ksm kss];
% COMPUTING THE "T" VECTOR
dof=size(mmm);
dof=dof(1);
identity=zeros(size(mmm));
for n=1:dof;
    identity(n,n)=1;
end;
Ts=[identity;-inv(kss)*(ksm)];

```

```

% REDUCED MASS AND STIFFNESS
mrr=Ts'*Ms*Ts;krr=Ts'*Ks*Ts;
%
s1=[zeros(size(kmm))];s2=[zeros(size(kms))];
s3=[zeros(size(ksm))];s4=inv(kss);
S=[s1 s2;s3 s4];
Ti=Ts+S*Ms*Ts*inv(mrr)*krr;
mrr=Ti'*Ms*Ti;krr=Ti'*Ks*Ti;
%
dof_f=size(IIf);
dof_w=dof_f(1);
dof=dof_f(2);
ZERO=zeros(dof,1);
ZERO(3)=1;
% alfa=E(13)/1000;beta=E(14)/1000;
alfa=0;beta=0;
for n=1:dof_w;
    crr=j*(alfa*mrr+beta*krr)*Iiw(n);
    er_ror1=(-Iiw(n).^2*mrr+crr+krr)*IIf(n,:)+ZERO;
    error(n)=sum((abs(er_ror1)).^2);
end;
func=sqrt(sum(error));
func=0;
% USING MODAL APPROACH
% COMPUTE MASS NORMALISED NORMAL MODES
[mode1,freq1]=fe_eig(mrr,krr);
mode1=mode1(:,3:6);
freq1=freq1(3:6);
load m_dame2;
mode=fe_norm(mode,mrr);
for n=1:4;
    error1(n)=-((freqw(n).^2*mode(:,n)'+mrr*mode(:,n))+(mode(:,n)'+krr*mode(:,n)));
end;
func=sqrt(sum(error1.^2))+func;

```

(C.2.3) Program Used to Load Measured Data

```

% BEAM.M
% Programmed by Tshilidzi Marwala
% 24 February 1997
%
clear all;
% DEFINITION OF GEOMETRY
% Length (x) L [m] Adjust L as required
L=1.1;
% Width (y) b [m] Adjust b as required
b=0.0292;
% Thickness (z) h [m] Adjust h as required
h=0.0096;
% CONSIDER BEAM WITH 11 ELEMENTS
d=L/11;
Iz=(1/12)*b*h^3; % See Meriam & Kraige p706
Iy=(1/12)*h*b^3;
Jx=(1/12)*b*h*(b^2 + h^2);
Area =b*h;
%

```

```

% COORDINATES OF NODES
% node# unused x y z
node=[ 1 0 0 0 0 0 0
      2 0 0 0      d 0 0
      3 0 0 0      2*d 0 0
      4 0 0 0      3*d 0 0
      5 0 0 0      4*d 0 0
      6 0 0 0      5*d 0 0
      7 0 0 0      6*d 0 0
      8 0 0 0      7*d 0 0
      9 0 0 0      8*d 0 0
     10 0 0 0      9*d 0 0
     11 0 0 0     10*d 0 0
     12 0 0 0     11*d 0 0
     13 0 0 0      0 1 0];

%
% USE BEAM ELEMENTS
elt=[ Inf abs('beam1')
% n#1 n#2 pl# il# nr 0
  1 2  1 1 13 0
  2 3  1 1 13 0
  3 4  1 1 13 0
  4 5  1 1 13 0
  5 6  1 1 13 0
  6 7  1 1 13 0
  7 8  1 1 13 0
  8 9  1 1 13 0
  9 10 1 1 13 0
 10 11 1 1 13 0
 11 12 1 1 13 0];

% MATERIAL PROPERTIES FOR ALUMINIUM
% MatId MatType E [N/m^2] nu rho [kg/m^3]
pl=[  1  1  7.0e10  0.35  2700];
% SECTION PROPERTIES
% SecId SecType Jx [kgm^2] Iz [kgm^2] Iy [kgm^2] A [m^2]
il=[  1  1  Jx  Iy  Iz  Area];
% ASSEMBLE MASS AND STIFFNESS MATRIX
[m,k,mdof]=fe_mk(node,elt,pl,il);
% "Active" degrees of freedom
% Consider x, y, Tx and Ty degrees of freedom
[adof,ind]=fe_c(mdof,[.01 .02 .06]);
% COMPUTE MASS NORMALISED NORMAL MODES
[mode,freq]=fe_eig(m,k,[0],mdof,adof);
% LOADING EXPERIMENTAL DATA
load t002.tra;
a1=t002(5:201,1);
Iiw=t002(5:201,2);
load t002.trb;
a11=t002(5:201,1);
FRF2=a1.*exp(i*a11*pi/180);

load t003.tra;
a1=t003(5:201,1);
load t003.trb;
a11=t003(5:201,1);
FRF3=a1.*exp(i*a11*pi/180);

```

```

load t004.tra;
a1=t004(5:201,1);
load t004.trb;
a11=t004(5:201,1);
FRF4=a1.*exp(i*a11*pi/180);

load t005.tra;
a1=t005(5:201,1);
load t005.trb;
a11=t005(5:201,1);
FRF5=a1.*exp(i*a11*pi/180);

load t006.tra;
a1=t006(5:201,1);
load t006.trb;
a11=t006(5:201,1);
FRF6=a1.*exp(i*a11*pi/180);

load t007.tra;
a1=t007(5:201,1);
load t007.trb;
a11=t007(5:201,1);
FRF7=a1.*exp(i*a11*pi/180);

load t008.tra;
a1=t008(5:201,1);
load t008.trb;
a11=t008(5:201,1);
FRF8=a1.*exp(i*a11*pi/180);

load t009.tra;
a1=t009(5:201,1);
load t009.trb;
a11=t009(5:201,1);
FRF9=a1.*exp(i*a11*pi/180);

load t010.tra;
a1=t010(5:201,1);
load t010.trb;
a11=t010(5:201,1);
FRF10=a1.*exp(i*a11*pi/180);

load t001.tra;
a1=t001(5:201,1);
load t001.trb;
a11=t001(5:201,1);
FRF1=a1.*exp(i*a11*pi/180);
IIw=2*pi*IIw;
FRF_1=FRF1./(-IIw.^2);FRF_2=FRF2./(-IIw.^2);FRF_3=FRF3./(-IIw.^2);
FRF_4=FRF4./(-IIw.^2);FRF_5=FRF5./(-IIw.^2);FRF_6=FRF6./(-IIw.^2);
FRF_7=FRF7./(-IIw.^2);FRF_8=FRF8./(-IIw.^2);FRF_9=FRF9./(-IIw.^2);
FRF_10=FRF10./(-IIw.^2);
IIxe=[FRF_1 FRF_2 FRF_3 FRF_4 FRF_5 FRF_6 FRF_7 FRF_8 FRF_9 FRF_10];
% INPUT/OUTPUT MATRIX
b=fe_c(m dof,[4.08]);
cd=fe_c(m dof,[2.02 3.02 4.02 5.02 6.02 7.02 8.02 9.02 10.02 11.02]);
pb=mode'*b; % actuator

```



```

cp=cd*mode; % mode shapes from sensors
Iixf=nor2xf(freq,0.01,pb,cp,Iiw); % FE normal 2 complex data file
save c:\final\f_dame11 Iiw Iixe
% PLOTTING THE "FRF's" TOGETHER
IDopt = [3 0 22 1 size(Iixf,1) 1 9 1 0 0 0 1 7];
iigui
iicom('IixeOn'); % commode('iicom','IixeOn');
if exist('legend')==2 legend('Toolbox','Alternatief');iimouse; end

```

(C.3) EXAMPLE 3: Freely Suspended Irregular H-Shaped Structure

(C.3.1) Program Used For Damage 3

This program takes the measured FRF and use them to update
% the FEA

% Written by Tshilidzi Marwala

% 24 February 1997

clear all;

for n=1:12;

 E(n)=70;

end;

E(13)=0;

E(14)=0;

for n=1:12;

 vlb(n)=66;

end;

vlb(5)=54;

vlb(13)=0;

vlb(14)=0;

for n=1:12;

 vub(n)=74;

end;

vub(13)=50;

vub(14)=50;

options(1)=1;

options(2)=0.1;

options(3)=1e-4;

options(7)=1;

options(14)=10000;

options(16)=1e-8;

options(17)=0.1;

% options(18)=1;

E=constr('funa_bim',E,options,vlb,vub);

(C.3.1) Program funa_bim

load f_dame1;

a=0.4;

b=0.6;

c=0.2;

E=E*10^9;

% DEFINITION OF GEOMETRY

% Width (y) b [m]

Adjust b as required

br=0.0322;

```

% Thickness (z) h [m]
h=0.0098;
t=h/2;
%
% CONSIDER BEAM WITH 11 ELEMENTS
Iz=(1/12)*br*h^3;
Iy=(1/12)*h*br^3;
Jx=(1/12)*br*h*(br^2 + h^2);
Area =br*h;
%
% COORDINATES OF NODES
% node# unused x y z
node=[ 1 0 0 0 0 0 0
      2 0 0 0 0 a/4 0
      3 0 0 0 0 a/2 0
      4 0 0 0 0 3*a/4 0
      5 0 0 0 0 a 0
      6 0 0 0 (t+b/6) a/2 0
      7 0 0 0 (t+b/3) a/2 0
      8 0 0 0 (t+b/2) a/2 0
      9 0 0 0 (t+4*b/6) a/2 0
      10 0 0 0 (t+5*b/6) a/2 0
      11 0 0 0 (2*t+b) a/2 0
      12 0 0 0 (2*t+b) a/4 0
      13 0 0 0 (2*t+b) 3*a/4 0];
%
% USE BEAM ELEMENTS
elt=[ Inf abs('beam1')
% n#1 n#2 pl# il# nr 0
1 2 1 1 6 0
2 3 2 1 6 0
3 4 3 1 6 0
4 5 4 1 6 0
3 6 5 1 5 0
6 7 6 1 5 0
7 8 7 1 5 0
8 9 8 1 5 0
9 10 9 1 5 0
10 11 10 1 5 0
11 12 11 1 10 0
11 13 12 1 10 0];
% MATERIAL PROPERTIES FOR ALUMINIUM
% MatId MatType E [N/m^2] nu rho [kg/m^3]
pl=[ 1 1 E(1) 0.3 2700
     2 1 E(2) 0.3 2700
     3 1 E(3) 0.3 2700
     4 1 E(4) 0.3 2700
     5 1 E(5) 0.3 2700
     6 1 E(6) 0.3 2700
     7 1 E(7) 0.3 2700
     8 1 E(8) 0.3 2700
     9 1 E(9) 0.3 2700
    10 1 E(10) 0.3 2700
    11 1 E(11) 0.3 2700
    12 1 E(12) 0.3 2700];
% SECTION PROPERTIES
% SecId SecType Jx [kgm^2] Iz [kgm^2] Iy [kgm^2] A [m^2]

```

Adjust h as required

% See Meriam & Kraige p706

```

il=[ 1 1 Jx Iy Iz Area];
% ASSEMBLE MASS AND STIFFNESS MATRIX
[m,k,mdof]=fe_mk(node,elt,pl,il);
% "Active" degrees of freedom
% Consider x, y, Tx and Ty degrees of freedom
[adof,ind]=fe_c(mdof,[.01 .02 .06]);
% COMPUTE MASS NORMALISED NORMAL MODES
[mode,freq]=fe_eig(m,k,[0],mdof,adof);
Ms=m(ind,ind);Ks=k(ind,ind);
master=[1 2 4 10 13 14 17 20 23 26 29 34 35 37 38];
slave=[3 5 6 7 8 9 11 12 15 16 18 19 21 22 24 25 27 28 30 31 32 33 ...
36 39];
% PARTITION STIFFNESS AND MASS MATRICES
kmm=Ks(master,master);
kms=Ks(master,slave);
ksm=Ks(slave,master);
kss=Ks(slave,slave);
mmm=Ms(master,master);
mms=Ms(master,slave);
msm=Ms(slave,master);
mss=Ms(slave,slave);
% REARRANGE THE MASS AND STIFFNESS MATRICES
Ms=[mmm mms;msm mss];
Ks=[kmm kms;ksm kss];
% COMPUTING THE T VECTOR
dof=size(mmm);
dof=dof(1);
identity=zeros(size(mmm));
for n=1:dof;
    identity(n,n)=1;
end;
Ts=[identity;-inv(kss)*(ksm)];
% Reduced mass and stiffness
mrr=Ts*Ms*Ts;krr=Ts*Ks*Ts;
s1=[zeros(size(kmm));s2=[zeros(size(kms))];
s3=[zeros(size(ksm));s4=inv(kss);
S=[s1 s2;s3 s4];
Ti=Ts+S*Ms*Ts*inv(mrr)*krr;
mrr=Ti*Ms*Ti;krr=Ti*Ks*Ti;
dof_f=size(IIXe);
dof_w=dof_f(1);
dof=dof_f(2);
ZERO=zeros(dof,1);
ZERO(7)=1;
alfa=E(13)/100;beta=E(14)/100;
ZERO=zeros(dof,1);
ZERO(7)=1;
for n=1:dof_w;
    crr=j*(alfa*mrr+beta*krr)*IIw(n);
    er_ror1=real((-IIw(n).^2*mrr+crr+krr)*IIXe(n,:))+ZERO;
    error(n)=sum((abs(er_ror1)).^2);
end;
func=sqrt(sum(error))/10.6272;
% func=0;
% USING MODAL APPROACH
% COMPUTE MASS NORMALISED NORMAL MODES
[mode1,freq1]=fe_eig(mrr,krr);

```

```

model=model(:,4:7);
load m_dame1;
mode=fe_norm(mode,mrr);
for n=1:4;
    error1(n)=model(:,n)*(-freqw(n).^2*mrr+krr)*mode(:,n);
end;
func=sqrt(sum(error1.^2))/100889+func;

```

(C.3.2) Program Used Down-load Measured Data

```

% BEAM.M
% Tshilidzi Marwala July 1997
clear all;
a=0.4;
b=0.6;
c=0.2;
% DEFINITION OF GEOMETRY
% Width (y) b [m] Adjust b as required
br=0.0322;
% Thickness (z) h [m] Adjust h as required
h=0.0098;
t=h/2;
%
% CONSIDER BEAM WITH 11 ELEMENTS
Iz=(1/12)*br*h^3; % See Meriam & Kraige p706
Iy=(1/12)*h*br^3;
Jx=(1/12)*br*h*(br^2 + h^2);
Area =br*h;
%
% COORDINATES OF NODES
% node# unused x y z
node=[ 1 0 0 0 0 0 0
      2 0 0 0 0 a/4 0
      3 0 0 0 0 a/2 0
      4 0 0 0 0 3*a/4 0
      5 0 0 0 0 a 0
      6 0 0 0 (t+b/6) a/2 0
      7 0 0 0 (t+b/3) a/2 0
      8 0 0 0 (t+b/2) a/2 0
      9 0 0 0 (t+4*b/6) a/2 0
     10 0 0 0 (t+5*b/6) a/2 0
     11 0 0 0 (2*t+b) a/2 0
     12 0 0 0 (2*t+b) a/4 0
     13 0 0 0 (2*t+b) 3*a/4 0];
% USE BEAM ELEMENTS
elt=[ Inf abs('beam1')
% n#1 n#2 pl# il# nr 0
  1 2 1 1 6 0
  2 3 1 1 6 0
  3 4 1 1 6 0
  4 5 1 1 6 0
  3 6 1 1 5 0
  6 7 1 1 5 0
  7 8 1 1 5 0
  8 9 1 1 5 0
  9 10 1 1 5 0

```

```

10 11 1 1 5 0
11 12 1 1 10 0
11 13 1 1 10 0];
% MATERIAL PROPERTIES FOR ALUMINIUM
% MatId MatType E [N/m^2] nu rho [kg/m^3]
pl=[ 1 1 7.0e10 0.3 2700];
% SECTION PROPERTIES
% SecId SecType Jx [kgm^2] Iz [kgm^2] Iy [kgm^2] A [m^2]
il=[ 1 1 Jx Iy Iz Area];
% ASSEMBLE MASS AND STIFFNESS MATRIX
[m,k,mdof]=fe_mk(node,elt,pl,il);
% "Active" degrees of freedom
% Consider x, y, Tx and Ty degrees of freedom
[adof,ind]=fe_c(mdof,[.01 .02 .06]);
[adof1,ind1]=fe_c(adof,[5.07 5.02 4.07 2.07 1.07 6.02 7.02 8.02 9.02 10.02 ...
13.07 13.02 12.01 11.08]);
% COMPUTE MASS NORMALISED NORMAL MODES
[mode,freq]=fe_eig(m,k,[0],mdof,adof);

% LOADING EXPERIMENTAL DATA
load T02.tra;
a1=T02(5:201,1);
I1w=T02(5:201,2);
load T02.trb;
a11=T02(5:201,1);
FRF2=a1.*exp(i*a11*pi/180);

load T03.tra;
a1=T03(5:201,1);
load T03.trb;
a11=T03(5:201,1);
FRF3=a1.*exp(i*a11*pi/180);

load T04.tra;
a1=T04(5:201,1);
load T04.trb;
a11=T04(5:201,1);
FRF4=a1.*exp(i*a11*pi/180);

load T05.tra;
a1=T05(5:201,1);
load T05.trb;
a11=T05(5:201,1);
FRF5=a1.*exp(i*a11*pi/180);

load T06.tra;
a1=T06(5:201,1);
load T06.trb;
a11=T06(5:201,1);
FRF6=a1.*exp(i*a11*pi/180);

load T07.tra;
a1=T07(5:201,1);
load T07.trb;
a11=T07(5:201,1);
FRF7=a1.*exp(i*a11*pi/180);

```

```
load T08.tra;  
a1=T08(5:201,1);  
load T08.trb;  
a11=T08(5:201,1);  
FRF8=a1.*exp(i*a11*pi/180);
```

```
load T09.tra;  
a1=T09(5:201,1);  
load T09.trb;  
a11=T09(5:201,1);  
FRF9=a1.*exp(i*a11*pi/180);
```

```
load T10.tra;  
a1=T10(5:201,1);  
load T10.trb;  
a11=T10(5:201,1);  
FRF10=a1.*exp(i*a11*pi/180);
```

```
load T01.tra;  
a1=T01(5:201,1);  
load T01.trb;  
a11=T01(5:201,1);  
FRF1=a1.*exp(i*a11*pi/180);
```

```
load T11.tra;  
a1=T11(5:201,1);  
load T11.trb;  
a11=T11(5:201,1);  
FRF11=a1.*exp(i*a11*pi/180);
```

```
load T12.tra;  
a1=T12(5:201,1);  
load T12.trb;  
a11=T12(5:201,1);  
FRF12=a1.*exp(i*a11*pi/180);
```

```
load T13.tra;  
a1=T13(5:201,1);  
load T13.trb;  
a11=T13(5:201,1);  
FRF13=a1.*exp(i*a11*pi/180);
```

```
load T14.tra;  
a1=T14(5:201,1);  
load T14.trb;  
a11=T14(5:201,1);  
FRF14=a1.*exp(i*a11*pi/180);
```

```
load T15.tra;  
a1=T15(5:201,1);  
load T15.trb;  
a11=T15(5:201,1);  
FRF15=a1.*exp(i*a11*pi/180);
```

```
load T16.tra;  
a1=T16(5:201,1);  
load T16.trb;
```

```

a11=T16(5:201,1);
FRF16=a1.*exp(i*a1*pi/180);

IIw=2*pi*IIw;
FRF_1=FRF1./(-IIw.^2);FRF_2=FRF2./(-IIw.^2);FRF_3=FRF3./(-IIw.^2);
FRF_4=FRF4./(-IIw.^2);FRF_5=FRF5./(-IIw.^2);FRF_6=FRF6./(-IIw.^2);
FRF_7=FRF7./(-IIw.^2);FRF_8=FRF8./(-IIw.^2);FRF_9=FRF9./(-IIw.^2);
FRF_10=FRF10./(-IIw.^2);FRF_11=FRF11./(-IIw.^2);FRF_12=FRF12./(-IIw.^2);
FRF_13=FRF13./(-IIw.^2);FRF_14=FRF14./(-IIw.^2);FRF_15=FRF15./(-IIw.^2);
FRF_16=FRF16./(-IIw.^2);
IIxe=[FRF_1 FRF_2 FRF_3 FRF_5 FRF_6 FRF_7 FRF_8 FRF_9 FRF_10 FRF_11 FRF_12 ...
FRF_13 FRF_15 FRF_16];

% INPUT/OUTPUT MATRIX
b=fe_c(m dof,[6.08])';
cd=fe_c(m dof,[5.07 5.02 4.07 2.07 1.07 6.02 7.02 8.02 9.02 10.02 ...
13.07 13.02 12.01 11.08]);
pb=mode*b; % actuator
cp=cd*mode; % mode shapes from sensors
IIxf=nor2xf(freq,0.01,pb,cp,IIw); % FE normal 2 complex data file
save c:\fina3\f_und01 IIw IIxe

% FIGURE(2)
IIw=IIw;
IDopt = [3 0 22 1 size(IIxf,1) 1 9 1 0 0 1 7];
iiGUI

```

Appendix D: Photographs of the Experiments Conducted

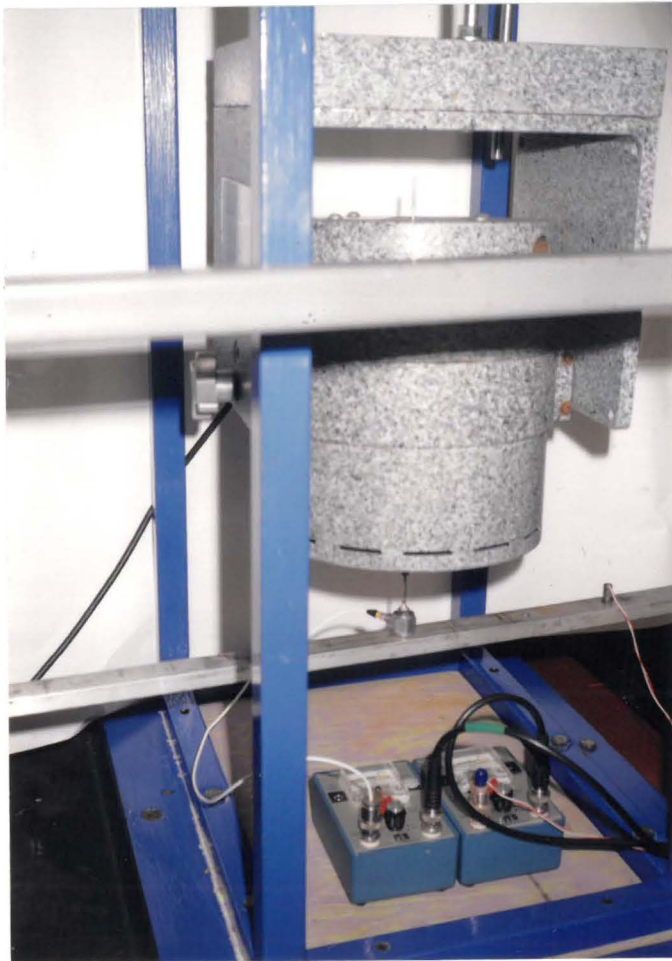


Figure D.1 Freely suspended beam

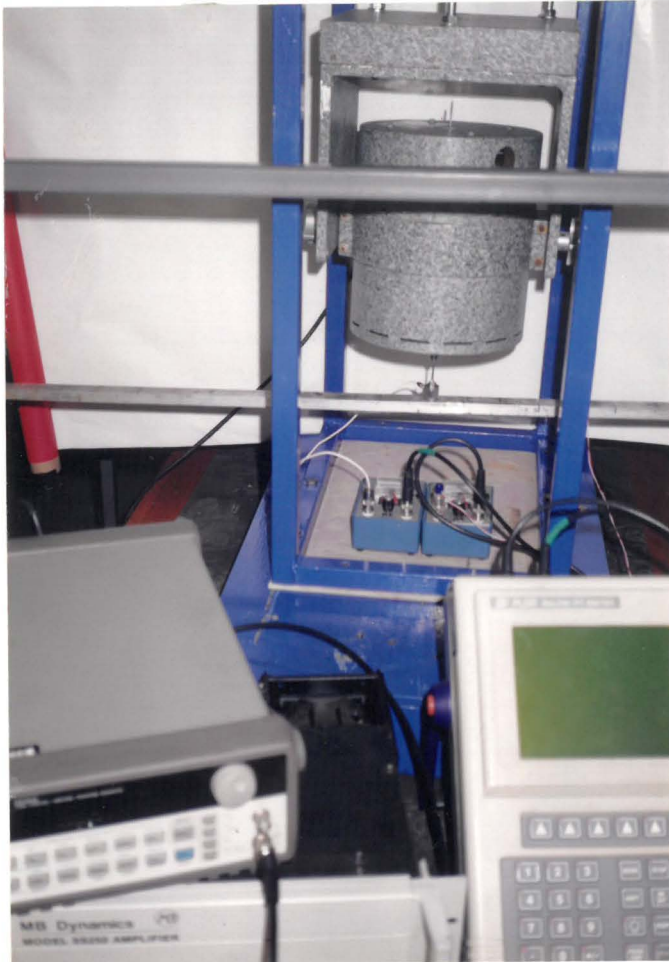


Figure D.2 Freely suspended beam with holes



Figure D.3 Freely suspended H-shaped structure

Appendix E: The Graphical Illustration of the Results

- The effect of damage on the FRFs (figures E.1, E.2, E.3).
- Effect of updating on the FRFs (figures E.4 and E.5).
- Illustration of the quality of modes measured.

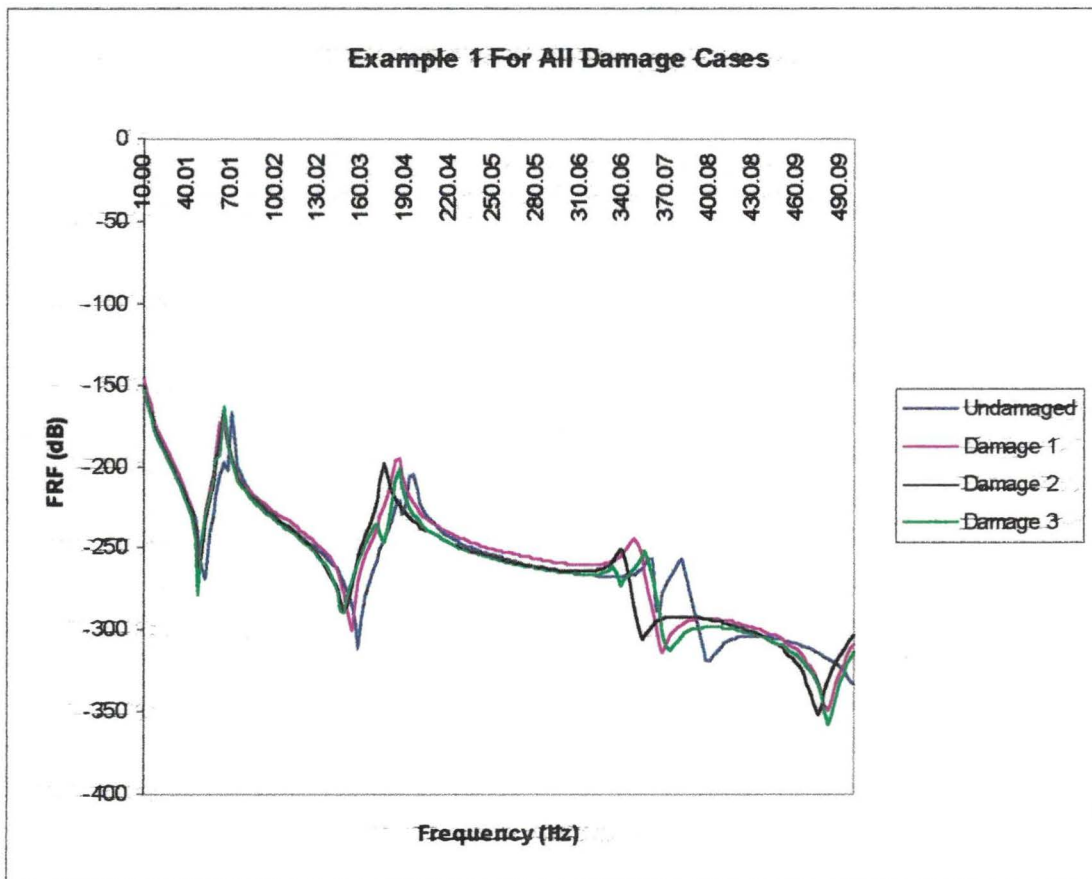


Figure E.1 The FRFs of the undamaged and the three damage cases (example 1)

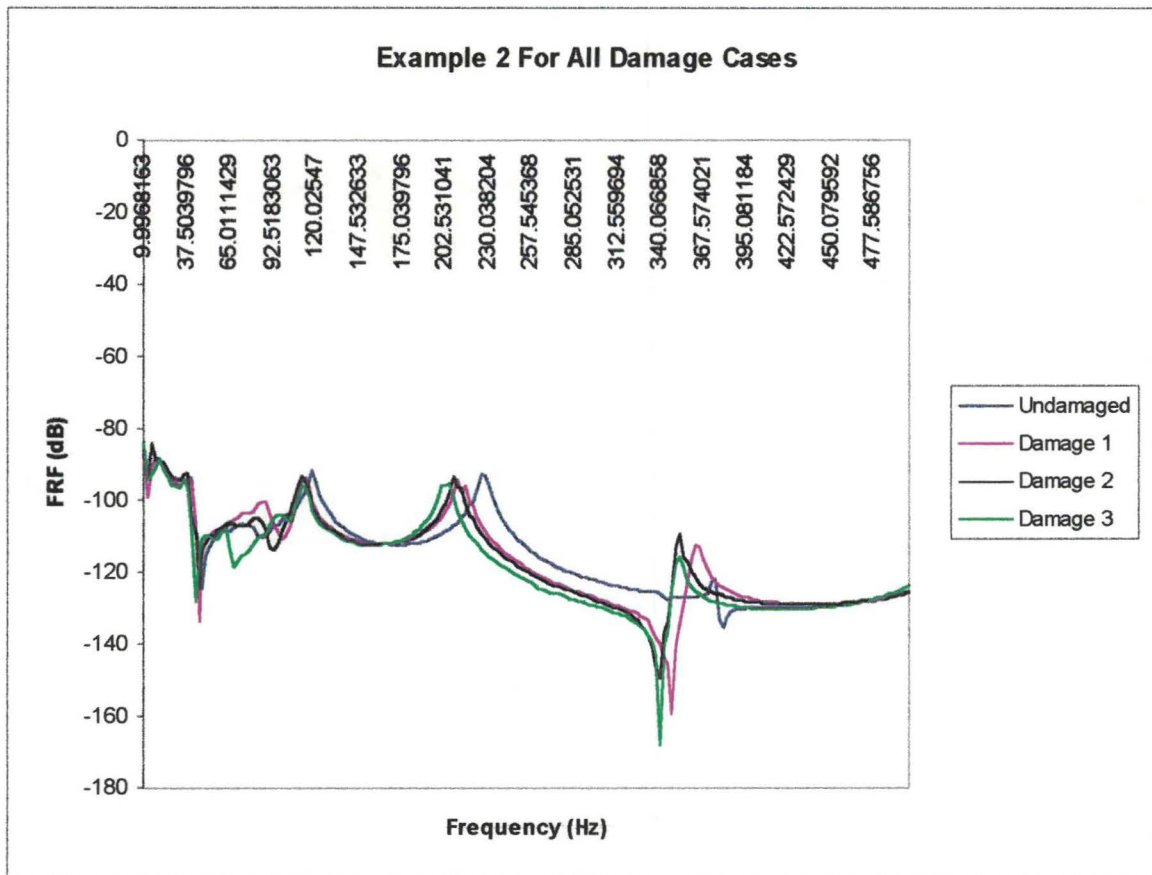


Figure E.2 The FRFs of the undamaged and the three damage cases (example 2)

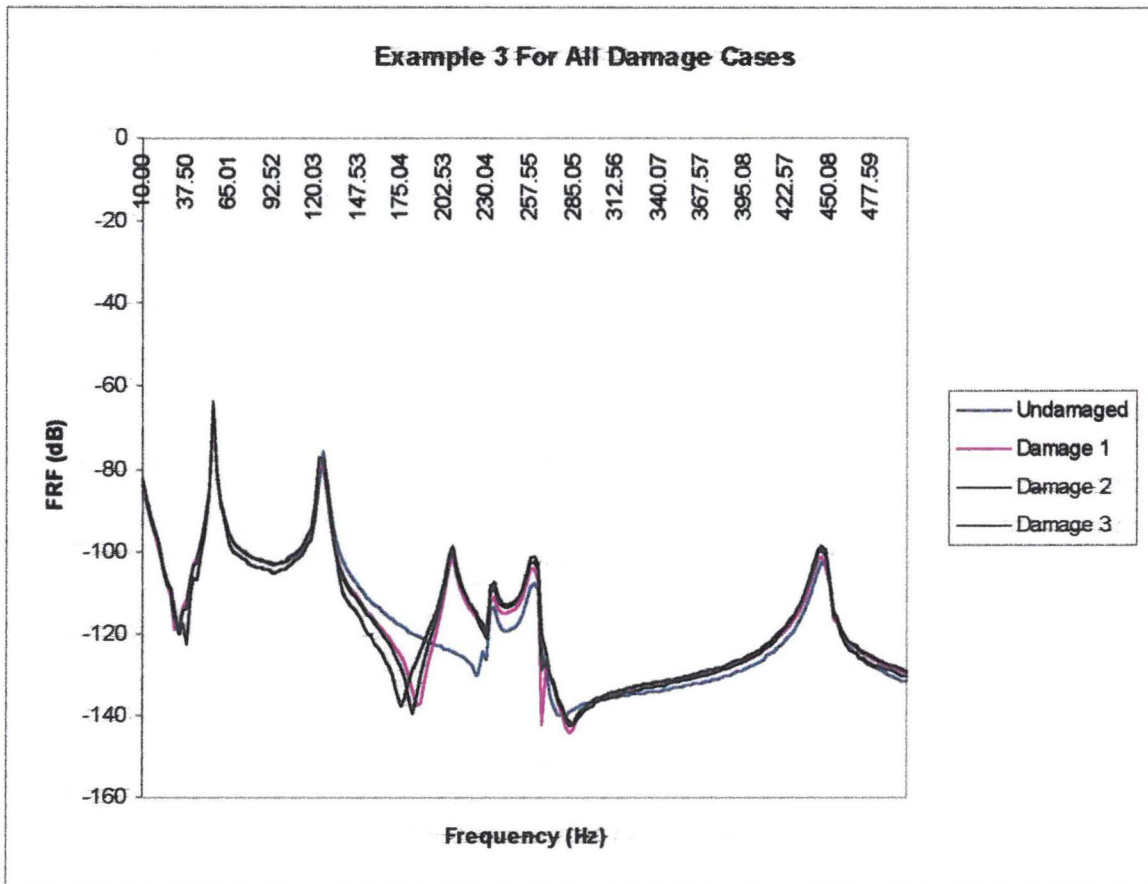


Figure E.3 The FRFs of the undamaged and the three damage cases (example 3)

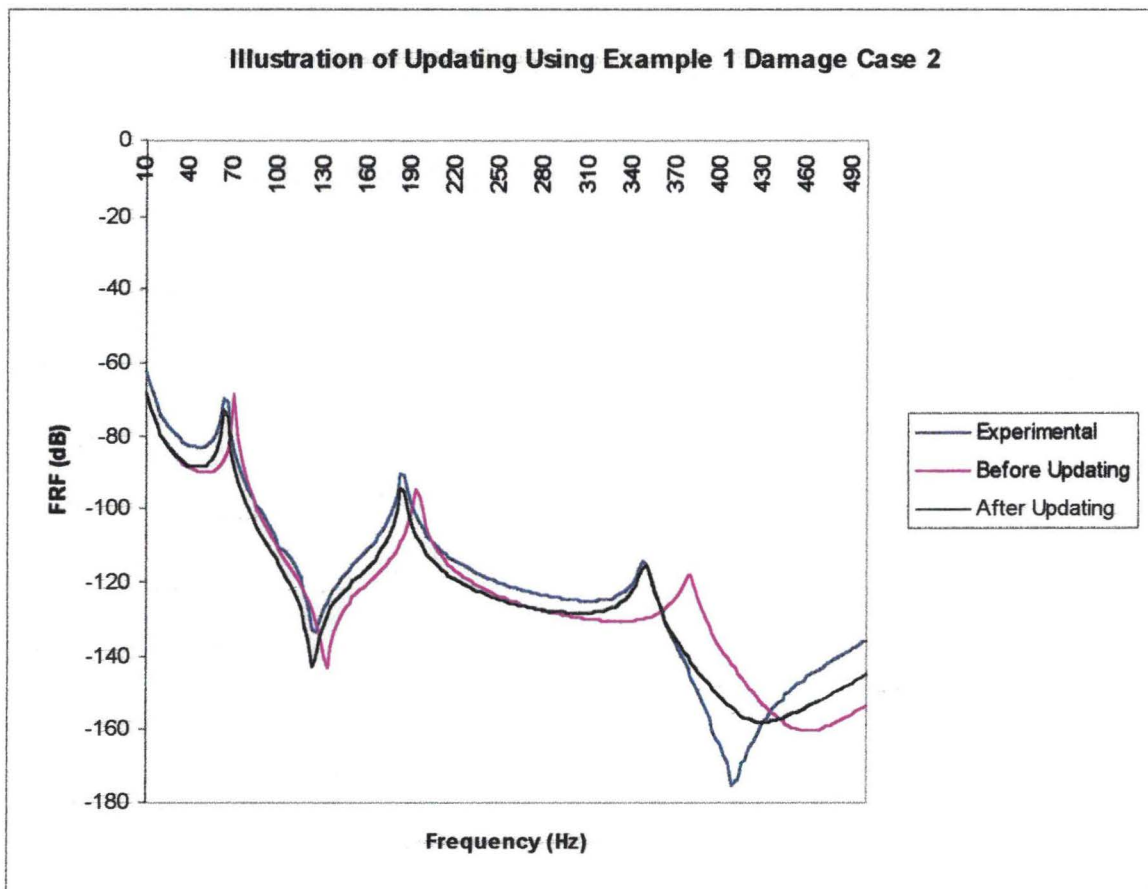


Figure E.4 Illustration of updating on the FRFs (case 1, example 1)

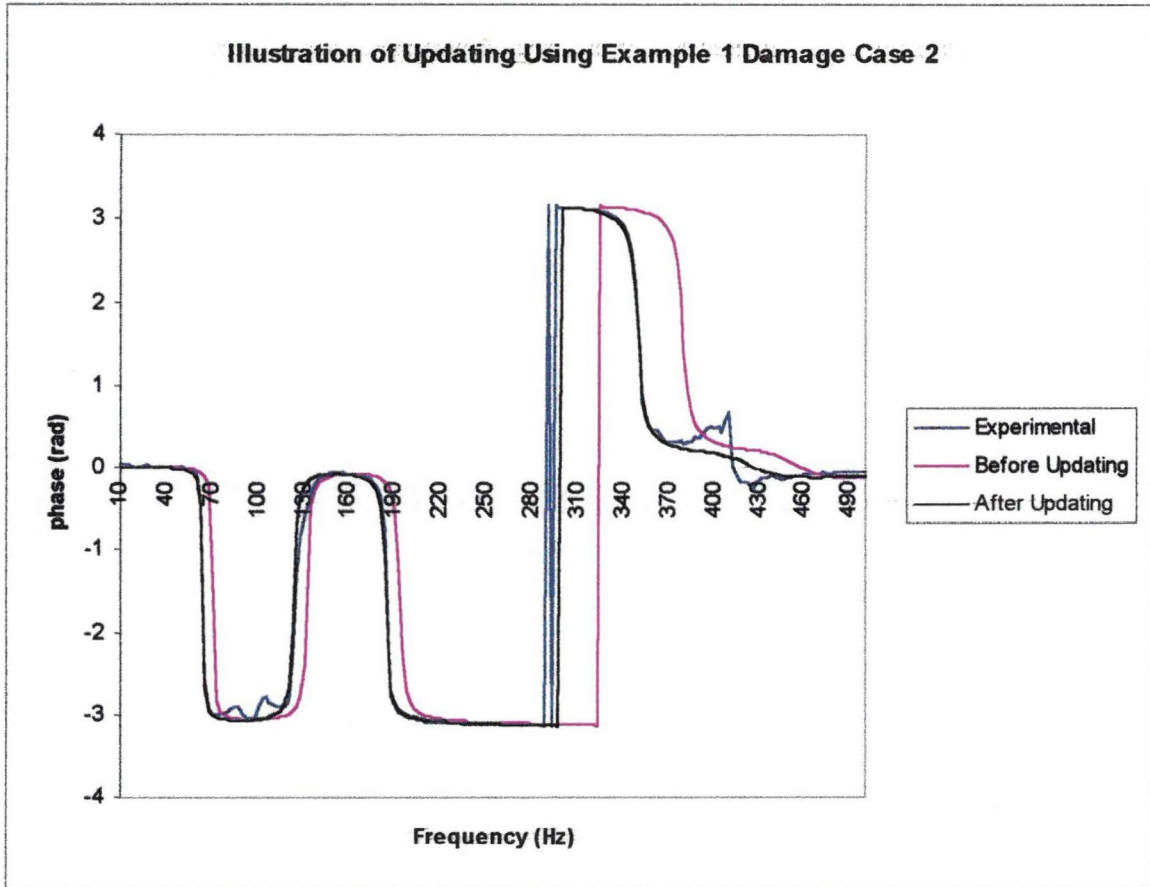


Figure E.5 Illustration of updating on phase (damage case 1, example 1)

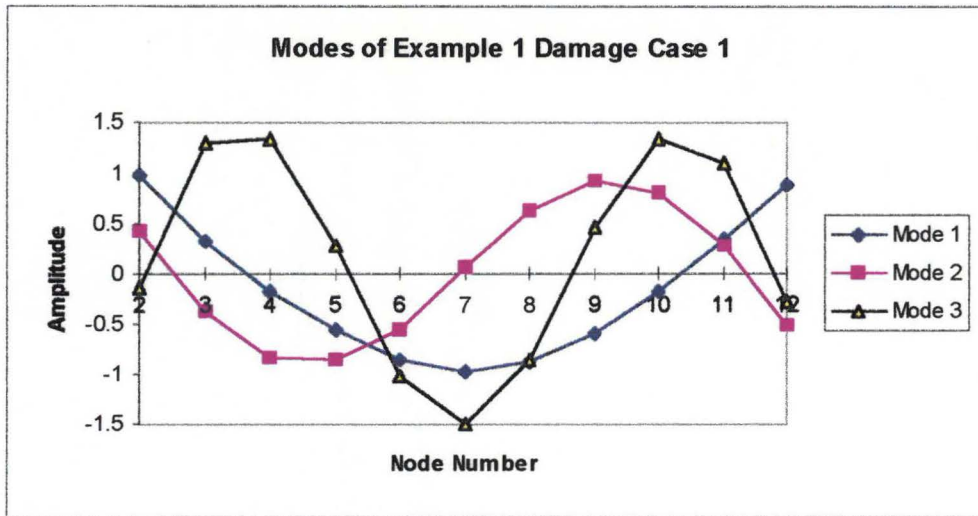


Figure E.6 The modes of damage case 1 of example 1

Appendix F: Details of the structures used

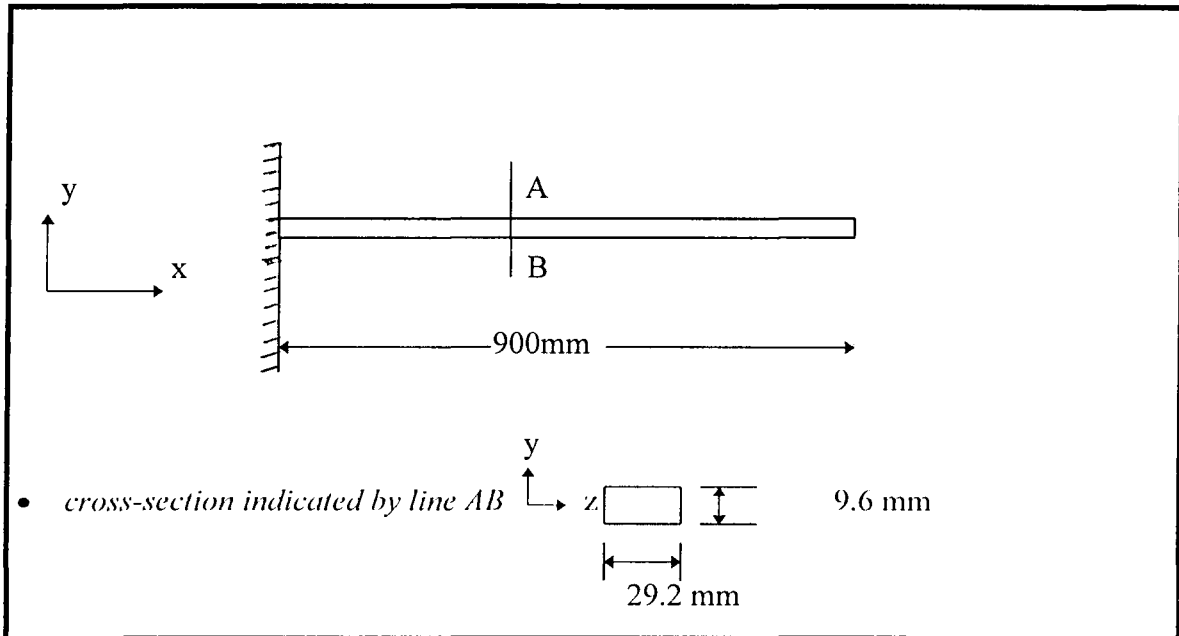


Figure F.1 The detailed diagram of a beam used to select a reduction/expansion method.

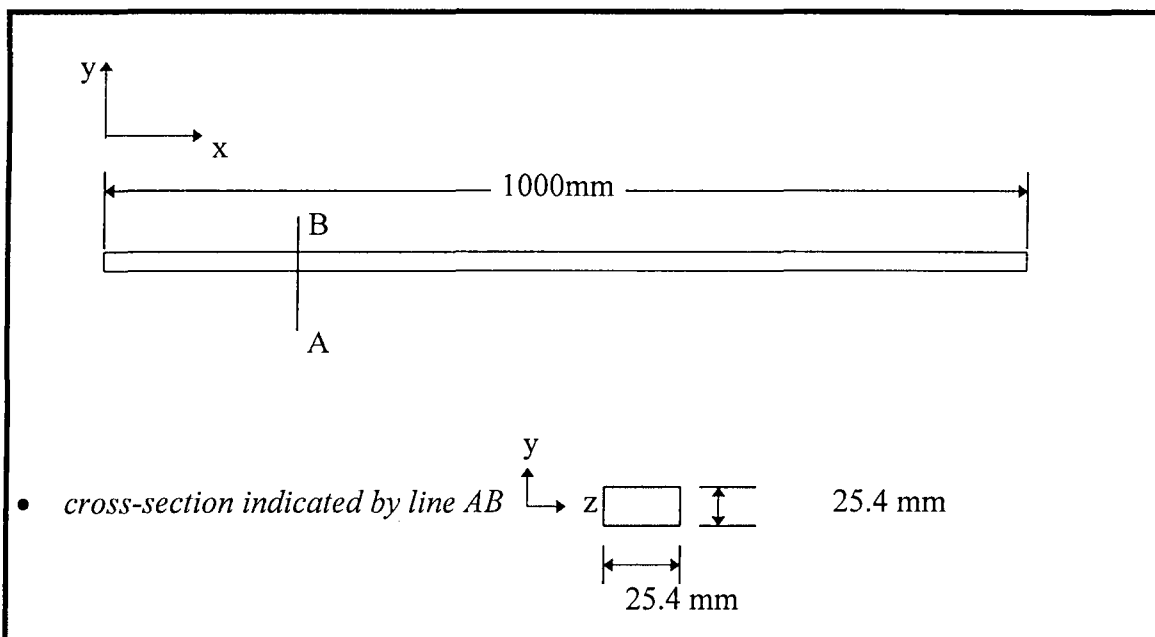


Figure F.2 The detailed diagram of a beam used in example 1.

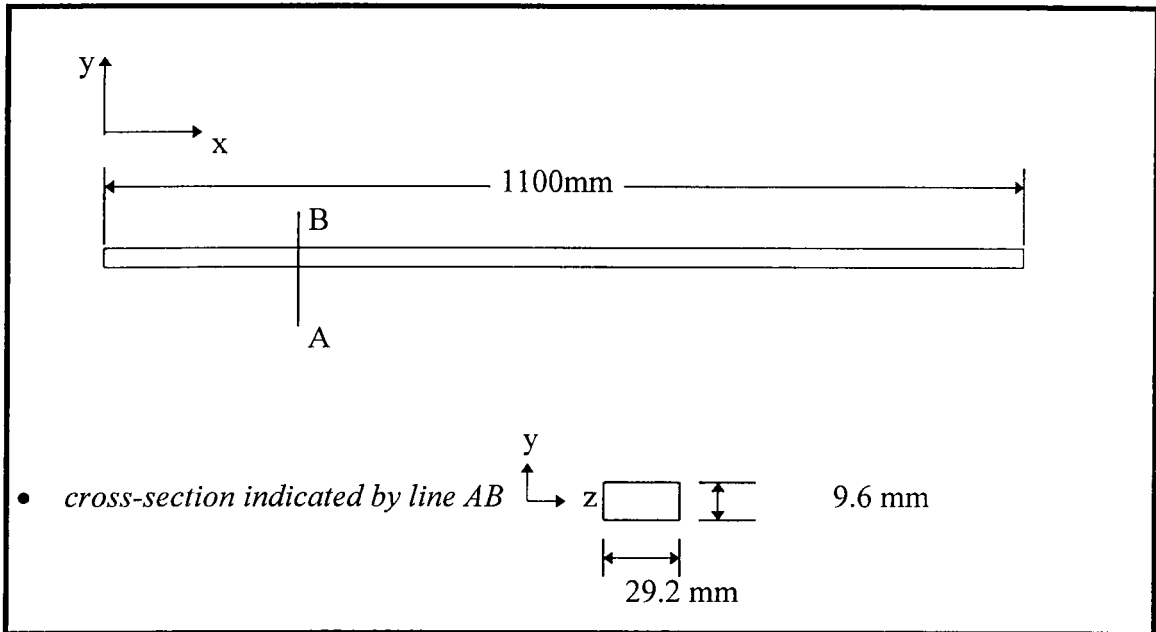


Figure F.3 The detailed diagram of a beam used in example 2.

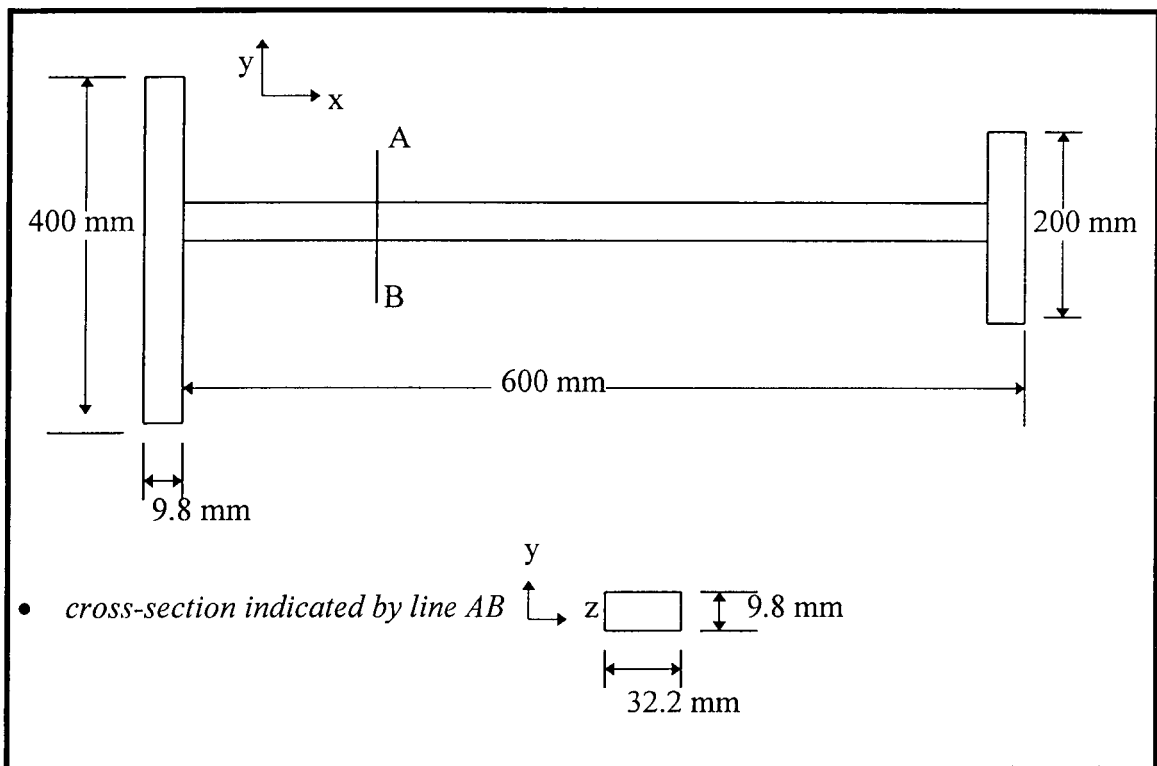


Figure F.4 Details of an irregular H-shaped structure used in example 3